Assessment of motions and loads of catamarans

Francisco Miguel Dos Santos Oliveira

Thesis to obtain the Master of Science Degree in

Naval Architecture and Ocean Engineering

Supervisor(s): Prof. Dr. Carlos Guedes Soares

Examination Committee

Chairperson: Prof. Dr. Yordan Garbatov
Supervisor: Prof. Dr. Carlos Guedes Soares
Member of the Committee: Prof. Dr. Ricardo Centeno

October 2018

”In memory of my dear sister.”

Acknowledgments

I would like to thank professor Carlos Guedes Soares for guiding this work, and the previous coordinator professor José Miguel Rodrigues who helped me in the initial phase of this dissertation.

To professor Ângelo Teixeira which contributed in the final part making possible the conclusion of this work. I would also like to thank professor Roberto Vettor for the availability in problem solving.

To Captain Arjen Töller who patiently accepted my refuses to join the ship during this last year, his support and understanding helped me to have a stable work.

To my friends and colleges present in both good and bad moments. Specially to the ones that encouraged me to return and complete this dissertation.

I would like to thank my parents for the support and guidance thought this years. Their help was crucial for my success and thankfully they never stop believing in my capabilities.

Resumo

Comparam-se métodos de cálculo de movimentos induzidos pelas ondas em catamarans, com o objectivo específico de avaliar como modelam a interação entre cascos. Aplicam-se três programas, representando o caso de não interação, o caso de interação bidimensional e por fim o caso de interação tridimensional, num total de 7 formas de cascos de catamarans encontrados na literatura. O primeiro caso é obtido utilizando resultados do método das faixas através de um código desenvolvido no CENTEC no IST, ao qual foram incluídos os termos dos extremos. O caso de interação bidimensional é resultante de um código desenvolvido por Centeno et al. (2000), baseado na teoria das faixas e em que os coeficientes hidrodinâmicos são calculados usando simetria dos cascos. Este código inclui o método de escoamento cruzado para inclusão dos efeitos viscosos nos movimentos. Para comparação o caso de interação tridimensional é obtido através do método dos painéis com fontes de Rankine, implementado no programa comercial Wasim da DNV-GL. Os resultados experimentais são comparados com os calculados pelos métodos através das funções transferência. A incerteza dos modelos numéricos é avaliada através de um modelo independente da frequência. Considerando as variáveis relevantes do problema, um estudo da correlação linear entre estas e os resultados da raiz do erro quadrático médio. Modelos de erros dependentes da frequência são criados com o resultado das correlações encontradas e comuns a todos os métodos. Os resultados indicam a relevância da interação hidrodinâmica e correlação com o número de Froude, sendo o método tridimensional o mais satisfatório.

Palavras-chave: catamaran; interação; método das faixas; método dos painéis Rankine; Modelo de erro

Abstract

Different methods to compute wave induced motion of catamarans are compared, with the special objective to evaluate how hydrodynamic hull interaction is modelled. Three numerical implementations, representing the no-interaction scheme, two-dimensional interaction and a three-dimensional interaction scheme, are applied in a total of 7 different hull forms of catamarans found in the literature. The first case is accomplished by post-processing of a strip theory method implemented in an in-house code developed at CENTEC in IST with additional end-terms inclusion. The two-dimensional interaction scheme results are obtained by a similar in-house code based on strip theory method, where the hydrodynamic coefficients are computed using symmetric demi-hulls. This code includes an empirical method, cross-flow for inclusion of viscous effects. For comparison it is included results using a commercial three-dimensional Rankine panel method, Wasim from DNV-GL. Motion results comparison between experimental and computed ones is done using transfer functions and Root Mean Square Error (RMSE). The uncertainty in numerical errors is evaluated using a frequency independent model error. Considering the relevant variables of the problem a linear correlations study is accomplished using the RMSE. A frequency dependent model error is studied using the best correlations found. Results indicate relevance of interaction schemes and strong dependence on Froude number, however better results are obtained using the three-dimensional interaction scheme.

Keywords: catamaran, interaction, strip theory, Rankine panel method, model error.

Contents

List of Tables

List of Figures

Nomenclature

Constants

ρ	Water dencity.
g	Acceleration of gravity.

Motion

α_l	Cross-flow lift coefficient.
β	Relative incident wave angle.
λ	Wave length.
ω	Incident wave frequency, rad/s.
ω_e	Encounter frequency.
ω_n	Natural frequency.
ω_c	Characteristic frequency.
$\zeta(x,t)$	Wave amplitude.
ζ_a	Incident wave amplitude.
A_{jk}	Added mass coefficient.
B_{jk}	Damping coefficient.
C_D	Cross-flow drag coefficient.
C_{jk}	Restoring coefficient.
F_j	Force or moment
Fn	Froude number, $\frac{U}{\sqrt{gL}}$
k	Wave number.

Coordinate systems

$O(x,y,z)$	Ship referencital.

$O_o(x, y, z)$ Earth referencital.

Ship

Δ Displacement.

∇ Under water volume.

A_{wl} Water line area.

B Beam.

B_{dh} Demi-hull beam.

C_b Block coefficient.

C_{wl} Water line area coefficient.

$GM_{t,l}$ Metacentric hight, transversal and longitudinal.

H Inner distance between demi-hulls.

L Length between perpendiculares.

LCB Longitudinal centre of bouyancy.

LCF Longitudinal centre of floatation.

r_{jk} Gyration radius.

S Demi-hulls centre line distance.

T Ship's draft.

U Forward velocity.

Chapter 1

Introduction

1.1 Motivation

The understanding of ship motions is today considered to have been developed to the stage of engineering accuracy. Even with relatively simple methods from the 70's, such as strip theory, that has been proven and widely used in computations of ship motions due to waves in a seaway, especially for single hulls. Other aspect of this advanced subject, ship motions, is the amount of methods existing to perform such computations, from thin theory, strip theories, three dimensional methods linear and non-linear based on potential theory, until recently CFD (computer fluid dynamics) that allow inclusion of viscosity. Compilations on such methods can be found in books and notes like, Fonseca (2009), Bertram (2012) and Faltinsen (2005). Nowadays it is the concern of general scientific community the comparison and evaluation of different methods. Comparing the results and the quality of the outcomes, sometimes regarding specific methods or conditions like linearity of solutions, or even general achievements in such computations are of most use for readers that are interested in the final ability to perform design optimisations regarding seakeeping criteria, Bunnik et al. (2010), Watanabe and Guedes Soares (1999), Dhavalikar (2011), Nestegard et al. (2008) and Temarel et al. (2016)

The study of ship motions in early stages of the project has been assumed as a benefit for the industry. This has led the researchers to investigate the motions of ships and create theories that can predict them with a good level of accuracy. This type of approaches to the project stage is based on the need to have a ship that can fully complete the task inherent to it. This is of higher importance when the type of vessel is somehow different or has extreme characteristics. These vessels such as fast ships, passenger ships, navy, investigation and others, have more parameters in account to make their operation successful or not. These type of ships are more likely to have discrepancies in the theoretical, numerical calculations and experiments. There are many factors that can influence these differences and also theories that try to overcome the problems. For the case of a multi-hull vessel such as the catamaran, considerations can be more elaborated. Catamaran's designs have been evolving rapidly and their ability to be a fast passenger transportation vessel is widely accepted, Faltinsen (2005). Two from the most important characteristics being fast vessels, namely faster then mono-hulls; and

the two demi-hulls configuration. Being fast is in itself an important aspect to have in consideration when performing hydrodynamic computations, which can be tackled in many different ways discussed along this work. Regarding being a vessel with two demi-hulls imposes a very important consideration for the type of methods to use in such computations because the interaction between hulls can play an important role. Prediction of motions on multi-hull vessels considering interaction of hulls have been needed since applications of strip theories in these cases, Jones (1972), Lee et al. (1973) and Van't Veer (1998a). This aspect together with high speeds, extreme characteristics of catamaran vessels, restrain the precision of results using simplified or commonly used theories of single hulls. Solutions to the interaction modelling can be found, from no-interaction to the fully three-dimensional wave problem case. In particular one publication developed at Instituto Superiror Técnico serves as starting point, Centeno et al. (2000), where a solution for the problem includes a cross-flow approach in a strip theory method. The implementation of that theory was available for this specific work being needed some revalidation after corrections were done, which were executed by Professor José Miguel Rodrigues at the time lecturing at the Institute.

Computations of seakeeping abilities of vessels need to have acceptable precision, since those vessels will carry persons on-board and/or need to perform operations of risk. To do this, different methods need to be studied, considering its different results and quantifying its level of precision. With the compiled information, processes can be defined and implementation of criteria in design stages of vessels regarding seakeeping can be done. Following this stages, found in single hull cases, this work fits in the comparison and evaluation of existing methods but for the case of multi-hull vessels. In sum, we will be comparing and evaluating different existing methods of seakeeping computations for vessels, with special focus on multi-hull.

1.2 Objectives and Outline

The focus of this work is a type of vessel that has peculiar characteristics, catamarans, even so those can be of a kind that is not contemplated in here. The catamarans on which this work is dedicated are twin-hull vessels, meaning that each of the hulls are completely symmetric and therefore demi-hulls. Many other types of catamarans exist from asymmetric hulls, wave piercing and SWATH (Small Waterplane Area Twin Hull), each one with it's own characteristics.

Catamarans are nowadays designed for a range of speed that place them in the category of semi-displacement vessels, they sail somewhere between being on their still waterline level and a planning condition, where the floating force is largely due to a lifting force produced by their speed trough the water. Being so, trim and sink due to dynamic condition is somehow important in computations regarding resistance and seakeeping. The demi-hulls of catamaran have different relations in dimensions from the single-hulls, being slender and in most cases having constant beam aft of mid-ship, ending typically in wet transoms with less draught then the midship section.

Inclusion of interaction between demi-hulls of catamarans can be significant for precision of results. Being available the work from Centeno et al. (2000), which includes a two dimensional approach, the

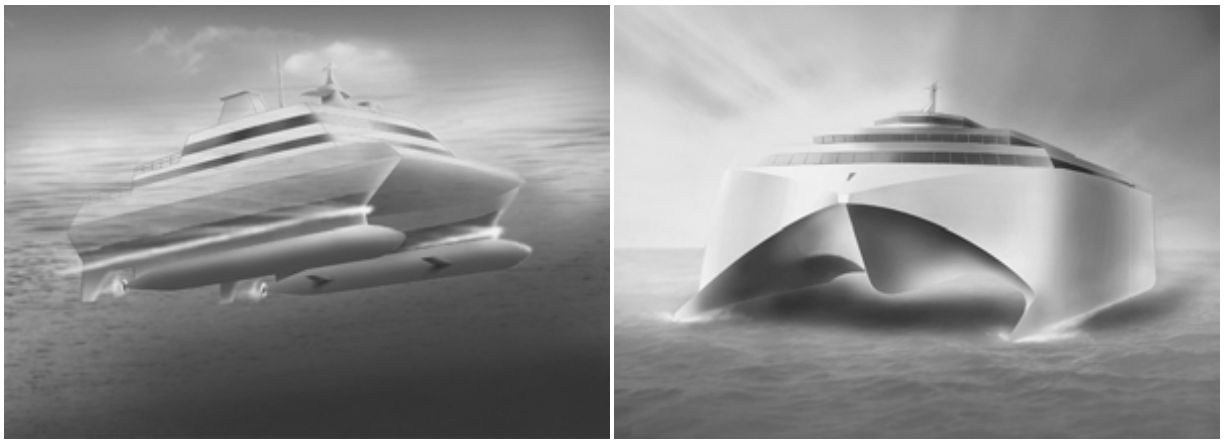

Figure 1.1: SWATH catamaran concept (left); Wave piercing catamaran concept (right), Faltinsen (2005).

study on this matter is a continuation on previous intern studies of the department. In seakeeping predictions advances, discussed at the beginning of this dissertation Chapter 2 ”Previous works done in the field”, several methods are explored and discussed with the objective of selecting the most relevant ones. Along side this selection, other important aspects such as improvements and post processing empirical methods are discussed. Namely *interaction*, *end terms* and *inclusion of viscous effects* in the computations until experimental work found for validation.

1.2.1 Numerical methods

In order to acquire results from the different methods, numerical computations are performed using a set methods available for this work. An in-house software, Fonseca built in FORTRAN, that uses strip theory based on Salvesen et al. (1970), from which results are subjected to post-processing, using MATLAB, in order to include end terms and a no-interaction scheme for catamaran transversal modes of motion. A two-dimensional interaction scheme is computed using CatCenteno, from Centeno et al. (2000). The software is based on the same strip theory as the previous but includes already ability to perform computations with end terms, more than that it also allows to apply an empirical method called ”cross-flow”. This method tries to include effects of viscosity in the motion results of fast vessels. The interaction effect is two-dimensional due to the computation of two-dimensional hydrodynamic coefficients of twin hulls placed side by side. As referred before the code was revised by the department. The software is build in FORTRAN and the use of MATLAB is extensive in the treatment of results. The third method is a three-dimensional scheme of a commercial software from DNV-GL. The package is called HydroD and in it the code used to perform computations is Wasim, a 3D Rankine panel method based code. This code among other features includes three-dimensional interactions between demi-hulls and also interaction with the standing wave created by the ship advancing on water, relevant for fast vessels. Strip theories solutions are solved in frequency domain, and Rankine panel method is solved in time domain, being treated by the software to give frequency domain solutions using fast Fourier transformation. Only linear motions are considered along this dissertation, although it has been present already for some time possibility to compute non-linear motions, case of Wasim software. The selection of methods to

implement in this work tries to traduce the possibilities that exist nowadays, keeping in mind that an important objective is the ability to include this type of computations in design stages. This is crucial since nowadays trend is to be able to create automatic loops of computations optimizing designs for specific criteria, such as seakeeping ones. An example of this will be justified by exclusion of CFD computations for this dissertation.

1.2.2 Results and experimental data comparison

Results from computations using the relevant methods will figure the work. Computations for prediction of ship motions are generally expressed in the form of RAO (Response Amplitude Operators), considering linear motions. The hydrodynamic coefficients of the methods will also be expressed for better understanding. Other possible results like phase angles between excitation forces and vessel motions will be neglected due to the amount of computations. Case studies will be used for validation of the methods. Experimental works used for this dissertation consider head waves conditions and in less cases bow or transversal waves, representing the availability of such experiments. The total number of different geometries used in this work is 7, with this hulls several combinations of conditions led to a total of 48 computations for heave, pitch and in relevant cases roll motions. For each one of this cases 3 interaction schemes, two of them with extra considerations leading to 288 RAO computations, creating a relevant pool of data for the next treatment and further conclusions.

1.2.3 Treatment of results

Commonly the experimental data produced for validations are discussed in a qualitative way. Comparison between experimental and computational results is done by overlapping curves in RAO figures. Recent works follow a trend of quantifying these differences by the mean of errors, root squared error for example. Performance metrics have been gaining ground as the precision of computations develops, such case is Castiglione et al. (2011) publication which presents a V&V (Validation and Verification) study characteristic of CFD computations. In other works when several methods are compared the amount of results is small and only direct comparisons are possible to accomplish, Bunnik et al. (2010). Due to the extension of this work a based on uncertainty quantification methodology is attempted, this way trying to quantify differences and showing concise results for further conclusions. This approach can be found for the case of single-hull vessels and has given good understanding regarding error modelling and even non-linearities presence on experimental results, Guedes Soares et al. (1999). With the objective of bringing this subject to catamaran motions results, the last work serves as base for a study on errors. Quantifying the errors and being able to locate them in the frequency means an attempt to understand the methods limits and their applicability.

1.3 Outline

The work is written in 8 chapters being the first one the introduction that includes the motivation of this work, followed by the three main components of the thesis: ”Numerical methods”, ”Results and experimental data comparison” and ”Results treatment”. Each one of these previous components is detailed in objectives subsection. The study on ”Previous works done in the field” is evident in Chapter 2, there, an overview of evolution and latest state-of-the-art works are explored, with focus on the case of catamaran motions computations. Chapter 3 includes the theoretical definitions of methods used in this work, catamaran motions computations using strip theories methods and a Rankine panel method. With the theoretical base a study on the problematic of hulls interaction is done, Chapter 4, in this chapter main differences in results by applying the different interaction methods are studied. ”Case studies” Chapter 5, has the compilation of all the catamaran models used to compute motions by the different methods and at the end includes descriptions of the software available for the work. The next two Chapters, 6 and 7, show the obtained results, being the first one direct comparison using RAO figures, which are showed in Appendix A. ”Study on model error” Chapter 7, has the treatment of results applying performance metrics and uncertainty models, first a frequency independent model and then a linear correlation study on the root mean square error that leads to a presentation of model correction factor dependent on the model’s speeds. Finally the last Chapter 8, compiles the work here produced, including conclusion remarks and recommendations of future directions of studies, concerning the central topic of catamaran motions.

Chapter 2

Previous work done in the field

In this chapter previous work done in the field is revised in order to describe the present state of knowledge. It is important to start with this part as a justification of the methods here used. This is done with a brief explanation about the ship motions and how this subject evolved throughout the time. Different theories have been created and it is important to refer some limitations inherent to them. More it is recommended to understand the effect of those limitations in today's ship motions studies. A generic overview of the need to study the ship's motions and a sequence of the most remarking development in the direction of methods applied in this work is done. More works are discussed including those that account for viscous effects representing the state-of-the-art at the present time. There are many methods to use when ship's motions are to be calculated, still here the focus will be those of interest when they include experimental validation, referent to strip theory methods, 3D Rankine panel methods and to computational fluid dynamics (CFD).

2.1 Ship motions

Ship motions have been studied since the 18th century, maybe not in a direct way as we do today, however since then there are publications on the evolution of seakeeping research. This first mile stone that is available was produced by Leonhard Euler in 1749 named ”Scientia Navalis”. In those times his study was far too mathematical, including theorems and corollaries.

A bigger need for correct calculations regarding the roll of ships appeared when the sailing ships were substituted by the steam vessels. The sails which were a damping device regarding the roll motion, for the sailing vessels, are replaced by steam engines. The work that marked this new era of ship motion calculations was produced by William Froude and A. N. Kriloff at the year 1861. Quite consequently of the development of the steam engines the pitch motion had to be considered when the vessels sailed with head waves. In 1896 Kriloff develops work regarding this matter and later in 1898 he presents the general six degrees of freedom theory. The works are based on the pressure field created by the underwater part of the vessels, considering that it is not disturbed by the ship. Froude-Kriloff hypothesis has dominated almost the works in seakeeping analysis till 1953 and is still nowadays used (Froude-

Kriloff excitation force). Being possible to consider the vessel a rigid body the equation of motion is written by Newton's second law; this results in a second order differential equation with respect to the derivative of displacement.

To correctly solve this equation experimental hydrodynamic coefficients where introduced, these coefficients are somehow special since they are frequency dependent. An extensive study on those coefficients was done with several theories proposed. One was Lewis (1929) work, who used the conformal mapping method to calculate the coefficients for sections oscillating. And exact solutions for the flow around circular cylinders with forced oscillation in the free surface were found by Ursell (1949). The two works combined provide the hydrodynamic coefficients for arbitrary sections and frequencies. A more sophisticated method to calculate the coefficients was developed by Frank (1967). He uses pulsating sources distributed along the hull shape. Known as Frank's close-fit method it works for any arbitrary body shape oscillating on the fluid surface and can be applied for multiple bodies, Lee et al. (1971). This coefficients tend to infinity when testing the zero frequency. To correct this, is necessary to introduce some three-dimensional effects on the formulation.

With the two-dimensional results previously described was possible to apply them in theories that are able to predict ship's motions. This first methods are named strip theory, and two-dimensional section coefficients are integrated along the length of the hull. Korvin-Kroukovsky (1955) presented the application of results from the two-dimensional to a strip theory that predicts the heave and pitch motions. Later ,Korvin-Kroukovsky and Jacobs (1957) brings some improvements and plenty experimental validations in the latter work. Problems with these theories were the intuitive way to introduce the effects of ship's forward speed. Also the coupling terms did not verify the relation of symmetry, Timman and Newman (1962). Similar strip theory was presented by Gerritsma and Beukelman (1967) but the work of Salvesen et al. (1970) is still considered one of the more acceptable and widely used. The mathematical analysis of the last strip theory is more accurate than the one presented by Korvin-Kroukovsky and Jacobs, simplifying the six degrees of freedom equations in a set of two coupled linear differential equations. The base assumption of the strip theories method is the linearisation of ship motions in respect to the incident wave, meaning that the wave hight is small compared to the ship's main dimensions. This assumption, which allows the solution in frequency domain represents very good accuracy and ability to include seakeeping criteria in design stages. Even so there are cases where more than the linear solution is required, extreme responses due to large incident waves are important when other then operability conditions can be found at the life time of a ship. To study this specific cases time domain theories are developed being able to solve the non-linear equations resulting from the excitation forces, Elsimillawy and Miller (1986), Xia and Wang (1997) and Fonseca and Guedes Soares (1998). There are plenty methods that vary from the strip theory, but this last mile stone lead to developments on a different type of vessels such as the catamaran.

2.2 Catamaran motions

With the achievements of methods described previously, attempts to apply the same mathematical models were not successful for catamarans at the beginning. With this same models the US Navy started the operation of USNS Hayes. This vessel faced big problems relative to the heave and pitching motions, making it not possible to operate as research vessel for the Navy, Van't Veer (1998a). One of the conclusions was that the wave interaction between hulls was not taken in account with the available strip theory. This failure lead to a more exhausting research and model test related to the multi-hull vessels and at the same time other variations of hulls types like the SWATH were incorporated in the same type of problem.

Ohkusu (1970) presents a method to calculate the hydrodynamic coefficients for a multi-hull vessel and applied them in the strip theory with satisfactory results. The sequence of reports published show consideration of interference effects on floating structures shaped as cylinders without forward speed. Calculations of the hydrodynamic coefficients and forces acting upon sets of cylinders are preformed by experimental and a theoretical approximation, having in mind that knowing these quantities the results can be used in strip theories calculations and even applying Lewis transformations for different forms of hulls corresponding to catamarans. The publication presenting theoretical calculations assumes a two dimensional interaction scheme that discard the standing waves in the vicinity of one cylinder, considering only the radiated waves in the problem. Calculations of the added mass and damping coefficients show profound effect considering interaction in all frequency ranges. For the case of twin cylinders, several configurations of spacing over radius, S/R, are explored with significantly different results in the location of maximum values versus minimums of the hydrodynamic coefficients. This abrupt, but not necessarily discontinuous changes in the curves of coefficients are due to the high waves existing in the space between the cylinders. Following this work an experimental study of a catamaran hull form produced for the purpose was presented, Ohkusu and Takaki (1971). The hulls used are symmetric longitudinally and two spacings were tested. Small forward speed, $Fn = 0.1$ was imposed and the response was compared with the theory discussed in his previous publication. The results shown response peaks in heave and pitch motions due the interaction between demi-hulls, this with the reasonable agreement between the experimental results. Observations on the experiments give notice that the wave between demi-hulls had significant high amplitude even when the heaving motions was small. As for the peak over-prediction is found to be related to the smaller damping force compared to the single hulls at resonant frequency.

Other of the very first works published, is by Jones (1972). In this work the simplified theory is applied to roll motion and the strip theory is adapted to the SWATH catamaran type for heave and pitch motions. As conclusions the author mentions over prediction of motion for the scenario of a higher ship's speed, even that the resonance frequency is well predicted using the ratio between wave length and ship's length. The possible solutions for the major problem of failure to predict the catamaran motions started with Lee et al. (1973). They mention three-dimensional influences regarding the hull spacing and viscous effects already assuming the catamaran as a fast vessel. The work presents conclusions about

displacement multi-hull and SWATH type of catamarans. By applying a strip theory approximation to calculate the hydrodynamic coefficients to include on the motion equations, the conclusions are similar to the previous works having results with a over-shoot in the motions response, noting that for the case of the SWATH type of catamaran the discrepancies are substantial, Lee et al. (1973).

Even being a study for the SWATH type of vessel, multiple remarks have to be done to the work completed by Lee and Curphey (1977). In this work discussions about the importance of viscous effects on the motions and correct formulation of the full three-dimensional problem are presented. One of the characteristics of this work is the guide to use of cross-flow method justified by the typical shape of the SWATH vessels. Lifting theory combined with strip theory led to good analytical results. The inclusion of viscous effects by the cross-flow approach is also present in the three-dimensional methods. Works like Chan (1993) and Fang et al. (1996) show some results even that the case of study is the SWATH type of catamaran. The three-dimensional linearised potential theory is applied including the effects between sections of the hull and taking account the end terms which are significant at low frequencies. By representing the mean wetted hull surface by an oscillating source distribution along the hull surface, it is concluded that discrepancies can be caused by not taking in account interaction between the steady and unsteady wave potentials while having forward speed. This can be solved by the use of a more correct formulation of the problem, that include viscous effects on the ship motions. The cross-flow method, witch is originally an adaptation from the simplified aerodynamic theory, Thwaites (1960), is a well tested way to include the effects of viscosity in ship motions. Even for the mono-hull case it has given better results compared with experimental data, works like Fonseca and Guedes Soares (2000) for vertical motion on container vessel and Begovic et al. (2002) and a later comparison work Arribas and Fernández (2006) show that the inclusion of the viscous effects is useful in the calculation of mono-hull ship-motions. This approach by the cross-flow to include the viscous effects can be applied to the strip theory, by an iterative method that introduced the new damping and added mass coefficient and recalculates the ship's motions till an accepted convergence is found in the results. Centeno et al. (2000) work presents this combination and with this formulation the results possible to compute are very well in agreement with the present necessities, fast calculations and simple implementation for an earlier stage of the ship design. Being the target of this work the multi-hull type of vessel the inclusion of viscous effects and the interaction between the hulls seam to be needed for more correct results with the necessary quickness of application.

Trying to solve the problematic of the three-dimension effects on the multi-hulls applications with the strip theory by van't Veer and Siregar (1995), shown that the strip theory is less realistic when the forward speed increases. In sequence the use of a three-dimensional panel method is presented in van't Veer (1997), in witch the interaction effects are included automatically Peng (2001). Regarding the three dimensional aspect of the catamaran motion problem there are several works of interest, but they are of some complexity level for the fast calculations required in the naval industry, specially in the preliminary design stage. Some works as, Hudson et al. (1995), Van't Veer (1998a), Varyani et al. (2000), Peng (2001) and Fang and Chan (2004) show an interest of research with this type of formulation and still compared with two-dimensional or directly with experimental tests.

Using the fundamental equations of Navier-Stokes the problem will be solved in all variables. Solvers that implement these equations are constructed with all the parameters of the problem into them, this means that with a solver of this type the solution of the problem will have in it the free surface water elevation (kelvin wake) and boundary layer. Applications of Reynolds averaged Navier-Stokes (RANS) methods in seakeeping and manoeuvring problems represent a new approach in numerical methods which implies the effects of viscosity and turbulence in the flow equations. The work of Castiglione et al. (2011) presents CFD results for a high speed multi-hull with rigorous verification and validation. Results using unsteady Reynolds-Average Navier-Stokes (U-RANS) are compared with experimental data and strip theory, for heave and pitch motions. The amount of computations present in the work are small due to the method applied. The comparison of results is done with a two-dimensional fast strip theory Faltinsen and Zhao (1991), that includes the interference effects, Hermundstad et al. (1999), and the experimental results of the hull in study. In both cases fully three-dimensional and U-RANS methods, the computational effort is very high or the methods are difficult to implement, even for the case of mono-hulls that do not have the problem with the interference effects.

Chapter 3

Theoretical background

In this chapter the theoretical formulations on which the numerical applications are based are introduced. From the ship motions mathematical problem that starts with the regular wave theory passing to the rigid body motion equations of a ship. Two different methods are used in this work, strip theory with and without interaction, and three-dimensional Rankine panel method. For each one the base theoretical assumptions are here described. Some variances of specific cases such as cross-flow method are also included and commented in this chapter. Regarding the numerical and software considerations the reader will be provided with relevant information later in Chapter 5.

3.1 Coordinate systems

To define the mathematical problem a set of referential axis where the object is placed has to be defined. Two Cartesian referential can be set, one that is fixed to the Earth referential, $O_0(x, y, z)$ and other that is fixed to the object with forward speed U, $O(x, y, z)$. With the first one, wave definition can be done and the second will be mainly referent to the motions of ships in study. The surface waves can be considered as linear superposition of harmonic components, and the next part defines the simple harmonic component that will be applied to the problem. This using the first referential, $O_0(x, y, z)$ that is placed with the origin at undisturbed surface of the ocean. The z axis direction is directed upwards and x axis is positive in the direction of wave propagation. Figure 3.1 is taken form Journee and Adegeest (2003) and shows the wave definitions on referential $O_0(x, y, z)$.

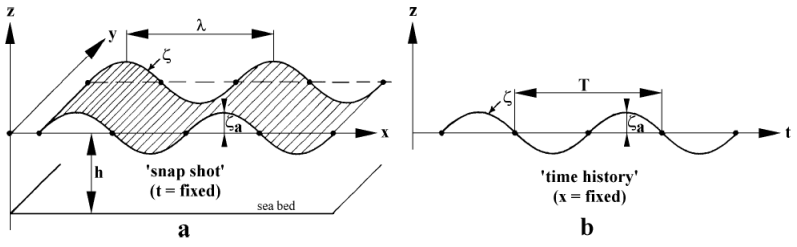

Figure 3.1: Harmonic wave definitions, Journee and Adegeest (2003)

The wave is shaped as sinusoidal function and the distance between highest point, crest, or the lower point, trough, to the undisturbed water surface is the wave amplitude ζ_a. In any other point of the wave its amplitude can be calculated and is denoted by $\zeta(x,t)$. The λ refers to wave length and if the "time history" is taken then T is the period of the wave. In here the depth of sea bed is represented as h, but for this work it will be considered tending to infinite as the problem is for deep waters case. With this definitions the relations of interest that can be calculated are the conversion to the sine or cosine angular arguments.

$$k\lambda = 2\pi \Leftrightarrow k = \frac{2\pi}{\lambda} \tag{3.1}$$

$$\omega T = 2\pi \Leftrightarrow \omega = \frac{2\pi}{T} \tag{3.2}$$

Where ω is the wave frequency in rad/s and if divided by the wave number, k in rad/m, it gives the wave velocity c , with this the mathematical description of the water elevation due to the existence of an harmonic wave can be translated to the following cosine Equation 3.4,

$$c = \frac{\omega}{k} = \frac{\lambda}{T} \tag{3.3}$$

$$\zeta = \zeta_a \cos(\omega t - kx) \tag{3.4}$$

For the ship that is exited by the wave the following coordinate system, $O(x,y,z)$ is located in a way that the x-y plan is coincident with the undisturbed surface of the water and z axe passing by the longitudinal centre of gravity. The six degrees of freedom are represented in the following figure 3.2. The linear motions of the ship are surge ξ_1 along the x axis, sway ξ_2 along the y axis, and heave ξ_3 along the z axis. For the rotational motions of the ship that are around the axes of the right handed coordinate system they are, roll ξ_4 around the x axis, pitch ξ_5 around the y axis and yaw ξ_6 around z axis.

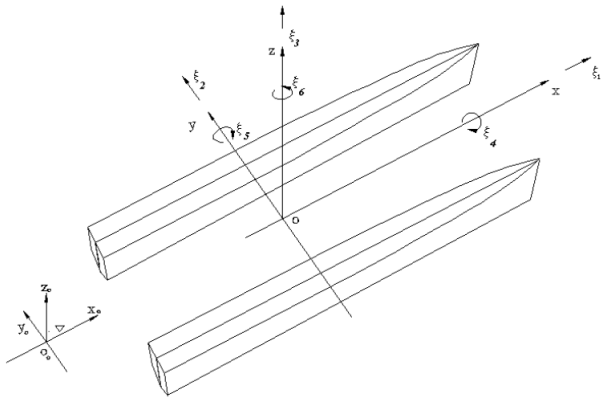

Figure 3.2: Catamaran coordinate system and the six degrees of freedom, Centeno et al. (2000)

The ship forward speed in relation with the incident wave direction, β, can be written in the coordinate system of the ship itself $O(x,y,z)$, this due to the encounter frequency.

$$\omega_e = \omega - kU\cos\beta \tag{3.5}$$

The direction of the wave propagation is then,

$$x_O = Ut\cos\beta + x\cos\beta + ysin\beta \tag{3.6}$$

resulting the wave elevation in the ship's referential $O(x, y, z)$,

$$\zeta = \zeta_a \cos(\omega_e t - kx\cos\beta - ky\sin\beta) \tag{3.7}$$

3.2 Ship equations of motion

As stated before the ship is modelled as a rigid body that now is subjected to excitation forces from the incident waves, resulting from those motions can be expressed in the equations for all the six degrees of freedom. From the dynamic equilibrium applying the second law of Newton the following equation can be written.

$$\sum_{k=1}^{6}[(M_{jk} + A_{jk})\ddot{\xi_k} + B_{jk}\dot{\xi_k} + C_{jk}\xi_k] = F_j^E \quad , \quad j = 1, 2, ..., 6 \tag{3.8}$$

$(A_{jk}\ddot{\xi_k})$, refers to the force (moment) component in the j-direction because of the motion in k-direction.

- M_{jk} - matrix of mass for the ship,
- $A_{jk} \quad B_{jk}$ - added mass and damping coefficient
- C_{jk} - restoring coefficients from the hydrostatic part of the forces
- F_j^E - the external forces in the k node of motion.

The hull has lateral symmetry, about the x, z plane, and that the centre of gravity is located at $(0, 0, z_g)$ the generalized mass matrix is,

$$M_{jk} = \begin{bmatrix} M & 0 & 0 & 0 & Mz_g & 0 \\ 0 & M & 0 & -Mz_g & 0 & 0 \\ 0 & 0 & M & 0 & 0 & 0 \\ 0 & -Mz_g & 0 & I_{44} & 0 & -I_{46} \\ Mz_g & 0 & 0 & 0 & I_{55} & 0 \\ 0 & 0 & 0 & -I_{46} & 0 & I_{66} \end{bmatrix} \tag{3.9}$$

In the matrix, M stands for the mass of ship and I_{jk} for the mass moment of inertia in the j, k node. If the j, k are different then is the product of mass inertial moment. The only one that appears is the product between 4th and 6th node of motion, this tends to zero if the ship presents strong symmetry along the y, z plane, in general terms it is comparatively smaller than the mass inertial moments. Since the origin of the referential system is usually taken on the water line plane the other diagonal, mass

times the vertical hight of gravity terms will not become zero. The moments of inertia can also be written in radius of gyration form.

$$I_{jk} = Mr_{jk}^2 \tag{3.10}$$

The added mass and damping coefficients matrices also become simplified due to the symmetry of ship.

$$A_{jk} \quad (or \quad B_{jk}) = \begin{bmatrix} A_{11} & 0 & A_{13} & 0 & A_{15} & 0 \\ 0 & A_{22} & 0 & A_{24} & 0 & A_{26} \\ A_{31} & 0 & A_{33} & 0 & A_{34} & 0 \\ 0 & A_{42} & 0 & A_{44} & 0 & A_{46} \\ A_{51} & 0 & A_{53} & 0 & I_{55} & 0 \\ 0 & A_{62} & 0 & A_{64} & 0 & A_{66} \end{bmatrix} \tag{3.11}$$

as for the restoring coefficients they are from the hydrostatic properties of the ship.

$$\begin{aligned} F_k &= -C_{kj}\xi_j \\ C_{35} &= C_{53} = -\rho g \iint_{A_{wl}} x ds \\ C_{33} &= 2\rho g \int_{A_{wl}} ds = \rho g A_{wl} \\ C_{55} &= \rho g \nabla G M_l \\ C_{44} &= \rho g \nabla G M_t \end{aligned} \tag{3.12}$$

Due to the symmetry of the ship that results in non diagonal matrices for the hydrodynamic coefficients, coupled motions can be treated separately. For the heave and pitch, nodes of motion heave and pitch the coupled equation is,

$$(M + A_{33})\ddot{\xi_3} + B_{33}\dot{\xi_3} + C_{33}\xi_3 + A_{35}\ddot{\xi_5} + B_{35}\dot{\xi_5} + C_{35}\xi_5 = F_3^E \tag{3.13}$$

$$A_{53}\ddot{\xi_3} + B_{53}\dot{\xi_3} + C_{53}\xi_3 + (I_{55} + A_{55})\ddot{\xi_5} + B_{55}\dot{\xi_5} + C_{53}\xi_5 = F_5^E \tag{3.14}$$

And for the other degrees of motion the roll, sway and yaw the motions equation is,

$$(A_{22} + M)\ddot{\xi_2} + B_{22}\dot{\xi_2} + (A_{24} - Mz_g)\ddot{\xi_4} + B_{24}\dot{\xi_4} + A_{26}\ddot{\xi_6} + B_{26}\dot{\xi_6} = F_2^E \tag{3.15}$$

$$(A_{42} - Mz_g)\ddot{\xi_2} + B_{42}\dot{\xi_2} + (A_{44} + I_{44})\ddot{\xi_4} + B_{44}\dot{\xi_4} + C_{44}\xi_4 + (A_{46} - I_{46})\ddot{\xi_6} + B_{46}\dot{\xi_6} = F_4^E \tag{3.16}$$

$$A_{62}\ddot{\xi_2} + B_{62}\dot{\xi_2} + (A_{64} + I_{46})\ddot{\xi_4} + B_{64}\dot{\xi_4} + B_{64}\xi_4 + (A_{66} + I_{66})\ddot{\xi_6} + B_{66}\dot{\xi_6} = F_6^E \tag{3.17}$$

In here the surge motion is not treated, there are formulations that creates approximations in order to have the surge motions solved but when using strip theory, two dimensional approach, the effects of a section do not interfere with the section next to it.

3.3 Strip Theory

Strip theory methods do not take in account longitudinal interaction between transversal strips. Being possible to have the bi-dimensional hydrodynamic coefficients for each strip considered to be an infinite cylinder. These values can be integrated longitudinally and total hydrodynamic coefficients values are obtained for the ship.

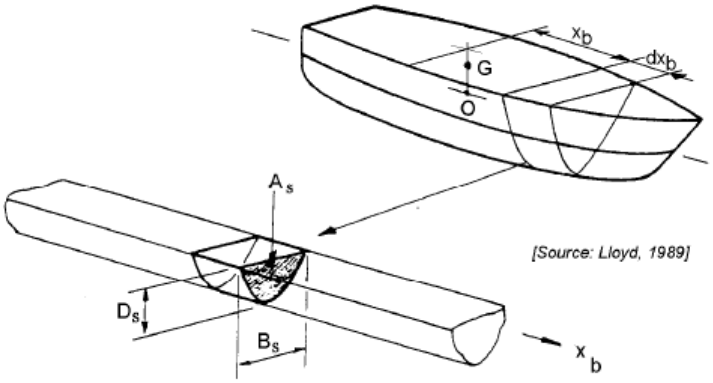

Figure 3.3: Strip Theory representation, Journee and Adegeest (2003)

For each strip the hydrodynamic coefficients and the forces are calculated using linearised potential flow theory as wave making, without forward speed. The next step is to follow the method to integrate these sectional values in other to obtain the total ones that will be included in the equation of motion.

3.3.1 Strip theory hydrodynamic coefficients

The hydrodynamic coefficients from each section are then integrated along the length of ship. To do this the formulation present in the work Salvesen et al. (1970) is demonstrated. First the heave and pitch hydrodynamic coefficients that are frequency dependent,

$$\begin{aligned} A_{33}(\omega) &= \int a_{33} d\xi - \frac{U}{\omega^2} b_{33}^A \\ B_{33}(\omega) &= \int b_{33} d\xi + U a_{33}^A \end{aligned} \tag{3.18}$$

$$\begin{aligned} A_{35}(\omega) &= -\int \xi a_{33} d\xi - \frac{U}{\omega^2} B_{33}^0 + \frac{U}{\omega^2} x_A b_{33}^A - \frac{U^2}{\omega^2} a_{33}^A \\ B_{35}(\omega) &= -\int \xi b_{33} d\xi + U A_{53}^0 - U x_A a_{33}^A - \frac{U^2}{\omega^2} b_{33}^A \end{aligned} \tag{3.19}$$

$$\begin{aligned} A_{53}(\omega) &= -\int \xi a_{33} d\xi + \frac{U}{\omega^2} B_{33}^0 + \frac{U}{\omega^2} x_A b_{33}^A \\ B_{53}(\omega) &= -\int \xi b_{33} d\xi - U A_{33}^0 - U x_A a_{33}^A \end{aligned} \tag{3.20}$$

$$\begin{aligned} A_{55}(\omega) &= \int \xi^2 a_{33} d\xi + \frac{U^2}{\omega^2} A_{33}^0 - \frac{U}{\omega^2} x_A^2 b_{33}^A + \frac{U^2}{\omega^2} x_A a_{33}^A \\ B_{55}(\omega) &= \int \xi^2 b_{33} d\xi + \frac{U^2}{\omega^2} B_{33}^0 + U x_A^2 a_{33}^A + \frac{U^2}{\omega^2} x_A b_{33}^A \end{aligned} \tag{3.21}$$

The two-dimensional sectional coefficients are for added mass, a_{33} and for damping, b_{33} from the heave motion. The notation A^0_{33} and B^0_{33} are the speed dependent part of the coefficients. The x_A is the longitudinal coordinate of the most aft section of the ship where a^A_{33} and b^A_{33} coefficients are calculated, these are the so called end-terms, that exist for ships that have a submerged transom.

$$A_{22}(\omega) = \int a_{22}d\xi - \frac{U}{\omega^2}b^A_{22}$$
$$B_{22}(\omega) = \int b_{22}d\xi + Ua^A_{22} \tag{3.22}$$

$$A_{24}(\omega) = A_{42}(\omega) = \int a_{24}d\xi - \frac{U}{\omega^2}b^A_{24}$$
$$B_{24}(\omega) = B_{42}(\omega) = \int b_{24}d\xi + Ua^A_{24} \tag{3.23}$$

$$A_{26}(\omega) = \int \xi a_{22}d\xi + \frac{U}{\omega^2}B^0_{22} - \frac{U}{\omega^2}x_A b^A_{22} + \frac{U^2}{\omega^2}a^A_{22}$$
$$B_{26}(\omega) = \int \xi b_{22}d\xi - UA^0_{22} + Ux_A a^A_{22} + \frac{U^2}{\omega^2}b^A_{22} \tag{3.24}$$

$$A_{44}(\omega) = \int a_{44}d\xi - \frac{U}{\omega^2}b^A_{44}$$
$$B_{44}(\omega) = \int b_{44}d\xi + Ua^A_{22} + B44^* \tag{3.25}$$

$$A_{46}(\omega) = \int \xi a_{24}d\xi + \frac{U}{\omega^2}B^0_{24} - \frac{U}{\omega^2}x_A b^A_{24} + \frac{U^2}{\omega^2}a^A_{24}$$
$$B_{46}(\omega) = \int \xi b_{24}d\xi - UA^0_{24} + Ux_A a^A_{24} + \frac{U^2}{\omega^2}b^A_{24} \tag{3.26}$$

$$A_{62}(\omega) = \int \xi a_{22}d\xi - \frac{U}{\omega^2}B^0_{22} - \frac{U}{\omega^2}x_A b^A_{22}$$
$$B_{62}(\omega) = \int \xi b_{22}d\xi + UA^0_{22} + Ux_A a^A_{22} \tag{3.27}$$

$$A_{64}(\omega) = \int \xi a_{24}d\xi - \frac{U}{\omega^2}B^0_{24} - \frac{U}{\omega^2}x_A b^A_{24}$$
$$B_{64}(\omega) = \int \xi b_{24}d\xi + UA^0_{24} + Ux_A a^A_{24} \tag{3.28}$$

$$A_{66}(\omega) = \int \xi^2 a_{22}d\xi + \frac{U^2}{\omega^2}A^0_{22} - \frac{U}{\omega^2}x^2_A b^A_{22} + \frac{U^2}{\omega^2}x_A a^A_{22}$$
$$B_{66}(\omega) = \int \xi^2 b_{22}d\xi + \frac{U^2}{\omega^2}B^0_{22} + Ux_A a^A_{22} + \frac{U^2}{\omega^2}x_A b^A_{22} \tag{3.29}$$

In this set of equations the a_{22} and b_{22} are the sectional added mass and damping coefficient for sway motion. a_{44} b_{44} are the coefficients for the roll motion, in equation 3.25 the $B44^*$ stands for the inclusion of a viscous roll parameter that gives an extra damping factor to the motion. The coupled terms are a_{24} and b_{24} for the sway and roll motions. The same as for the heave and pitch coefficients the designation ^{A} stands for the two dimensional coefficient of the most aft section of the ship, and ^{0} is for the speed dependent coefficients.

The mathematical explication is given in the work of Salvesen et al. (1970), and therefore not presented here. A remark that is to be done is regarding the end terms that appear in the coefficients calculations. These terms are from a vectorial transformations present in Ogilvie and Tuck (1969) and uses the two-dimensional coefficients of the most aft section of the hull. To calculate the two-dimensional sectional coefficients the use of Frank's close-fit method, Frank (1967), is applied to the catamaran demi-hull, further considerations regarding the interaction problem that is possible to include in this phase of the calculations are explicit in chapter 4.

3.3.2 Exciting forces

The incident wave potential can be written in the complex form.

$$\Phi_w = \frac{ig\zeta_a}{\omega} e^{kz} e^{-ik(x\cos\beta + y\sin\beta)} \tag{3.30}$$

Due to restraining the ship advancing in the incident waves, incident and diffracted potentials can be separated resulting in the forces as the following equation,

$$F_j = F_j^W + F_j^D \tag{3.31}$$

where the incident wave forces will lead to the Froude-Kriloff force and moment. This force is caused by the unsteady pressure created by the undisturbed waves that the ship encounters. The diffraction force and moment is due to the ship changing the pressure field, condition that exists due to restraining the ship to it's average position,

$$F_j^D = \rho \iint_S n_j (i\omega_e + U\frac{\partial}{\partial x})\Phi_d ds \tag{3.32}$$

$$F_j^W = \rho i \iint_S n_j (\omega - kU\cos\beta)\Phi_w ds \tag{3.33}$$

that can be reduced to.

$$F_j^W = \rho i\omega \iint_S n_j \Phi_w ds \tag{3.34}$$

Applying the Stokes theorem the force is expanded to a contour integration,

$$F_j^D = \rho \iint_S (i\omega_e n_j + U m_j)\Phi_d ds + \rho U \int_{C_A} n_j \Phi_d dl \tag{3.35}$$

the sectional Froude-Krylov force,

$$f_j(x) = ige^{-ikx\cos\beta} \int_{C_x} N_j e^{kz} e^{-iky\sin\beta} dl, \quad j = 2,3,4 \tag{3.36}$$

the sectional diffraction force is

$$\begin{aligned} \phi_D &= \psi_D \zeta_a e^{-ikx\cos\beta} \\ h_j(x) &= i\omega_e e^{-ikx\cos\beta} \int_{C_x} N_j \psi_D dl, \quad j = 2,3,4 \end{aligned} \tag{3.37}$$

The integration along the ship length gives the exciting force and moment that can now be written.

$$\begin{aligned} F_j &= \rho\zeta_a \int_L (f_j + h_j) d\xi + \rho\zeta_a \frac{U}{i\omega_e} h_j^A, \quad j = 2,3,4 \\ F_5 &= -\rho\zeta_a \int_L [x(f_3 + h_3) d\xi + \frac{U}{i\omega_e} h_3] d\xi - \rho\zeta_a \frac{U}{i\omega_e} x_A h_3^A \\ F_6 &= \rho\zeta_a \int_L [x(f_2 + h_2) d\xi - \frac{U}{i\omega_e} h_2] d\xi - \rho\zeta_a \frac{U}{i\omega_e} x_A h_2^A \end{aligned} \tag{3.38}$$

To obtain te two dimensional hydrodynamic coefficients the method used is the Frank's close fit. This

formulation is based largely from the theory manual of software *VERES*, Fathi and Hoff (2004).

Regarding the two dimensional potential solution used in the radiated and diffraction forces the method here commented is the Frank's close fit. It will be stated that both strip theory software used in for this work compute using this method, Centeno et al. (2000) and Fonseca and Guedes Soares (1998).

This method calculates the coefficients by a distribution of sources over the mean wetted surface of the ship. Satisfying the boundary conditions Green functions are applied to represent the unit strength sources that satisfy the potentials. The density of the sources are unknown functions to be determined by applying the kinematic surface boundary condition on the submerged part of the cross section with infinite length.

To note that this method has associated to it, irregular frequencies, which are uniqueness solutions, especially in the very high frequency range. This can be overcome by introducing an extra segment on the average waterline. The full formulation is presented in some published works. Of interest is the original one, Frank (1967) and an explanation is present in Journee and Adegeest (2003).

3.4 Rankine panel method

Rankine panel method theoretical formulation can be found in the literature, Kring (1994), or with practical examples in Bertram (2012). In this text only the base considerations are included specially regarding the linearisation of the boundary conditions and boundary integral formulations characteristic of the method. From Kring, the linearisation of the problem is summarized, starting with a decomposition of the potentials in basis Φ, local, ϕ, and memory, φ.

$$\Psi(\vec{x},t) = \Phi(\vec{x}) + \phi(\vec{x},t) + \varphi(\vec{x},t) \tag{3.39}$$

The memory flow is governed by an initial boundary value problem in which the memory potential represents the solutions of the steady, radiated, and, if present scattered wave patterns. The basis flow provides the linearisation and the local flow provides the forcing for unsteady motion. Considering the dominant basis condition component, Φ, and a perturbation correction memory, φ, the linear form of the kinematic and dynamic free surface conditions reduce to the form,

$$\frac{\partial \zeta}{\partial t} - (\vec{W} - \nabla\Phi)\cdot\nabla\zeta = \frac{\partial^2\Phi}{\partial t^2}\zeta + \frac{\partial\varphi}{\partial z} \tag{3.40}$$

$$\frac{\partial \varphi}{\partial t} - (\vec{W} - \nabla\Phi)\cdot\nabla\varphi = -g\zeta + [\vec{W}\cdot\nabla\Phi - \frac{1}{2}\nabla\Phi\cdot\nabla\Phi] \tag{3.41}$$

applied on $z = 0$, where is the $\vec{W}$ mean translational velocity of the ship. A decomposition of the perturbation potential into instantaneous and memory components as indicated in equation 3.39 generates better and stable form in the integral equation of motions. Decomposition of the incident, radiated and diffracted wave disturbances. The linear radiation body boundary conditions become,

$$\frac{\partial \varphi}{\partial n} = \sum_{i=1}^{6} (\frac{d\xi_j}{dt} + \xi_j m_j) \quad on \quad S_B \tag{3.42}$$

applied to the mean wetted surface of the hull. Here the m-terms, m_j, provide a coupling between the steady basis flow and the unsteady ship motion.

$$\vec{m} = (\vec{n}\nabla)\nabla\Phi \tag{3.43}$$

The diffraction body boundary condition merely states that the normal velocity of the sum of the incident and diffraction velocity potentials vanishes over the hull mean position. The Laplace equation is enforced in the fluid domain by a distribution of Rankine sources and dipoles over the free surface and wetted hull surface. Application of Green's second identity leads to a boundary integral formulation for the perturbation potential,

$$2\pi\varphi(\vec{x}) - \iint_{S_F \cup S_B} \frac{\partial \varphi(\vec{x}')}{\partial n} G(\vec{x}'; \vec{x}) dx' + \iint_{S_F \cup S_B} \varphi(\vec{x}') \frac{\partial G(\vec{x}'; \vec{x})}{\partial n} dx' = 0 \tag{3.44}$$

Where $G(\vec{x}'; \vec{x}) = 1/|\vec{x} - \vec{x}'|$ is the Rankine source potential, S_F is the mean position of the free surface, and S_B is the mean position of the hull. Many ways to implement the transom effects in the mathematical formulations, the Consideration in here present are the ones indicated in Kring (1994), since it is the base of software in this work used, Wasim linear (SWAN1). Having correlation to the lifting flow theory the conditions imposed at the stern of the hull are called Kutta conditions. This because, if the stern is well designed, the detachment of flow happens at the trailing edge. Due to this consideration the boundary conditions are imposed at the aft position, location of the transom stern, $_A$. Along the stern flow detachment line, where free surface conditions are applied.

$$\frac{\partial \varphi}{\partial z} = -\frac{\partial \zeta_T}{\partial t} + (\vec{W} - \nabla\Phi) \cdot \nabla\zeta_A + \frac{\partial^2 \Phi}{\partial z^2}\zeta_A + \frac{\partial \phi}{\partial z} \quad on \quad (x, y, z) = (x_A, y_A, 0) \tag{3.45}$$

$$\frac{\partial}{\partial t} - (\vec{W} - \nabla\Phi) \cdot \nabla)(\phi + \varphi) = -g\zeta_A + [\vec{W} \cdot \nabla\Phi - \frac{1}{2}\nabla\Phi \cdot \nabla\Phi] \quad on \quad (x, y, z) = (x_A, y_A, 0) \tag{3.46}$$

With the first, dynamic condition the total pressure at the trailing edge is equal to the atmospheric pressure. The second, kinematic condition ensures the continuity of the pressure along the detaching streamline. As indicated in Kring (1994), a two dimensional example of this is found in Schmidt (1981).

Chapter 4

Modelling hulls interaction

To consider the interaction effect for motion computations of catamarans three levels of numerical implementations are used, considering the base case of no-interaction to the two-dimensional interactions scheme and finally a three-dimensional. The relevance of interaction schemes may differ from the conditions that vessels are subjected to, as it will be discussed a no-interaction method can be valid for a combination of speed, heading and hull spacing. However a two-dimensional interaction scheme can be very precise at low speeds situations or no forward speed. The last method is way more complete, and it is used in this work as a comparison for the motions results. Due to the availability of commercial program, Wasim, only the strip theory based methods are discussed in the present chapter.

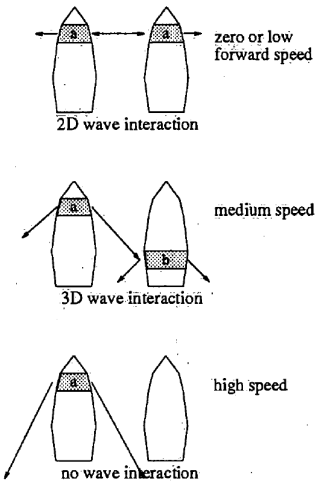

Figure 4.1: Interaction schemes, van't Veer and Siregar (1995)

Considering the two-dimensional interaction scheme, with the radiated waves travelling traversal to the hulls centre lines like the first case shown in Figure 4.1, it is possible to predict in a simple way the interaction relevance and limit. Following formulation from van't Veer and Siregar (1995) for the condition in which the radiated wave from one hull interacts with the other hull is as in Equation 4.1.

$$\tau = \frac{U}{V_p} = \frac{U}{\lambda_e / T_e} = \frac{U k_e}{\omega_e} = \frac{U \omega_e}{g} \tag{4.1}$$

When τ is greater then the relation between length and inner hull distance L/H, the wave generated at the bow of one demi-hull does not interact with the other demi-hull, since it will pass behind the most aft section of it. Such is the case of last example shown in Figure 4.1. Likewise the limit frequency where this interaction occurs for a certain forward speed is deducted by the Equation 4.2.

$$\omega_e > \frac{L}{H} \cdot \frac{g}{U} \tag{4.2}$$

4.1 Catamaran without interaction using strip theory

In order to represent the base scheme of a catamaran the no-interference case is included in this work. Because the following study will consider other than 180 degrees of headings a general form is shown for heave, pitch and roll motions. Considering the demi-hulls independent, wave loads can be calculated for each demi-hull and then transformed to the case of catamaran. To do so it is required that the two hulls are equal and that the centre lines of each one is at a constant distance from each other, $S = 2y_T$.

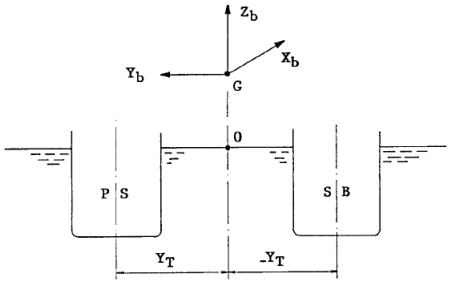

Figure 4.2: Catamaran without interaction, Journee and Adegeest (2003)

In general if the catamaran is subjected only to head waves the result is exactly the same as only one of the demi-hulls was considered, but this changes if the heading is different from $\beta = 180°$. When predicting roll motion it can be possible to consider the catamaran in total as a single-hull case, which is applicable to small hull spacing configurations, such is discussed in Bulian et al. (2008). Other formulation that is widely adopted and more versatile regarding hull spacings considers roll motion of catamarans a function of each demi-hull heave motion, with the demi-hulls rigidly connected. This formulation leads to a characteristic difference in the results, due to the phase of excitation on each demi-hull. Excitation forces are in different phases on each demi-hull and in some frequencies, heading and hull spacing the difference in phase can be 180 degrees, resulting in very low or even no-exciting forces at all. This is used in the present work when post processing the results from Fonseca motion results and it is based on strip theory explicit in 3.3, which is modified to obtain a general formulation for the case of a catamaran. Such type of implementations can found in texts like Journee and Adegeest (2003) or Faltinsen (2005).

For mass matrix referent to the twin hull ship comes that the mass is simply the double, and therefore the connecting platform mass isn't included. The inertial mass moments are computed using data like the radii of gyration, with especial attention when considering the roll motion. Since catamaran's beam

over all are substantially bigger then a single-hull ship and the masses are located further away from the catamaran centre line. In this transformation the mass moment of inertia I_{46} is not considered, regardless that for catamarans this can actually have significance, Faltinsen (2005). For the hydrodynamic coefficients they are as the mass consideration, simply the double. But when modelling rotational motions, roll and yaw some considerations have to be done. Because this dissertation refers only to heave, pitch and roll motion only the equations for those modes of motions are shown next.

$$(2M + 2A_{33})\ddot{\xi_3} + 2B_{33}\dot{\xi_3} + 2C_{33}\xi_3 + 2A_{35}\ddot{\xi_5} + 2B_{35}\dot{\xi_5} + 2C_{35}\xi_5 = F_3^{Cat} \tag{4.3}$$

$$2A_{53}\ddot{\xi_3} + 2B_{53}\dot{\xi_3} + 2C_{53}\xi_3 + (2I_{55} + 2A_{55})\ddot{\xi_5} + 2B_{55}\dot{\xi_5} + 2C_{53}\xi_5 = F_5^{Cat} \tag{4.4}$$

$$\begin{aligned}&(2A_{42} - 2Mz_g)\ddot{\xi_2} + 2B_{42}\dot{\xi_2} + \\ &(2A_{44} + 2y_T^2A_{33} + I_{44}^{Cat})\ddot{\xi_4} + (2B_{44} + 2y_T^2B_{33})\dot{\xi_4} + (2C_{44} + 2y_T^2C_{33})\xi_4 + \\ &(2A_{46} - I_{46}^{Cat})\ddot{\xi_6} + 2B_{46}\dot{\xi_6} \qquad\qquad = F_4^{Cat} + y_TF_3^{Cat}\end{aligned} \tag{4.5}$$

Regarding the roll motion it is possible to see the effect of heave coefficients in Equation 4.5, where it is added a term in the form $2y_T^2\cdot$ that multiplies by the heave added mass, damping and restoring coefficients. The terms that include ^{Cat} are calculated regarding catamaran specific case, inertia and exciting forces that are discussed next. For the excitation forces and moments other consideration has to be modelled. Considering each one of the demi-hulls separately, starboard and port side, the exciting forces have the same absolute value. However since the demi-hulls are apart of a distance S and with other values of β than $180°$, the phase experienced by each demi-hull will differ. Therefore the excitation forces have to be added considering the phase angles. Based on a local referential system it is possible to write the incident wave potential, Equation 3.30, felt by one demi-hull at the time with origin in $y' = (0, \pm y_T, 0)$.

$$\Phi_w = \frac{ig\zeta_a}{\omega}e^{kz}e^{-ik(x\cos\beta \pm y'\sin\beta)}(\cos(ky_T sin(\beta)) - i\sin(ky_T\sin(\beta))) \tag{4.6}$$

Equation 4.6 can be considered for the port side demi-hull with a different signal since the local origin is placed on the other side of the ship's referential system. Adding both starboard and port side in excitation forces equations leads to Equations 4.7, 4.8 and 4.9 for heave, pitch and roll modes of motion. For roll motion case the total moment is the sum of both local roll excitations forces felt by each demi-hull and the moment created by the heave excitation force of each demi-hull.

$$F_3^{Cat}e^{i\omega_e t} = 2F_3^E\cos(ky_T\sin\beta)e^{i\omega_e t} \tag{4.7}$$

$$F_5^{Cat}e^{i\omega_e t} = 2F_5^E\cos(ky_T\sin\beta)e^{i\omega_e t} \tag{4.8}$$

$$F_4^{Cat}e^{i\omega_e t} = [2(F_4^E\cos(ky_T\sin\beta - iy_TF_3^E\sin(ky_T\sin\beta))]e^{i\omega_e t} \tag{4.9}$$

4.2 Two dimensional hull interaction using strip theory

Other way to consider interaction between the demi-hulls of a catamaran is accomplished at the computation stage of added mass and damping coefficients. This is the case of Centeno et al. (2000) work, where the radiated waves from one demi-hull interfere with the other hull and vis-versa. The way this is accomplished is by creating the symmetry of catamaran in the input file and computing the side-by-side hulls hydrodynamic coefficients using Frank's close fit. Because the demi-hulls are placed at y_T distance from the symmetry plan-xz, the solutions for sources placed around the surface have effects of the symmetric result. When including this in a strip theory method, the calculation of coefficients dictates that the radiation problem from one strip affects only the corresponding strip on the other demi-hull. Therefore it is considered a two-dimensional interaction scheme, just like the strip theory method that does not include effects from strip located forward of the one being calculated. Results of this method were studied by Ohkusu (1970) and Wang and Wahab (1971) with an analytical solutions, and for the case of a stopped catamaran the hydrodynamic coefficients are computed with high precision compared to experimental results.

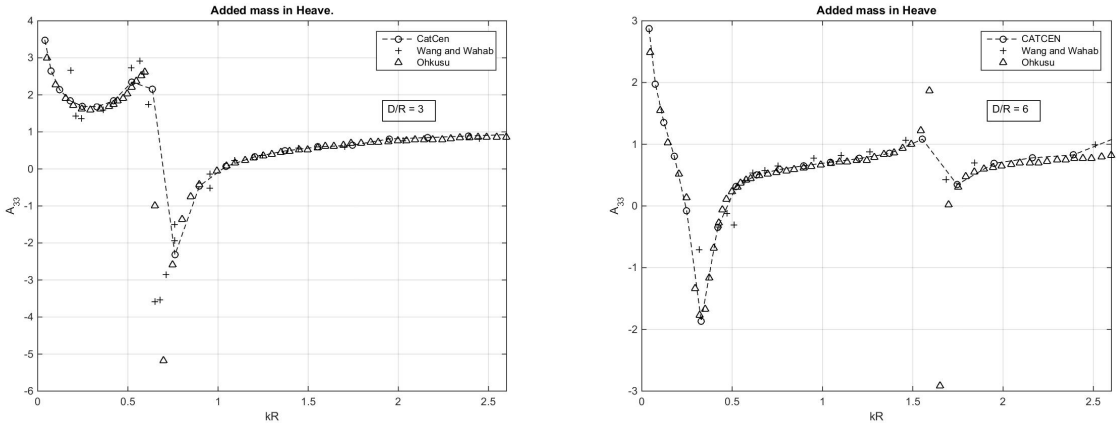

Figure 4.3: Added mass of twin cylinders in Heave motion.

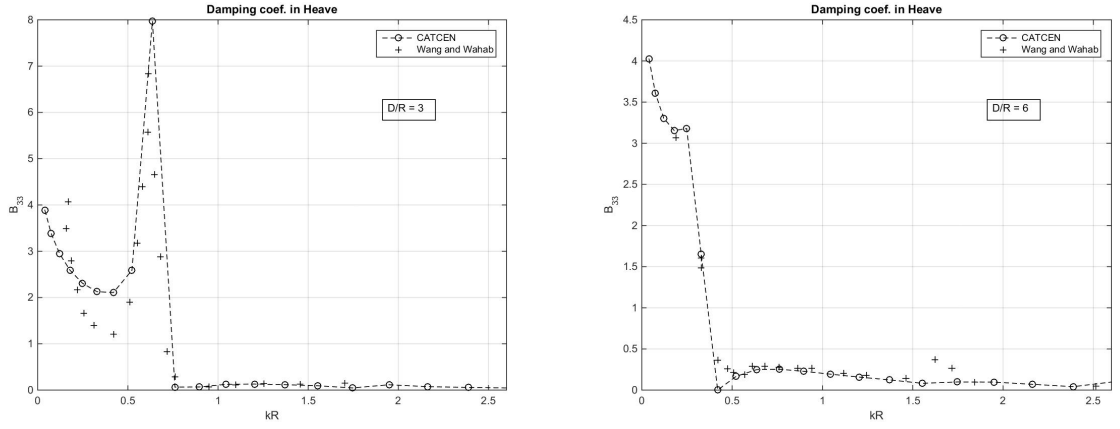

Figure 4.4: Damping coefficient of twin cylinders in Heave motion.

In Figures 4.3 and 4.4, added mass and damping coefficients calculated using CatCenteno and compared with results from Ohkusu (1970) and Wang and Wahab (1971). Two configurations of hull spacing are used, $D/R = 3$ and $D/R = 6$, where D is in this case the distance between centre lines of the cylinders and R their radius under water. The length of experimented cylinders is $L = 2.29m$ and the volume of a demi-hull $\nabla = 83.54m^3$. The non-dimensional coefficients, A_{jk} and B_{jk}, are obtained by dividing the added mass by the twin cylinders mass, $L\rho\pi R^2$, and the damping coefficient by the mass times incident wave frequency, $L\rho\pi R^2\omega$. Results that are interesting in this interaction scheme, implemented in CatCenteno, are the modelling of resonance frequencies caused by the standing wave between the demi-hulls. This will depend on the space between cylinders and are shown in the added mass curves. The negative values obtained for the added mass are very characteristic of this interaction, representing very well the location in frequency where the standing-wave phenomenon happens. This standing-wave is also associated with a quick decrease of the damping coefficient showing a peak and then a close to zero value at the same frequency as the added mass abrupt change.

Considering the heave motion case, the natural frequency of the body can be calculated by Equation 4.10, for the twin cylinders case this results in the non-dimensional value $kR = 0.64$.

$$\omega_{n3} = \sqrt{\frac{\rho g A_{wl}}{2Mass}} \tag{4.10}$$

Still in Figure 4.3 showing added mass for heave curves, it is possible to observe negative values for the low frequencies which differ from hull spacing configuration. To predict the frequencies at which this happens, van't Veer and Siregar (1995) indicates a formula that calculating the natural frequency of the water column moving together with the model.

$$\omega = \sqrt{\frac{\rho g A_c}{\rho \nabla_c + A_{c33}}} \approx \sqrt{\frac{gH}{HT + \pi \frac{H}{2}^2}} \tag{4.11}$$

In Equation 4.11 the volume of water column that is between the hulls is expressed as ∇_c and the added mass can be approximated by the half mass of a cylinder with diameter H. As for the restoring coefficient it is the area between cylinders at water line level. The result, $kR_{D/R=3} = 0.72$ and $kR_{D/R=6} = 0.39$ from this approximation fits very well with the first abrupt changes in Figure 4.3. Other ways to predict this resonance peaks exist, Faltinsen (2005) shows such calculations using Molin (1999) method, which calculates the piston mode resonance based on the approach of moon pools resonance frequency. The main difference is that one considers a two-dimensional source problem, Molin, and van't Veer derives Equation 4.11 from the natural frequency of an equivalent water mass representing the standing wave.

This way to model the interaction between demi-hulls has a big limitation regarding the applicability for big Froude numbers, meaning higher forward speed. But considering low Froude numbers it can give very good results, such results are shown in a comparison using the model from Ohkusu and Takaki (1971). The model with length $L = 4m$ is subjected to experiments with head waves at a $Fn = 0.1$, being study two hull spacing configurations, $S/T = 3$ (TW1) and $S/T = 5$ (TW2). In the published work, Ohkusu and Takaki (1971) a very complete description of the data is available and therefore not totally

presented here, where the results from interaction are meaningful for this work.

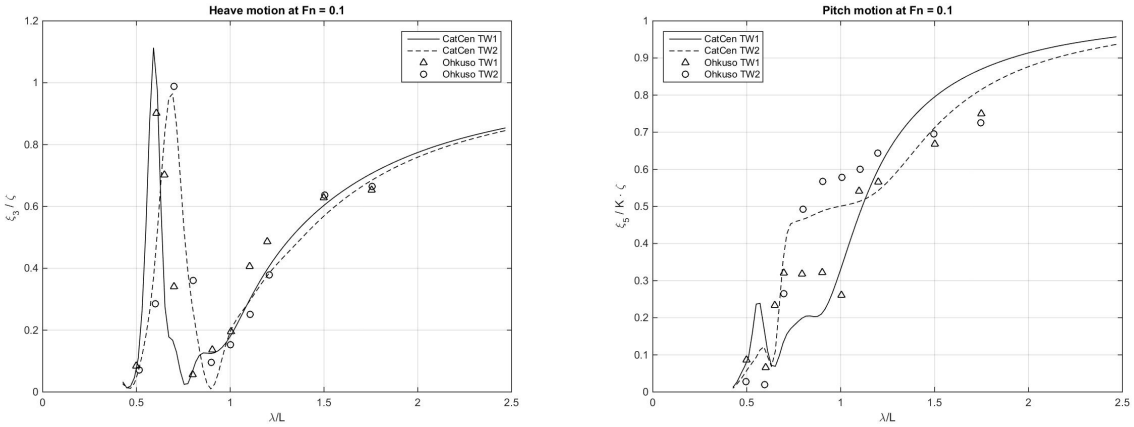

Figure 4.5: Heave and pitch responses, Ohkusu models TW1 and TW2 at $Fn = 0.1$

Figure 4.5 shows RAO results for the two cases with different spacings. The results of two-dimensional interaction scheme fits with the experimental ones, by having the peaks at same locations and with similar values. The peak on heave motion response exists due to the results expressed in previous Figures, 4.3 and 4.4. The distance between hulls, S is different for the configurations meaning different characteristic frequencies, using equation 4.11, for $TW1$ model that has the smaller distance between the demi-hulls this characteristic frequency comes at $\lambda/L = 0.5$, while for the bigger spacing configuration the frequency is lower appearing at $\lambda/L = 0.95$. The second does not agree with the peak in heave motion but the shift in frequency exists. This means that the resonance frequency is a combination of both factors, where the standing wave phenomena looses relevance with increased forward speed. Considering this, placing both the frequencies near each other creates a considerable peak in the heave motion at low Froude numbers.

Before the next results are discussed an introduction on cross-flow empirical method is done, it is included in the software used for two-dimensional interaction scheme CatCenteno. The complete formulation of the method applied to the catamaran case can be found in Centeno et al. (2000), and here only the base considerations are presented for the understanding of results further to obtain. This way to include viscous effects on the ship's motions is applicable to the case of strip theories computations and uses a set of two empirical coefficients, α_l and C_D. Accordingly with Thwaites (1960) the side force due to viscous lift and cross-flow drag on a body with length dA_p is expressed as Equation 4.12.

$$F = \frac{1}{2}\rho V dA_p \sin\alpha(\alpha_l|U\cos\alpha| + C_D|V\sin\alpha|) \tag{4.12}$$

In Equation 4.12, α is the angle of attack of the body, V is the relative fluid velocity, A_p is the projected area, α_l and C_D are the lift and drag coefficients respectively. If the body has a harmonic oscillatory motion of small amplitude like the hull of a ship with constant forward speed the expression can be

written for the j node of motion.

$$\widehat{F}_j = \frac{1}{2}\rho A_j(U^2\alpha_l\alpha_j(x) + C_D\nu_j(x)|\nu_j(x)|) \quad j = 1,2,3 \tag{4.13}$$

α_j is the angle of attack of the flow, U is the forward speed of the ship, ν_j is the relative fluid velocity with respect to the body in j node of motion, A_j is the projected area of the body in j direction. The coefficients α_l and C_D depend on the geometrical characteristics of the body, mode of motion and frequency. They are usually determined experimentally, but according to Lee and Curphey (1977) the angle α_l is about 0.07 and the drag coefficient, C_D is from 0.4 to 0.7. However in this work and for all computations regarding this method, the values are set to recommended one by Centeno et al. (2000), $\alpha_l = 0.07$ and $C_D = 0.01$. Writing the relative velocities of the water particles on each strip of the demi-hulls, it is possible to decompose the resulting equations by the terms multiplying ship's velocity and displacement for each mode of motion, $\dot{\xi_k}$ and ξ_k respectively. This leads the solution to an iterative method that seeks convergence in the result. Final equations have the following form and can be added to the 6DOF equations system, like in equations 4.14 and 4.15.

$$\widehat{F}_j = \sum_{k=2}^{6}(\widehat{B}_{jk}\dot{\xi_k} + \widehat{C}_{jk}\xi_k) - F_j^V, \quad j = 2,3,...6 \tag{4.14}$$

$$\sum_{k=1}^{6}[-\omega^2(M_{jk} + A_{jk}) + i\omega(B_{jk} + \widehat{B}_{jk}) + (C_{jk} + \widehat{C}_{jk})]\xi_k = F_j^w + F_j^d + F_j^v \tag{4.15}$$

With this method the next results show the effect of forward speed in two-dimensional interaction scheme when including of viscous effects in the motions results. The model here tested is the Wigley hull form, a mathematical description of the hull allows authors with greater possibility of repetition and therefore a more accurate way to validate results form software. The description of this hull can be found in publication van't Veer and Siregar (1995), where numerical implementation is similar CatCenteno software.

Note that the increase in forward speed will make the generated waves sweep back until the wake of the vessel. Meaning that the wave which was generated by a section of the ship will interfere with a section located more aft of the other demi-hull, as the second case in Figure 4.1 illustrates. This means that a three-dimensional approach will be more correct.

Table 4.1: Wigley single hull characteristics and catamaran configurations

Wigley single hull			WH1	WH2
$L[m]$	2.5	S/B	2.10	3.140
$B[m]$	0.357	$H[m]$	0.39	0.764
$T[m]$	0.139	$B[m]$	1.11	1.480
$\Delta[kg]$	69.5	Fn	0.3	0.45

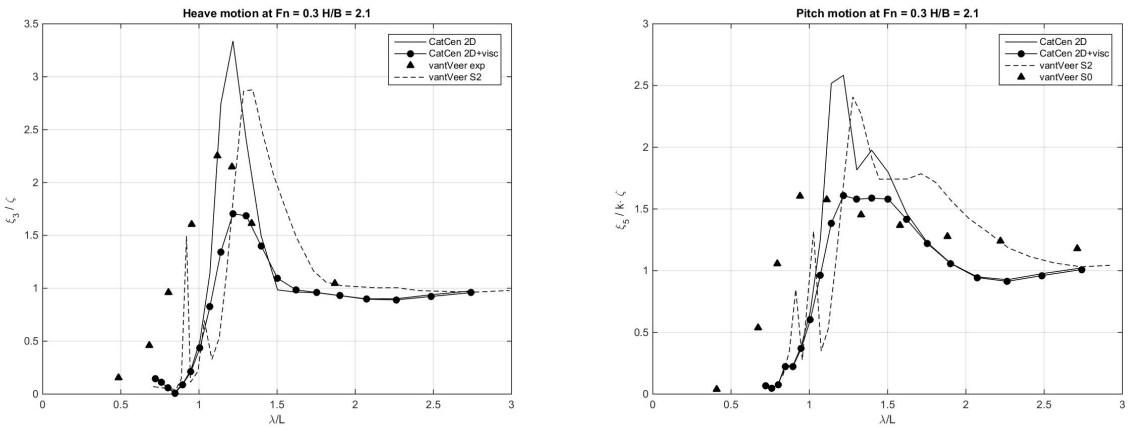

Figure 4.6: Wigley, WH1 heave (left) and pitch (right) response.

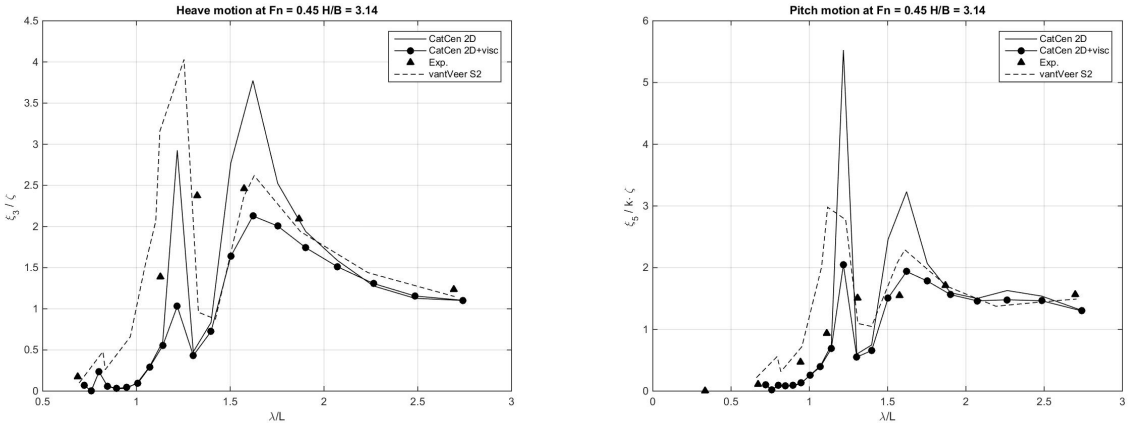

Figure 4.7: Wigley, WH2 heave (left) and pitch (right) response.

In Table 4.1, the main values of the catamaran configuration are shown and the results of RAO computations can be found in Figures 4.6 and 4.7. Results form experiments and computations from van't Veer and CatCenteno are shown, being possible to see the big impact that inclusion of viscous effects has on the results. Inclusion of this method, cross-flow, brings the overly predicted peaks due to the interaction of hulls to reasonable values as the computations indicate. This is especially the case for low Froude number, where the hull spacing is small and closer to practical values seen in actual catamarans. For WH2 the same does not apply, the response shows errors with two different peaks that do not fit in the experiments. In this case the inclusion of viscous effects is not able to improve the results. Interestingly CatCenteno results are highly similar to van't Veer computations, with the problem that may be due to the exaggerated hull spacing and possibly errors in numerical implementation. Regarding the limit of interaction by Equation 4.1, where it expresses the frequency at which it stops to occur, it can be derived in a different form. With the objective of using the frequency domain experimented, it is possible to compute the percentage of demi-hull that is subjected by radiated waves from the other demi-hull. With the frequencies ranging from $\omega 1 = 3rad/s$ the lowest and $\omega 20 = 5.85rad/s$ interaction results are expressed in Table 4.2.

$$\tau = \frac{U\omega_e}{g} = \frac{L}{H}$$
$$x_{st}/L = 1 - \tau\frac{H}{L} \tag{4.16}$$

Table 4.2: Wigley interaction

	$WH1$	$WH2$
L/H	3.33	2.23
$x_{st}/L_{\omega 1}$	83%	57%
$x_{st}/L_{\omega 20}$	59%	no interaction

In the first case represented in Figure 4.6 at the lower frequency 83% of the hulls suffer from the waves radiated by the other hull, as for the highest frequency this values lowers to 59%, adding to this higher frequencies means less impact on the motions amplitude and therefore losing relevance. Considering now the second configuration where the results are presented in Figure 4.7, it is shown that the limit of validity for two-dimensional interference is reached. Table 4.3 shows the water column natural frequency and the incident wave characteristic frequencies for both models. The Last one is calculated considering $\lambda/2 = H$ and the results are expressed as λ/L.

Once applying two-dimensional interference scheme the motions will show the same type of peaks as if the Froude number was smaller, for the same frequency intervals. To change these peaks the cross-flow method is applied. This brings down the over-prediction of ship's motion, as it can be seen from the figures modifying peak amplitudes and bringing them closer to experimental results from van't Veer and Siregar (1995). Other aspect regarding cross-flow method, is that it changed the restoring coefficients from the original strip theory and it can shift the frequency at which the resonance occurs.

Table 4.3: Wigley models frequencies.

Characteristic frequencies	$WH1$	$WH2$
$\omega_c[rad/s]$	1.13	1.86
λ/L	2.04	1.05

Chapter 5

Case studies

Experimental works have been used for validation of theories and computations on the subject, the number of these regarding the problem with catamaran is less then the amount for the single hull type of vessels, Guedes Soares et al. (1999). It is common that the experimental works are produced for the verification and validation of numerical methods, being associated with works of numerical implementations and direct comparison between results. In this work the collection of experimental works is found in the literature in the form of publish reports or articles with the objective to expand the pool of data available over the theme.

As the information included in previous works and studies is sometimes insufficient, assumptions need to be done in the scope of this work. This is a task that is preformed cautiously, matching and representing the original works whenever possible. The important data that such works should present can be found in ITTC Recommendations and Guidelines, pro (2017). International Towing Tank Conference is a voluntary association that establishes conducts for the maritime hydrodynamic performance of ships, test facilities and numerical experiments. For this case aspects like the following are of importance when data is being collected,

- Scale, model dimensions and shape.
- Ratios of model to tank dimensions which can limit the interaction of ship's waves with the basin walls.
- Hull configurations and loading conditions, which have to be scaled traducing the hull shape characteristics.
- Mass of the model characteristics, representing the location of centre of gravity and inertial radii of gyration.
- Speeds and headings, being the speed needed to be scaled properly trough the Froude number by the assumption of gravitational forces importance.
- Wave characteristics, that for the motions studies has to be scaled maintaining the linearity assumption for the results.

- Towing and restraining device characteristics affecting the degrees of freedom model and the possible errors in the results due to applied forces by the towing device.

From the above list of items that indicate important parameters to be explicit for numerical comparisons, some are in truth difficult to replicate. A common practice is to represent the model shape in the form of transversal line plans, sometimes the offset table is present in the report which is preferable. In some works the lines plan is somehow not clarifying, the representation of bow shape requires a longitudinal projection of the lines plan which is omitted in most of the cases. Even with this data available it is most likely that the impression of the document is old and/or distorted, this problems can be very significant since the study of ship motions is largely connected with the interaction of hull shape with the tank environment. The same type of issue is found in way results are expressed, for motion studies the RAO's are commonly used but this is sometimes only presented in the form of graphics. Requiring careful reading and data collection from the reader in order to minimize errors. Other important aspect is the uncertainty associated with the evaluation of the experimental results, more recent experimental studies on the motion of ships are introducing this aspect in the publish data Bouscasse et al. (2013). This is of importance for the validation studies in numerical studies, the need to understand the value of experimental data and also the error mitigation trough instruments will possibly define a more reliable result to compare.

5.1 Experimental data

For this work the experimental data collected derived from published data regarding computations for catamaran motions. In the text can be found specifications on the experimental methodologies, concise information is found in Table 5.1. About the models data Table 5.2 shows dimension relations and for their mass Table 5.3 has the needed values considering the motion studies. Hull geometry definition can be found in the literature from which the data is taken, this will be explicit when the experimental conditions are commented.

Table 5.1: Experimental set-up characteristics

Model	Local	Basin LxBxD [m]	Propulsion	Free motions	Fn range	Headings [$^\circ$]
NPL	SITT	60 x 3.7 x 1.8	Carriage	Heave and Pitch	0.2, 0.53, 0.8	180
MARINTEK	MARIN	152 x 30 x 5	Propeller	Heave, Pitch and Roll	0.49, 0.66	180, 150, 90
DELFT372	DSHL	145 x 4.2 x 2.6	Carriage	Heave and Pitch	0.3, 0.45, 0.6, 0.75	180
DELFT372	MARIN	100 x 24 x 2.5	Water jet	All	0.3, 0.6, 0.75	180, 195, 225
El Pardo	CEHIPAR	152 x 30 x 5	Carriage	Heave, Pitch and Roll	0, 0.2, 0.4, 0.6	180, 165, 150
VOSPER	HLUG	77 x 4.6 x 2.7	Carriage	Heave and Pitch	0, 0.25, 0.625, 0.75	180

Table 5.2: Model hulls characteristics

Model	S/L	L	L/B	B/T	L/∇^3	C_b	C_{wl}	$LCB\%$	$LCF\%$
NPL4b	0.20 & 0.40	1.60	9.00	2.00	7.40	0.40	0.77	-6.34	-8.24
NPL5b	0.20 & 0.40	1.60	11.00	2.00	8.50	0.40	0.77	-6.34	-8.24
NPL6b	0.20 & 0.40	2.10	13.10	2.00	9.50	0.40	0.77	-6.34	-8.23
MARINTEK	0.20	3.78	14.15	1.33	7.49	0.50	0.81	-6.34	-8.57
DELFT 372	0.23	3.00	12.50	1.60	8.53	0.40	0.76	-2.70	-8.56
El Pardo	0.20	4.30	15.93	1.93	9.60	0.55	0.78	-7.86	-9.04
VOSPER	0.20 & 0.29	2.05	12.98	1.86	7.65	0.70	0.87	-10.14	-5.87

Table 5.3: Model mass.

Model	$\Delta[kg]$	$LCG(AP)[m]$	$KG[m]$	$r_x[m]$	$r_y[m]$	$r_z[m]$
NPL4b	20.22	0.70	0.13	...	0.40	0.40
NPL5b	13.34	0.70	0.11	...	0.40	0.40
NPL6b	21.60	0.96	0.12	...	0.53	0.53
MARINTEK	203.00	1.65	0.35	0.38	1.03	1.09
DELFT 372 (HW)	87.07	1.41	0.34	0.53	0.78	0.75
DELFT 372 (OW)	87.07	1.41	0.28	0.39	0.81	0.93
El Pardo	184.10	1.85	0.37	0.50	1.15	1.15
VOSPER	39.46	0.83	0.06	...	0.51	0.52

MARINTEK (1992) and Hermundstad(1999): In the sequence of a new numerical strip wise method to calculate motions of fast displacement vessels, Faltinsen and Zhao (1991) a experimental work, is published in order to validate the global loads on the case of catamarans. Using this 2.5D theory other work is published, Faltinsen et al. (1992), where the motions and global loads of a model are tested in the Ocean Environment Laboratory of MARINTEK. The model was subjected to regular wave system with incident angles of 90 and 45 degrees, studying the most severe conditions for the global loads on the connecting deck of a catamaran. The model was self propelled set with an auto-pilot system to keep the relative heading to the waves. The system used had a significant signal lag time, used for the control system, which traduced in a variation of the heading thought run time. Regarding the motion results heave, pitch and roll motions are presented in RAO graphics, lacking some refinement in the resonance peak. On the same Laboratory, MARINTEK, a variance of the previous model was extensively tested by Hermundstad (1995), the variations included a tunnel stern for accommodation of the propeller and shaft on each demi-hull and the spacing S was different. The same type of automation in the control of model speed and direction was used. As for the tests conditions, they were made for still water condition, regular waves and transient. For the present work the accessible publication, Hermundstad et al. (1999) includes experimental results of four regular wave conditions. Combination of two Froude numbers, $Fn = 0.49$ and $Fn = 0.66$ and three directions, $\beta = 180, 150, 90$ degrees, with frequencies well scattered around the natural frequencies generated a very good set of results in the form of RAO's for heave pitch and roll. Linearity in the results is assumed by having the $2\zeta/\lambda$ between 0.0067 and 0.02 for

long waves and 0.02 and 0.03 for shorter waves.

NPL round bilge series (1995): A report of experiments with NPL round bilge series, Wellicome et al. (1995) describes the seakeeping properties of catamarans for three geometrical similar hull forms. This work is the continuation on studies of NPL series hull forms, that started with calm water resistance tests. It is referred that the importance of hull forms saekeeping abilities, since nowadays operation speeds have increased. The tests were performed in the Southampton Institute test tank (SITT). The program related the longitudinal degrees of freedom of catamaran and single hull cases. Test were for head waves systems with incident wave angle of 180 degrees. Froude numbers were set between 0.2 and 0.8, with encounter frequencies ranging from 6 to 16 rad/s. Although it is not presented as data in the report there is a brief consideration on the wave height, stating that it had some degree of variation with frequency. The measured quantities are the model motions, the root mean square (RMS) accelerations and motions as it is used for irregular waves criteria in design. The added resistance due to waves is also measured and since information in previous works was available for calm water tests these last were not performed. Three hull forms are used, 4b, 5b and 6b. These models have symmetrical round bilges and include wet transom sterns, representing under water forms of catamarans in service or under construction at the time. They were also fitted with turbulent flow stimulator at the bow in form of strip studs. The towing point was placed at the location of centre gravity, longitudinal and vertical, the last was fixed as relation to draught of each model, 1.5 draught above base line. Due to the weight displacement balance of the model 6b this had a bigger length dimension then the others. The hull forms in the report are presented in transversal lines plans lacking the bow definition, which is defined by a single point intersecting the water line. Other data like dimensions and mass characteristics are present in the form of tables. The results obtained by the experimental work is presented in the form of graphics which were handled with extreme caution for data acquisition.

DELFT372 (1998): In the sequence of studies for PhD thesis of Mr. Riaan van't Veer, Van't Veer (1998a), the author performed a series of tests to a catamaran hull form designed in DELFT University of Technology for the purpose. Two different tests are preformed in distinct towing tank facilities, the initial one was performed in Delft Ship Hydrodynamic Laboratory (DSHl) considering only head waves, and the second one in Seakeeping basin at MARIN (Maritime Research Institute in Wageningen, The Netherlands), with three different headings, Van't Veer (1998b) and Van't Veer (1998c). The main purposes of the tests were to evaluate the resistance measurements including trim and sinkage, steady wave pattern, heave and pitch motions in head waves with free motion results and forces oscillations test in order to evaluate the hydrodynamic coefficients and finally wave forces measurements. The second report for the same project aimed for the measurement of resistance including trim, sinkage and motions tests in regular waves with oblique headings. The design of this model followed the ratios of overall dimensions on common practice for catamaran designs, lacking only the effective submerge transom stern. This feature was not totally possible to execute due to the need of installing a water jet propulsion system later on the second report. Due to the different experimental set-ups, the mass characteristics of the models are different. Because the oblique wave tests were performed with the model loaded with all the instruments for data acquisition. In both of the reports hull geometry is well defined

in the form of geometric plan and also with the offset table of the hull. Results are expressed either in tabular form and in graphic form which facilitates the collection of data.

P2 El Pardo (1999): Other used publication for the study of catamaran motions computations is experimental work referent to Guedes Soares et al. (1999). The work produced by the authors focused on the heave, pitch and roll motions of a model catamaran produced for the experiments. The motion results considered the effect of headings and speed of the model and some derived responses were calculated, such as vertical accelerations and mean added resistance in waves. The tests were executed in the Laboratory of ship Dynamics of El Pardo Model Basin (CEHIPAR) in Madrid. A complete description of the test facilities is found in the published document, indicating the type of wave making system and procedures in the reception of instrumentation signals. The tests focused on the linear responses of the model using waves with characteristics of small wave sloop, $k\zeta_a$. Value that varied from 0.06 for short waves and 0.01 for long waves. The speed range of Froude numbers is between 0 and 0.6 being the variation of heading studied for the design speed which meets Froude number equal to 0.4. The model used was build in FRP (fibre reinforced plastic) to a scale of 1:10, it is a wave piercing type that was experimented with a third bow placed in front. When impact loads were found in the appendage tests are repeated without it. The mass inertias were adjusted for the values on Table 5.3. The motions of catamaran model were measured by a non-contact optical tracking system, the incoming wave hight was measured by a capacitive wave probe placed forward of the model and two load cell at the towing bar in order to acquire added resistance values. The experimental results represented as RAO, regarding heave, shown resonance peak at a non-dimensional frequency of $\omega\sqrt{L/g} = 2.5$, corresponding to $\lambda/L = 1$. For pitch this is seen at a $\lambda/L = 1.4$. Both responses tend to decrease with the increasing angle of incident wave. The numerical model of the hull was available for the work. Not being possible to model the entire bow shape of the model due to the numerical implementation of one code, CatCenteno, the bow is altered to a single point intersecting the water line. As the hull shape the motions results were available in numerical form.

VOSPER (2001): Connected with the validation of CatCenteno code is an experimental work studying the influence of hull spacing on catamarans, Centeno et al. (2001). The experiments were performed at the Hydrodynamic Laboratory at the University of Glasgow (HLUG) with the purpose of study heave and pitch for two different spacings between the catamaran demi-hulls. The experimental program consisted in the study of heave and pitch motions with incident wave angle of 180 degrees and a range of Froude number between 0 and 0.75. The model used in this work had the hull form of VOSPER international, Incecik et al. (1991), with different draft and hull spacing. The catamaran was designed as a passenger platform with a ship's length target of $L = 43.5$ meters. The hulls are set with two different spacings, 40 and 60 centimetres between the demi-hulls centre line, corresponding to the abbreviation V40 and V60 respectively. Important characteristics o the demi-hull shape is the hard shine and wet transom stern. The numerical model of the demi-hull shape and the needed values for the mass inertial values were available in the form of input for the code CatCenteno. Being later scaled and treated for other software used in this work.

5.2 Software used

Regarding the numerical computations, three different available software are used. Availability was given to the author of this work and their characteristics are connected with the objective of increasing the understanding on interaction effects. The main characteristics of each software is presented in table 5.4.

Table 5.4: General specifications of the software.

Acronym:	Fonseca	CatCenteno	Wasim
Reference:	Fonseca and Guedes Soares (1998)	Centeno et al. (2000)	Kring (1994)
Method:	Strip Theory	Strip Theory	Rankine panel method
Domain:	Frequency	Frequency	Time & Fourier
Linearity:	Linear	Linear	Linear & Non-linear
Transom terms:	No	Yes	Kutta conditions
Multi-hull:	No	Two-dimensional	Three-dimensional
User-face:	Input file	Input file	Graphical, command line

Fonseca: A frequency domain strip theory code which is the linear version of the time-domain software presented in Fonseca and Guedes Soares (1998), is used to perform computations for the base case. The transformation to catamaran case is done by computing the demi-hull motions as a single hull case and then post-processing the results to represent the catamaran motions, implying no interaction between the demi-hulls. The software, Fonseca, was provided by the department CENTEC University of Lisbon. It's calculations are based on the strip theory from Salvesen et al. (1970). To acquire the two-dimensional sectional added masses, damping coefficients and diffractions forces the Frank's close fit method is applied. This linear version is not published and validated as the non-linear version from Fonseca and Guedes Soares (1998), but it has been widely used in intern computational works and lectures. Post-processing of results from this code include the transformation from single hull motion results to catamaran, modifying the hydrodynamic coefficients and solving the equation of motion. Other computation done is the inclusion of end-terms, this is possible since there are two-dimensional sectional outputs with damping and added mass coefficients together with sectional diffraction forces. The equations and considerations are present in the Chapter 4.

CatCenteno: A step in the interaction scheme is done by including computations of motions using a two-dimensional interaction scheme. Centeno et al. (2000) have developed a software that is based on strip theory method. The work aimed for motions computations on catamaran vessels. On top of the interaction feature the author included cross-flow method in order to account for viscous effects. The software uses Frank's close fit to calculate the hydrodynamic coefficients. The interaction method is coded in a way that the diffraction problem of one demi-hull affects the other demi-hull directly on the same longitudinal coordinate. To do so, one of the demi-hulls is created in the input file with the central axis away from the central line of the catamaran. With sectional shapes along the length of the ship, hydrodynamic coefficients and exciting forces are calculated and then integrated using the strip theory of Salvesen et al. (1970). The inclusion of the cross flow method in the computations leads to an iterative

process that seeks convergence in the motion response, this method as a very good applicability in the SWATH type of ships and here is applied to the catamaran type, Lee et al. (1973).

Wasim: In the effort of including a fully three-dimensional interaction study for catamarans, a state-of-the-art method is used. WASIM software is already used in classification societies as an everyday motions computations tool in a very wide range of cases, Nestegard et al. (2008). This software is originated from a cooperation between DNV and MIT starting in beginning of the 90's, its basic implementation had two stages of evolution, SWAN1 and SWAN2. From its beginning the software was applied to practical applications in the new-building activities. Nowadays it is included in a package provided by DNV-GL called HydroD - SESAM. Within this, analysis can be done for either stationary floating structures or with forward speed. For the case of this work only the Wasim package was used, Veritas (2011). Based on potential flow theory the program uses a three-dimensional Rankine panel method creating a fully three-dimensional solution. The panels are located in the hull surface and the ship's surrounding free surface, generated by an included program for the purpose. The specifications of theory and numerical implementations schemes are well described in the reference, Kring et al. (1997). In this work the reader is guided to several other important publications about the specifications of used methods. Being important for the comparison the main features of WASIM are briefly described.

The solution of equations is done in the time domain, being needed to post process the results using a fast Fourier transform to build the RAO's. The radiation to infinite condition is satisfied by a numerical beach on the free surface. The beach has the ability to treat the zero speed case and the critical frequency problem ($\tau = 0.25$), when the radiated wave travels at the same speed as the ship). The panel method implies the use of Boundary Element Method (BEM), and WASIM has the peculiarity of using B-splines for the velocity potentials which satisfy the continuity of value and first derivative across panels. Other feature of the program is to enforce the continuity of velocity potentials and free surface elevation across grid patches on the free surface. The program requires a stability caution when preparing the simulation. This is dependent in terms of ship speed, ship's length, panel size, aspect ratio of the panels and time-step size. Because of the last the time required for the computations is affected strongly. The information that allows this subject to be correctly modelled is found in Veritas (2011). The hull shapes can be introduced in the program either in the form of structural elements (.FEM) or simply by sections description (.PLN). The last was enough for the study necessities, providing a good correlation to the strip theory methods. The mass model, as it is called in the program, is introduced using the user system of coordinates which are defined in the shape input file. With the difference that for the inertias input uses the radii of gyration.

Because the user interface of Wasim, the ability to implement a sequential computation for all the models was not attempted, even that it may be possible to do using the command line. For the case of strip theory based software this was accomplished, mainly because it only uses input files in the form of .DAT. The total time to compute all the cases considered with Fonseca and CatCenteno was significantly smaller than the time needed to perform the same with Wasim.

Table 5.5: Programs limitations in hull shape definition.

Acronym	Input type	Number of sections	Points number per section	Longitudinal coordinates	Stems definition
Fonseca	sectional points	40	20	Yes	Bow & Stern
CatCenteno	sectional points	40	20	No	Bow
Wasim	sectional patches + FEM	200	200	Yes	Curves

From the above Table 5.5, there are two differences that had an important influence in modelling of hulls geometries. Both of the strip theory codes require that the bow is modelled by a single point, intersection between the bow stem and mean water line. This limits the type of hull forms possible to include in the calculations, specially if the bow is of a not conventional form, as bulbous or wave piercing. Fonseca code requires the longitudinal location of the sections, and both the bow and stern have to be defined with a singular point. Because longitudinal position of sections can be defined the previous problem, when modelling the bow shape, can be improved. For the case of CatCenteno the sectional description of the models starts with a single point at the bow. From this point the code will split the ship's length in constant spaced sections. The number of sections has to be the number of shaped sections plus one for the bow point. Which does not allow a very precise hull form definition. This problem was found for El Pardo catamaran, it's wave piercing bow was not modelled in any of the three programs. Differently, Wasim allows the user to create a curve that defines the stems shapes and therefore it allows such types of bows and others. In this software the sections are introduced in sequences that generates patches representing the hull surface. Because of this the types of hull forms possible to create are incredibility big, from SWATH to Trimarans and others. For the Wasim three-dimensional panel method the geometry definition had firstly considered the stability issue. Because it is in time domain, time step has to be defined and for the case of high speed cases this is strongly defined by the stability of integration methods. Keeping the solve process stable for this cases means that the time step used is already small enough and therefore accuracy of solution is obtained. Stability is connected with the panel size and Froude number at which the ship is sailing defining the minimum time step to be used. In result of this the grid definition lengthwise has a high impact in the computation time. In Veritas (2011) a complete description regarding this topic can be found.

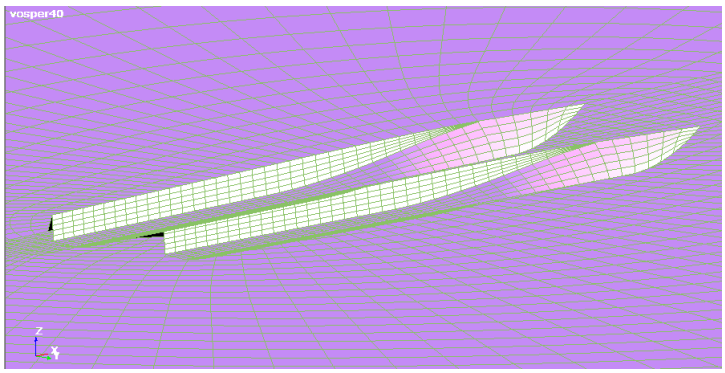

Figure 5.1: Example of Wasim panels, VOSPER V40.

A brief study on the grid convergence was done in order to better understand the possible results and implications of grid differences. The main objectives are to have convergence in the results, keep the time of computations acceptable and finally have some degree of correlation to the strip methods software used by the geometry definition. Using DELFT 372 model scaled to 30 meters in length, the number of longitudinal panels is set to 30. With such number of panels the time step at the highest Froude number, $Fn = 0.75$, has to be set in $t_{step} = 0.02s$. In terms of transversal number of panels the influence in computational time is not so significant, setting a base case of 10 panels in each side of the demi-hull. With this base case the time of computation, for 10 frequencies is of $t_{comp.} = 750s$, at the highest Froude number. If the number of panels lengthwise is increased to 40, 1.3 times more, the results take 3.73 times more to be obtained, this with an increase of 3% in precision on the results. The increase of time due to the grid refinement are significantly more then the gain in precision, at least for lengthwise refinement. For the transversal number of panels the values in table 5.6 where used, noting that Fonseca and Wasim inputs only define half of the demi-hull, CatCenteno on the other hand defines points all around the sections of one demi-hull.

Table 5.6: Hull geometry discretization used.

Acronym	Number of sections	Number of Points per section	End terms
Fonseca	40	16	Yes & No
CatCenteno	39	18	Yes
Wasim (Panels)	30 to 40	12	Kutta Condition

Chapter 6

RAO computations

In this Chapter the computational results which are plotted in the form of RAO's (Appendix: A) are discussed. Response Amplitude Operators are displayed in non-dimensional form, and due to the objective of study catamaran motions with a large amount of computations phase angles are not displayed. Non-dimensional axis for displacement movements such as heave, are obtained by dividing the amplitude of motion by the wave amplitude in the vertical direction. Rotational motions such as pitch and roll are further divided by the wave number $k = \omega^2/g$, witch times the wave amplitude give the wave slope $k\zeta$. Frequencies can either be non-dimensional when in the form of wave length ratio over the ship's length, λ/L, or by the ITTC recommendation ,$\omega\sqrt{L/g}$, which is the one used in this work. The first one is common practice when presenting longitudinal motions for head waves, since it better gives an idea of what it should look like in such conditions. In the above case the considered wave frequency is the incident wave frequency and not the encounter.

The computations follow experimental works commented in Chapter 5.1. In an experimental environment ships have reduced dimensions for practicality. The case for numerical computations is somehow different, it is possible to scale the models to the target dimensions of the catamarans. This improves computational precision by reducing numerical errors provident from truncation. The Table 6.1 shows final scaled dimensions of the models and their main characteristics and in Table 6.2 the scaled values for the mass. Considerations for scaling are either related with direct information from the publication stating the design length target, or from the common size found in fast semi-displacement catamarans discussed in Faltinsen (2005), stating that their length are typically between 30 and 40 meters. With this in mind when a 1:10 scaled catamaran model was not within the target length, the scale was changed to meet the length between perpendiculars of 40 meters. The case is found for the NLP round bilge series that were tested with relatively small models of 1.6 and 2.1 meters long.

Table 6.1: Scaled ship hulls dimensions.

Ship	Scale	$L[m]$	$T[m]$	$B_{dh}[m]$	$S[m]$	$\nabla[m^3]$
NPL4b	1:25	40.00	2.222	4.444	8 & 16	315.875
NPL5b	1:25	40.00	2.222	3.636	8 & 16	208.427
NPL6b	1:19	40.00	1.527	3.053	8 & 16	149.293
MARINTEK	1:10	37.78	2.012	2.670	7.530	203.000
DELFT 372	1:10	30.00	1.500	2.400	7.000	87.070
El Pardo	1:10	43.00	1.354	2.700	8.600	179.600
VOSPER	1:20	41.00	1.700	3.160	6 & 12	308.000

Table 6.2: Scaled ship mass characteristics.

Ship	Scale	$\Delta[kg]$	$LCG[m]$	$KG[m]$	$GM_t[m]$	$r_x[m]$	$r_y[m]$	$r_z[m]$
NPL4b	1:25	323772	17.44	3.33	...	...	10.00	10.00
NPL5b	1:25	213637	17.44	2.73	...	...	10.00	10.00
NPL6b	1:19	153025	17.44	2.29	...	...	10.00	10.00
MARINTEK	1:10	203000	16.50	3.52	8.35	3.80	10.30	10.90
DELFT372 (HW)	1:10	87070	14.10	3.40	...	...	7.82	7.46
DELFT372 (OW)	1:10	87070	14.10	2.78	14.10	3.89	8.10	9.64
El Pardo	1:10	184100	18.50	3.71	16.23	5.01	11.48	11.48
VOSPER	1:20	315700	16.36	1.10	...	...	10.88	10.44

The results are divided in longitudinal modes of motion, the larger amount of computations, and later the transversal roll mode of motion. For each model and condition there is a figure in Appendix A comparing all the collected results from the methods. In Table 6.3 it is shown the values of natural encounter frequencies and results from two different formulations for the piston mode resonance frequency in heave, van't Veer and Siregar (1995) and Molin (1999). In Appendix B tables with the values computed for Root Mean Squared Error (RMSE) are shown. The values of interaction are calculated using the resonance frequency for heave motion in Equation 4.16. They are expressed in Int coefficient, that represents the length that one demi-hull is subjected to the radiated waves from the symmetric demi-hull. The difference in natural frequency between heave and pitch are relatively small and computation of interaction coefficient for both is unnecessary.

Table 6.3: Natural and heave piston resonance frequencies.

Non-dimensional values, $\omega_e\sqrt{L/g}$					
	Natural Frequencies			Piston mode	
Ship	Heave	Pitch	Roll	Molin	van't Veer
NPL 4b $S/L = 0.2$	4.17	4.07	...	1.06	2.26
NPL 4b $S/L = 0.4$	4.17	4.07	...	1.01	1.40
NPL 5b $S/L = 0.2$	4.63	4.52	...	1.44	2.15
NPL 5b $S/L = 0.4$	4.63	4.52	...	1.37	1.37
NPL 6b $S/L = 0.2$	5.02	4.90	...	1.88	2.07
NPL 6b $S/L = 0.4$	5.02	4.90	...	1.78	1.35
MARINTEK	3.90	3.59	3.94	1.53	1.98
DELFT 372 (HW)	4.35	4.07	...	1.91	1.85
DELFT 372 (OW)	4.35	3.93	3.97	1.91	1.85
El Pardo	4.65	4.28	4.05	2.32	0.95
VOSPER V60	3.88	3.79	...	1.64	1.62
VOSPER V60	3.88	3.79	...	1.69	2.10

6.1 Heave and Pitch results

The only computations that do not include wet transom effects is with the base case of no interaction, Fonseca. The inclusion of end-terms is as written in Chapter 3.3.1. For the other interaction schemes the use of either end-terms, for CatCenteno or kutta condition for Wasim is present in all the computations. Speed interval of experimental works range from 0 to 0.8 Froude number. The majority of experimented wave directions are head and bow waves, ranging from $\beta = 180^\circ$ to $\beta = 150^\circ$, some cases are found with $\beta = 90$ but none with following waves. Regarding the spacing between demi-hulls, Table 6.1 shows the absolute values. Especial note for the three NPL hull forms, where two different spacings are considered, $S/L = 0.20$ and $S/L = 0.40$. As for the VOSPER these varied between $S/L = 0.20$ and $S/L = 0.29$, the other models have values around $S/L = 0.20$. The results obtained from the variable hull spacing models are interesting, especially regarding the interaction schemes implemented with the Software used. Apart from this general tendency for different Froude numbers and headings can be reasonable found, meaning that the comments are to the methods applied and their results comparing to the experimental data available and not to the hull forms itself.

6.1.1 NPL round bilge

The first set of RAO figures included in the Appendix are results for NPL round bilge series tested for head waves, the three hull forms and each with two spacings are shown in Appendix A.1, A.2 and A.3 for hulls 4b, 5b and 6b respectively. The general behaviour of the experimental response amplitude operator for heave motion shows that for low frequencies the results start with $\xi_3/\zeta = 1$ and as the frequency tends to higher values the response reduces to zero. This shows the consideration from

linear response type, meaning that for long waves the ship's movement follows the wave amplitude and for very high frequencies the effect of short waves has less or none impact on the ship.

For heave, at lowest Froude number tested all the three hull types and configurations show a peak near the natural frequency below the value $\xi_3/\zeta = 1$, as like the response values for all the frequency domain. With the increase of Froude number to $Fn = 0.53$ the response in heave shows that the system is under-damped near the natural frequency and therefore the peaks values are higher than 1. The values of the response increases with the Froude number and the frequency range in which this happens becomes larger. Due to the natural encounter frequency, these peaks in response appear for lower non-dimensional frequencies. The peaks show higher values near the resonance frequency, since it is predicted that the exciting forces by long crested waves are larger than for short waves. Each each one of the three models that are tested and considering the two S/L values, differences can be noticed on heave peak values. This due to the hulls configurations and also connected with the forward speed. Generally the amplitude values at heave response peaks show bigger values when S/L is smaller. However such differences are less pronounced as the Froude number increases. For the two cases, NPL5b and NPL6b that includes tests for both spacings at $Fn = 0.8$, the response amplitude near the resonance frequency is of the same magnitude. As for the case of NPL4b the highest Froude number was not tested for configuration $S/L = 0.20$. Pitch amplitude resulting curves show similar tendency for high frequencies going to zero. As for the low frequencies it is possible to note that the domain does not allow to show results with $\xi_5/k\zeta = 1$, which for higher Froude numbers will be more noticeable. For low Froude numbers, $Fn = 0.2$, the pitch response curves show similar behaviour between the three types of hulls tested. Local humps can be found around natural frequencies. For $Fn = 0.53$ the curves start to show very well defined peak values that can reach relatively high numbers, $\xi_5/k\zeta = 1.45$ for NPL5b with $S/L = 0.20$. It is verified in those curves an additional hump that can be due to interaction between the hulls, this at a higher frequency than the natural. At maximum Froude number tested, $Fn = 0.80$, the responses show a wide range of frequencies in which the amplitude is above one. For pitch motion non-linearities at high speeds can be very important and may present in the experimental results. With $Fn = 0.53$ pitch response amplitude shows different values for the two hull spacing tested, following the same tendency as for the heave motion lowering the values for wider configurations. The higher frequency humps are shown for high speeds, however they tend to disappear for $S/L = 0.4$. Such example of this is both NPL5b and NPL6b at $Fn = 0.8$.

For all the range of Froude numbers Wasim gives very good fit of the experimental data. If the spacing is increased to $S/L = 0.40$ the computations using Wasim give over prediction of the peak for higher Froude numbers, 0.53 and 0.8. However, curve tendency and location of the peak at natural frequency are very well in agreement with experimental data. The first observation of CatCenteno results can be done regarding the curves tendency for higher hull spacings, where RAO curves show similar problems as van't Veer and Siregar (1995), having exaggerated peaks and discontinuities with very low response values. This is characteristic of the interaction scheme adopted regarding added mass and damping coefficients curves discontinuities, showing large damping near the frequency at which there is a discontinuity in the added mass curve. This is discussed and shown for twin cylinders in Chapter

4.2. Regarding the code, it is believed that the software is still not robust enough and implementation errors my be part of the cause of such results. At low Froude numbers the interaction scheme applied in CatCenteno has good results and the inclusion of viscous effects does not show an improvement in response values. When combination of low hull spacing with $Fn = 0.53$, CatCenteno gives over prediction on resonance frequency. In these cases the inclusion of viscous effects by the cross-flow method improves the results, giving values in agreement with experimental results. An example of this improvement is NPL5b hull, with Froude number 0.53 and spacing $S/L = 0.2$. Generally the results from Fonseca show well behavioured curves with continuity and smooth transitions in the peaks. The results from this computations show that for low Froude numbers the interaction between hulls has to be taken in account, since the peak at natural frequency is smaller than the experimental results. Mainly considering heave motion, the results using Fonseca, are very good for higher Froude numbers and for bigger spacings between hulls when including end-terms. For pitch motion the end-terms brings response values below the experimental for smaller frequencies. These are direct consequences of the interaction limit of catamarans demi-hulls and effect of end-terms in pitch motion. In the methods that account for interaction the response peak show better location then when using the no-interaction computations by Fonseca code.

6.1.2 MARINTEK

In Appendix A.4, the RAO computations for MARINTEK model are compared with experimental results, the figures show that experimental frequency domains tested are too high, this means that the results are in most of the cases close or equal to zero. The reasons experiments were done for are the comparison of cross-deck loads and not only focused in motions responses. Even with the experimented frequency domain it is possible to find a general tendency of heave response curves, starting near $\xi_3/\zeta = 1$ for low frequencies and tending to zero at high frequencies. The Froude numbers tested are relatively high, 0.46 and 0.66, meaning that peaks are present near the resonance frequencies.

Between the two speeds and for head waves it is possible to observe in the experimental curves an increase in the response value near the resonance frequency. $\xi_3/\zeta = 1.4$ for $Fn = 0.49$ and $\xi_3/\zeta = 1.5$ for $Fn = 0.66$, this with a change from 0.62 to 0.49 on interaction. For the fastest speed it was experimented other heading, $\beta = 150°$. The result for heave response is very similar but shows a wider peak. As for the 90° angle, the heave response shows a frequency where the ship's motion is very low, $\omega\sqrt{L/g} \approx 3.8$. All the pitch responses for this model show that for the smaller frequencies tested the amplitude, $\xi_5/k\zeta$ is above 1. For the higher Froude number tested it is possible to observe a hump in the response curve around $\omega\sqrt{L/g} \approx 2$, in both headings.

Due to the very high frequencies considered it is expected that RMSE metric is influenced by the small values of responses. Observing table B.4, CatCenteno with viscous effects shows the best performance for the head waves. If the heading is different then 180° , Fonseca with end-terms and Wasim give good predictions too, with RMSE around 0.15 at 90 degree heading; and $RMSE = 0.28, 0.28$ (heave and pitch respectively) at 150 degrees heading. For all the Froude numbers tested over predic-

tion can be found for all codes. Improvements by using end-terms and cross-flow for inclusion of viscous effects are significant since the range of speed is relevantly above the assumed limit of strip theories, $Fn = 0.45$. For beam waves there is an interesting result where Fonseca and Wasim show the best results and predict very well the low response value at the high frequency.

6.1.3 Delft 372

Two different mass models were used for the calculations, one used only for head waves motion study and the other that included oblique wave directions, $\beta = 195, 225°$. The second case also includes the head wave direction but since the mass and moment of inertias are different the cases are separated. The first four figures in annex, Appendix A.5 are RAO computations of the first case, being the rest of RAO figures in Appendix A.5 regarding to oblique headings cases. The general behaviour of heave response for this model at the tested conditions shows that the system is always at Froude numbers that results in under-damped type of response curves.

The peak amplitude of heave response increases with increased froward speed and the peak also becomes wider. For the second mass model some low frequencies are not included, which does not allow to understand if the maximum is actually obtained at that frequency domain. Adding to the speed, other reason why the peak shows wider is the change in heading, which is more noted by comparing the head waves case with the $\beta = 225°$. Besides a wider peak, the maximum amplitude obtained decreases. Pitch responses show the same problem regarding the frequency domain for higher speeds. In the response curves it is possible to observe the increase of resonance peak values due to the increase of forward speed, and a decrease when changing the headings.

For this model the general results of RMSE computations for the tested conditions show lower values using Wasim software. When considering the inclusionof viscous effect, CatCEnteno also has relatively low values of RMSE, however it happens mostly for the head waves cases. Values of this performance metric range from 0.07 till 0.39 on which the lower Froude numbers are better predicted than computations at higher Froude numbers. Big influence on the oblique heading where the predictions for all the codes decrease their precision.

Results from Wasim fit very well with the tendency and amplitude of motions for the set of Froude numbers, from 0.3 till 0.75. For the first mass model, head waves, it is seen that the situation of higher S/L relation and consequent over predictions in heave does not appear. CatCenteno when including the viscous effects have very similar results in heave, since the Froude numbers that the model is subjected to are high, bigger than 0.3. In such computations the lack of precision in the pitch motion is noticeable starting from $Fn = 0.6$. Wasim gives the location of peaks in pitch response with better accuracy. Fonseca code do follow the same tendency and can give reasonable results in heave and pitch at high speeds, $Fn = 0.6$. By comparing results from non-interaction schemes and the experimental results it is possible to see that the interaction influence in the amplitude of peaks is present at lower Froude numbers, this more significantly for oblique headings. For the model that was subjected to oblique waves three Froude numbers were tested, 0.3, 0.6 and 0.75. The previous situation regarding head waves can

be found, with pitch response peak due to interaction not computed by Fonseca at the lower Froude number. Increasing the heading of incident waves creates lower values of amplitude of motion at the predicted frequencies. From the experimental results this feature represents a decrease from 1.65 to 1.4 (ξ_3/ζ) in heave and from 1.4 to 1 ($\xi_5/k\zeta$) in pitch motion considering the lower Froude number of 0.3. For higher Froude numbers such does not happen equally, the decrease of amplitude of motion is only evident in heave and for the biggest value of $\beta = 225°$. Other observation is that with more oblique headings Wasim gives very accurate results in terms of location and extension of the peak in motions amplitude for heave and pitch, certainly regarding the interaction that is accounted with a fully three-dimensional method. Strip theory methods locate the maximum response at slighter bigger frequencies, this is especially for the case of pitch motion.

6.1.4 El Pardo

El Pardo model experimental tests include several headings ranging from $\beta = 180°$ until $\beta = 150°$, in Appendix A.6 RAO computations are shown for this model. Considering the case of head waves the motion response for heave has an evolution from 0 to 0.6 Froude number. For the case of no forward speed the figure shows that response decays with the frequency without showing any significant peak. As the speed increases peak in heave response are computed at the natural frequencies, and when Froude number is higher than 0.4 the response is of an under-damped system. It is noticeable too that this resonance peak increases its amplitude with higher speeds, where for $Fn = 0.4$ the amplitude is $\xi_3/\zeta \approx 1$ and for $Fn = 0.6$, $\xi_3/\zeta \approx 2$. Different headings where tested for $Fn = 0.4$, and the results show a decrease in the amplitude together with a wider peak of resonance. For the pitch responses experimental results show that the response has a very high peak of resonance for Froude number of 0.4 and 0.6, with $\beta = 180°$. Regarding the second hump in pitch RAO, it appears for head waves with $Fn = 0.6$ and for $Fn = 0.2$. For $Fn = 0.4$ it is possible that the refinement in frequency is not fine enough to show such behaviour. By changing the heading, results in pitch show a decrease of the amplitude at resonance peaks.

Comparing the software used in the computations it is possible to observe that Wasim shows very good fit in the tendency of RAO curves. CatCenteno predicts very well the peak amplitude in heave response when including the viscous effects at high speed, $Fn = 0.6$ and without it at low speed $Fn = 0.2$. As for pitch responses the inclusion of interaction effects gives better results. The range of Froude number that this model was subjected to does not have so high values as in the previous cases. With this, results show that strip theories can follow the experimental values and the inclusion of improvements on the codes, end-terms and cross-flow, do not show exaggerated differences in heave motion, matching good with the experimental data. However in pitch the end-terms have exaggerated effect and gives worst results.

6.1.5 VOSPER

The final model used for computations of motions is VOSPER catamaran, shown in Appendix A.7. This model is characteristic for the hard chine on the hull and a wet transom. This last model also includes two different spacings tested for the same conditions, but no change in the heading keeping it at $\beta = 180°$.

For heave motion the lower Froude number results show that the different spacing have almost the same amplitude for the tested frequencies. Only some discontinuity at van't Veer piston mode frequency for V60 model, $\omega\sqrt{L/g} \approx 2.1$. At a higher Froude number, $Fn = 0.25$, the responses show already a peak at the resonance frequency which is smaller for the bigger spacing model V60. The same difference in amplitudes is found for $Fn = 0.625$, where for both spacings the amplitudes are larger than for $Fn = 0.25$. The interaction coefficients are at this case $Int = 0.53$ for V40 and $Int = 0.29$ for V60. For the highest Froude number it is possible to observe the same effect of the increased spacing, however it is seen that it losses significance with increased speed. For pitch motion of VOSPER catamaran the results have the same type of sequence regarding the increasing of Froude number. But interestingly the experimental results do not show resonance peaks as high as previous models.

Results from the different methods used show the same tendencies as for the previous, with better correlation between experimental and computations for CatCenteno when using the cross-flow method. Again for very high Froude numbers and bigger spacing the computations using Fonseca when including end-terms can give good results, which is also true for pitch motion.

6.2 Roll results

For the roll motion of catamarans the main subject of study usually becomes the global loads at the cross-deck structure. Works like Faltinsen et al. (1992) present computations comparing experimental data on such variables. From the chosen experimental works available, only three models are subjected to oblique waves, MARINTEK, Delft 372 and El Pardo. This is possibly justified by the difficulties in creating experimental set-ups for these cases, which are in most of the cases conducted with self propelled models including autopilots that do not assure the same heading during the run, Hermundstad (1995) identifies this problematic.

All the resulting RAO figures for roll motion are shown in Appendix section A.8. Starting with the results for MARINTEK catamaran, it is possible to observe that the frequency domain tested for $\beta = 150°$ is very high, having very low motion amplitude values. However for $\beta = 90°$ inclusion of hydrodynamic interaction is very important, resulting in better predictions. Computations done with no-interaction show extreme over prediction in all the frequency domain. Also to note that due to the relatively high Froude number, $Fn = 0.49$ the inclusion of viscous effects in CatCenteno improves a lot the computation results. For the case of Delft 372 model the headings differ from 180 degrees, 15 and 45 degrees. In the first case calculated, roll motion responses are over predicted in the lower frequencies, only when the Froude number is high, $Fn = 0.75$ the computations from Wasim and Fonseca give better fitting to the experimental results. CatCenteno at high speed shows evident errors in the computations, possible

to observe for $\beta = 225°$. Peaks in characteristic frequencies show such error, which is observed at $\omega\sqrt{L/g} \approx 2.1$ for $Fn = 0.3$ and $\omega\sqrt{L/g} \approx 2.3$ for $Fn = 0.6$. The first example, has extremely good correlation for Wasim computations and the second with Catcenteno, but where experimental shows a hump the computations show a trough and the opposite, Figure A.50. For the last model that was subjected to roll motion, El Pardo, Wasim computations show very good correlation with the experimental data. However CatCenteno follows the tendency, if viscous effects are not included. Fonseca does not present the characteristic peak due to the interaction as expected, however it can also perform in average value, especially at the heading of $\beta = 165°$.

6.3 Root mean square error

As the analysis of results uses directly some values from calculation of RMSE, it is useful to demonstrate the average of RMSE metric. This average is computed for all the different conditions tested and only differentiates the methods used in the motions computations. This is shown in Table 6.4, where standard deviation is included for a better qualification of results. The result are expressed in the same units RAO figures for each mode of motion.

Table 6.4: Mean values of Root Mean Square Error.

	$\overline{RMSE_3}$	$\sigma(RMSE_3)$	$\overline{RMSE_5}$	$\sigma(RMSE_5)$	$\overline{RMSE_4}$	$\sigma(RMSE_4)$
Fonseca	0.25	0.20	0.25	0.16	0.37	0.36
Fonseca+ET	0.25	0.19	0.21	0.09	0.29	0.24
CatCenteno	0.43	0.29	0.28	0.14	0.18	0.10
CatCenteno+VISCO	0.26	0.15	0.21	0.08	0.17	0.07
Wasim	0.23	0.15	0.24	0.17	0.15	0.09

In Table 6.4 it is possible to observe that Wasim gives the lower value for heave and roll motions, $\overline{RMSE_3} = 0.23$ and $\overline{RMSE_4} = 0.15$. However for pitch motion the lower values are from CatCenteno when including viscous effects, and Fonseca when including end-terms, both with $\overline{RMSE_5} = 0.21$. These results show correlation with the previous discussion, where result from Wasim are consistently in agreement with experimental values, which for the case of roll motion it is shown that interaction is important for the computations. For pitch motion case the result shows that using strip theories, generally better agreement with experimental values is obtained. However the previous discussion shown that this may not be true, considering the amplitude and locations of resonance peaks may crucial when evaluating methods results. Developments on these considerations are done further in the work, when studying model errors.

By observing the tables in Annex B, from which values where used to compute the average, is possible to observe shaded table cells with the lower values for each tested condition. Considering the Froude number at which the catamarans are tested and the hull spacing, which combined represent the interaction level between the demi-hulls, conclusions can be drawn. As mentioned before the result of interaction level, $Int.$, is given at the natural heave frequency for each tested condition. Because of

the two-dimensional assumption for the results, differentiation due to the headings are not included in the discussion. To note also that the computations without forward speed gave results very close to the experimental values, with RMSE under 0.11 for all motion results.

The method that has the larger amount of relatively good results is Wasim, using the three-dimensional method gives a wide interval of interaction coefficients, ranging from $Int. = 0$ until $Int. = 0.83$. Considering the correspondent Froude numbers these results show the same wide range, with $Fn = 0.2$ until $Fn = 0.8$. These values show that computations using Wasim are the most reliable ones for any condition.

Other interaction schemes using trip theory methods can also result in lower RMSE values too. It is shown that CatCenteno accounting for viscous effects gives low RMSE values for high Froude numbers, $Fn > 0.6$. Only three cases with lower Froude numbers have good result in terms of RMSE. Regarding the interaction coefficients these range from $Int. = 0.2$ until $Int.0.72$. Indicating reduction of errors when accounting for viscous effects giving a relatively high range of interaction at which the results are acceptable. Good results using this method do not include hull spacing value of $S/L = 4$. Other cases using two-dimensional approach without cross-flow method are shown in the tables having low RMSE, with $Int. = 0.72$ until $Int. = 0.81$, however they are only three and at very low Froude number, $Fn = 0.2$.

For the case of no-interaction, using Fonseca, low RMSE values can be found when including end-terms, such cases are for relatively high Froude numbers, from $Fn = 0.53$ till $Fn = 0.8$. In combination with big hull spacings the interaction coefficient ranges from $Int. = 0$ until $Int. = 0.56$. Meaning that the computations from simple strip theory can perform good when considering catamarans at high speed. If end-terms are not included acceptable results can be found too, however the range of Froude number becomes lower, with $Fn = 0.2$ until $Fn = 0.6$. These low speeds indicate that even when interaction is relatively high, single hull strip theory when well implemented, can give good results

Chapter 7

Study on model errors

Significant experimental data is presented and directly compared with computations performed by different available methods. In this chapter the objective is post-processing of results in a performance metrics philosophy. This tries to evaluate important aspects relating the type of simulations and influence variables though quantified parameters. Uncertainty in data is to be treated for better determination of the information available, so a rational use of information is possible. With the study on uncertainty different characteristics can be found on methods allowing to distinguish between systematic and random errors, Tian et al. (2016). The commonly used performance metrics are bias (mean of the differences), MSE (Mean Square Error) and CC (Correlation coefficient).

During the work we discuss the comparisons used to validate the numerical computations, which were found and treated until now. The figures showing both theoretical and experimental results for RAO's are extremely valuable, however with the evolution of computation capabilities the fit of curves by observation and direct discussion may not be sufficient. The precision has increased and therefore better correlations between computations and experiments are expected if more modern and sophisticated methods are used. As stated in Chapter 5.1, the available data and the methodology to collect it contributes to variation on metrics treatment introducing uncertainty. Other aspect that is starting to be present in the experimental reports published is the uncertainty analysis of the experimental results. A recent example of such attention is the work of Bouscasse et al. (2013). Such considerations regarding experimental publications are shown in Chapters 2 and 5.1. Part of this discussion is the computations ability to represent the experimental results and with it having good correlation with the reality. Formulations and other aspects related to this are found in Chapter 3. These type of considerations may be connected to errors in failure representing and testing reality, however there are variables in the problem that simply mean different results. These variables are related directly either with the vessel in study or the conditions that it is subjected to. Following the work Guedes Soares et al. (1999) it is possible to asses these ones:

- Length between perpendiculars, L - general dimension of the vessel in question, will mainly define the range of interesting frequencies used in wave characterization, because of this it is used as reference dimension in scaling processes.

- C_b, relation of L/T, L/B and $L/\nabla^{1/3}$. The first parameter defines in a simple however important way the general nature of the hull geometry. Ratios such as L/B and L/T also translate hull geometry in transversal and longitudinal perspective respectively. This can very well have correlation to the radiated wave problem which is included in the motions computations.

- C_{wl}, natural frequencies are very dependent on the water line figure in conjunction with mass properties. The linearised equation of motion shows that the hydrostatics of a vessel is extremely important in the form of restoring coefficients and this is highly connected with area and area moments of the water line surface.

- Mass model considering centre of gravity location and radii of gyration lengths are important, mass distributions are not included since no loads distribution are calculated.

Three other important variables are the type of waves, directions and speed of the vessel which combined will translate in different encounter frequency. The waves here treated are regular and with small slope, $k\zeta$, in order to keep linearity being of sinusoidal shape with defined frequency, ω, incident direction β and of course the vessel speed in the form of Froude number, Fn.

7.1 Frequency independent model error

Several ways to model the uncertainty state clearly that experimental errors exist. However once good correlation between a model and experimental data is found, the experimental error should have an average deviation tending to zero. In Guedes Soares et al. (1999) several types for the uncertainty models are introduced, unbiased, constant, linear and quadratic. It is understood that by increasing the degree of Equation 7.2, a better fit can be found for the differences between computations and experimental results curves. However due to limited amount of data the determination of coefficients for polynomial model error is less significant as the degree increases.

$$\hat{H}(\omega) = \phi(\omega) \cdot H(\omega) + \epsilon(\omega) \tag{7.1}$$

$$\phi(\omega) = a + b\omega + c\omega^2 \tag{7.2}$$

H is the theoretical values from the computations performed, ϕ is any model error function that multiplied by the theoretical predictions results gives $\hat{H}$, the improved predictions. The random experimental errors are represented by the inclusion of term ϵ. The base generalization of the uncertainty in computations can be found by assuming a constant model error, Equation 7.3. To determinate the value of a random variable, a, the squared error resulting from application of the method in the entire frequency domain is minimized, equation 7.5. In both of the equations is included repetition of the experiments in same frequency, index$_j$, such repetitions were not found during the research for this dissertation.

$$X_{ij} = aH_i + \epsilon_{ij} \tag{7.3}$$

$$\hat{a} = \frac{\sum_i X_i H}{\sum H_i^2} \tag{7.4}$$

$$Q = \sum_i \sum_j (X_{ij} - aH_i)^2 = \sum_i \sum_j \epsilon^2 \tag{7.5}$$

Applying Equation 7.4 to the results obtained, a set of resulting tables similar to RMSE computations is obtained, which are included in Appendix C. For a quicker result interpretation the mean values of all the models and test conditions are computed, keeping segregated the different methods used. This can be found in Table 7.1 showing the mean values of the model error variable and it's standard deviation.

Table 7.1: Mean values of frequency independent model error.

	Mean values of FIME					
	$\overline{\hat{a_3}}$	$\sigma(\hat{a_3})$	$\overline{\hat{a_5}}$	$\sigma(\hat{a_5})$	$\overline{\hat{a_4}}$	$\sigma(\hat{a_4})$
Fonseca	0.98	0.13	0.88	0.21	0.55	0.17
Fonseca+ET	1.03	0.14	1.09	0.24	0.62	0.17
CatCenteno	0.81	0.16	0.89	0.21	0.82	0.21
CatCenteno+VISCO	0.97	0.15	1.00	0.20	1.00	0.54
Wasim	0.91	0.13	0.86	0.16	1.12	0.39

In this general view of results the method that needs less linear correction is CatCenteno when including viscous effects, with values closer to one for a random variable. The standard deviation of frequency independent model errors computed for pitch motion are relatively higher than for the heave motion. For roll motion the same high standard deviation values of results can be found when using higher order of interaction schemes, however keeping an average of satisfactory result. The conclusion is that when including interaction in roll motion results do not need a correction but are very inconstant, possibly due to test conditions. From these calculations an attempt to find linear correlation between the results and variables discussed in beginning of Chapter 7 was done. However relatively small values of correlation coefficients where obtained, therefore the use of frequency independent model error for variables correlation comes to a stop. The next part of uncertainty study, which includes dependency on the frequency, will be treated using RMSE results.

7.2 Frequency dependent model error

The natural choice after computing the frequency independent error is to compute the random variables, a and b for equation 7.2, and with that the linear frequency dependent model error. However when applying such model, the available data was not sufficient to obtain relevant values. In order to generate a metric that is frequency dependent, a different method is used. The following formulation is based on Model Correction Factor (MCF) method, which considers the influence of the deviation between ideal or calculated and realistic results of any model reflecting that real situation. In this case real catamaran motions obtained by experiments are considered as realistic results and motions computations as the calculated values that try to predict the complexity of the real problem. The factor is simply the ratio

between the experimental, X_i and computed, H_i values for the catamaran model, condition and that can be frequency dependent.

$$MCF(\omega_i) = \frac{X_i}{H_i}(\omega_i) \tag{7.6}$$

Figure 7.1 shows the results obtained when applying Equation 7.6 to every single case tested for all the catamarans, conditions and for each frequency. This figure shows the heave and pitch MCF for all the cases and already shows the differentiation in Froude numbers tested originated from a linear correlation study. The dashed line at $\frac{X_i}{H_i} = 1$ represents the computations that are equal to the experiments and therefore no correction is needed. If MCF becomes lower than 1 then the theoretical method over-predicts the motion at that frequency and if higher than 1 it under-predicts such result. With this type of result it is possible to attempt to generate some differentiation by the important variables of the problem. To do this a linear correlation study is done, which took the RMSE as the control variable to identify the variables that most explain the deviation of the theoretical model from the experimental results.

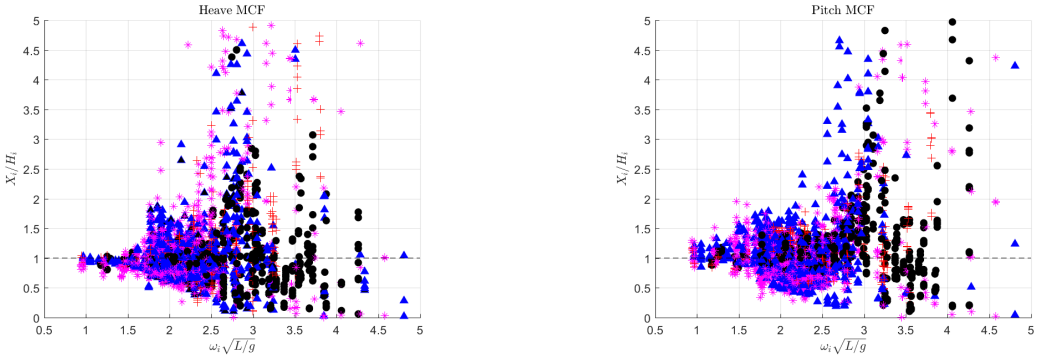

Figure 7.1: Model correction factor for heave (Left) and pitch (right) motion at all tested conditions.

7.2.1 Linear correlation study

Linear regression models are widely used where variable means are used to generate the best linear model dependent on two random variables. In this case the objective is to quantify the possible linearity between multiple variables and the control variable RMSE of the motions results. This result measures the goodness-of-fit of such linear regression model. A high correlation coefficient CC close to one implies the existence of a strong linear correlation between the variables, whereas a low correlation, close to zero, would mean the lack of a linear relationship. This method can be found in books like Ang et al. (2007), and its formulation is implemented in MATLAB software, which is used for such computations. In Tables 7.2, 7.3 and 7.4 the linear correlation coefficients are shown. The methods used in motions computations are separated and five variables are chosen, β, Fn, C_B, C_{wl} and S/L. The values in the tables show the dependency of RMSE results and the variables, were the values above 0.50 are highlighted. This represents the closer to linear correlations that are found.

Table 7.2: Linear correlation coefficients, heave.

Heave motion & Root Mean Square Error					
CC_3	Fonseca	Fonseca+ET	CatCenteno	CatCenteno+VISCO	Wasim
β	0.34	0.34	0.21	0.27	0.09
Fn	0.59	0.53	0.75	0.61	0.64
C_B	-0.31	-0.33	-0.37	-0.31	-0.22
C_{wl}	-0.28	-0.32	-0.28	-0.26	-0.13
S/L	-0.17	-0.20	0.07	0.27	0.14

Table 7.3: Linear correlation coefficients, pitch.

Pitch motion & Root Mean Square Error					
CC_5	Fonseca	Fonseca+ET	CatCenteno	CatCenteno+VISCO	Wasim
β	0.35	0.30	0.16	0.24	0.14
Fn	0.76	0.57	0.71	0.51	0.57
C_B	-0.20	-0.51	-0.27	-0.34	-0.13
C_{wl}	-0.14	-0.56	-0.15	-0.24	0.00
S/L	0.02	0.06	0.09	0.21	0.03

For heave and pitch motions it is predictable that possible correlation between results and Froude number could exist for all methods. This is very reasonable due to the importance of such variable in the different formulations. Strong influence of the block coefficient and the waterline coefficient in pitch motion can be found too, in the results of strip theory when included the end-terms, but since it is not found on the rest of methods this coefficient will not be studied.

Table 7.4: Linear correlation coefficients, roll.

Roll motion & Root Mean Square Error					
CC_4	Fonseca	Fonseca+ET	CatCenteno	CatCenteno+VISCO	Wasim
β	-0.59	-0.53	-0.04	0.50	-0.12
Fn	-0.04	-0.06	0.45	0.53	-0.04
C_B	0.14	0.09	-0.21	-0.42	-0.09
C_{wl}	0.64	0.61	0.20	-0.28	0.33
S/L	-0.33	-0.28	0.09	0.42	-0.05

Whereas in roll motion the case is significantly different, there is no case of correlation coefficients higher than 0.50 for all the methods at the same variable. Still some conclusions can be taken from here, heading influences the results precision for the modified strip theory Fonseca. This can be the result from post-processing implementation. Not only the heading dictates precision but also the water line coefficient, this is again possibly due to the method used to implement the roll of catamaran in the single hull software Fonseca. To note that the roll motion is implemented by the heave motion on each demi-hull.

7.2.2 Average model correction factor

Due to the correlation study, data can be treated by differentiating the MCF in terms of Froude number. This is done by creating 4 intervals of Froude numbers regarding the experimental data available. With the data that is included in each Froude number interval the average of MCF within a frequency interval is calculated and the resulting value plotted. A continuous line connects the values and figures are separated by the interaction methods relevance. Because of the end-terms at post-processing of Fonseca results, and inclusion of viscous effects by the cross-flow at CatCenteno, thin and thick curves are in the figures. The thick lines are the improved methods and the thin lines base methods. Because Wasim does not include such post-processing calculations it is only shown thick lines. In all the figures there is a horizontal line at 1 which helps to indicate if the computations are under or over-predicted.

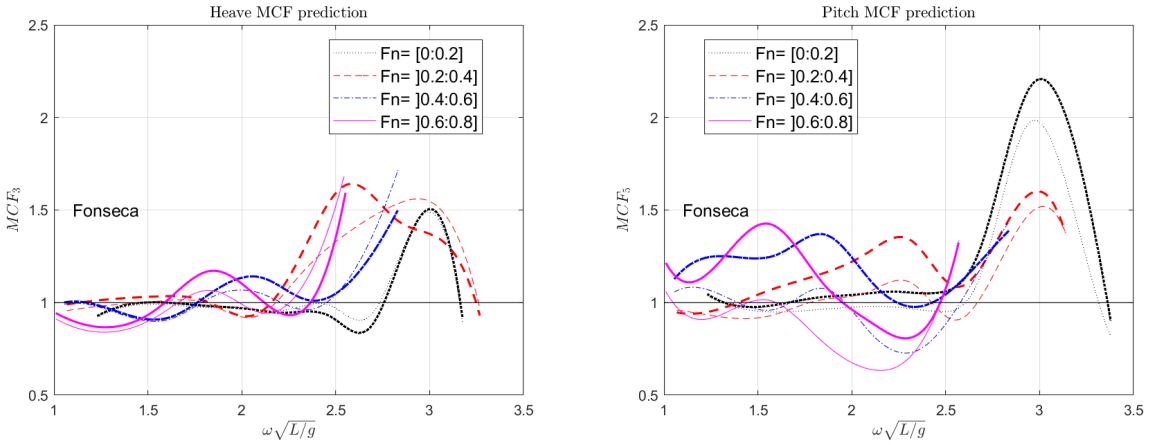

Figure 7.2: Averaged MCF of Fonseca results for heave (left) and pitch (right).

The no-interaction results can be found in Figure 7.2, using Fonseca software. Generally under-predicted results since the values are present largely above horizontal line. For higher speeds worst results are obtained at high frequency and with more oscillations along the frequency domain.

In the left side of Figure 7.2, which corresponds to the heave motion MCF, the lower Froude numbers interval, $Fn = [0 : 0.2]$, show very close to 1 values until $\omega\sqrt{L/g} \approx 2.5$. After this frequency and closer to $\omega\sqrt{L/g} \approx 3$ a peak is shown in the result, this is close to the natural encounter frequencies of the models tested. Because this method does not include interaction between the hulls it shows under-predicted of results. For the second Froude numbers interval, $Fn =]0.2 : 0.4]$, the peak is located at a lower non-dimensional frequency and the under-prediction is slightly bigger starting from $\omega\sqrt{L/g} \approx 2.25$ and until the end of frequency domain. Higher Froude numbers and high frequencies, results in high MCF values, which can be because the low amplitude results experimented. Because this MCF is a relation, any difference from zero is amplified largely showing very high values. For lower frequencies the results may be interpreted as before, where the first curves peak can be found near the average encounter resonance frequency. For the two intervals this peaks show smaller values of MFC representing better predictions. Due to the increased speed it is expected that the interaction has less relevance and because of that the no-interaction scheme can predict better the results. The inclusion of end-terms is noticeable at the higher Froude numbers intervals. The results in this case are not beneficial at the

peaks, and only gives better MCF at low and high frequency intervals. Since Fonseca's method does not take in account interaction resonance, peaks are under predicted. The inclusion of end-terms traduces in lower responses and MCF becomes higher at response peaks. Such cases are for $Fn =]0.4 : 0.6]$ at $\omega\sqrt{L/g} \approx 2$ and for $Fn =]0.6 : 0.8]$ at $\omega\sqrt{L/g} \approx 1.8$. The right side of Figure7.2, the case of pitch motions, the averaged MCF shows the same tendency of high values for higher frequency range. For low Froude numbers intervals, high frequency results are significant, but for higher Froude numbers intervals those results lose meaning due to the encounter frequency. This is possible to observe if considering the line of highest Froude numbers, $Fn =]0.6 : 0.8]$. At low Froude numbers MCF is close to one until about $\omega\sqrt{L/g} \approx 2.5$, where it starts to increase showing under-prediction of results at the resonance frequency. Inclusion of end-terms at lower Froude numbers intervals has less effect on the MCF as seen in RAO's. For the other Froude numbers interval it is possible to see that the pitch MCF is relatively good presenting an over-prediction that increases with the increase of speed. This over predictions are spread over a wider range of frequencies and move to lower ones as the Froude numbers increase. The results show that the inclusion of end-terms in pitch motions is not so beneficial, when including these the MCF becomes closer to one at the resonance frequencies but loses precision for the lower range of frequencies. For the pitch motion is understood that the interaction plays a more complex role, by having multiple humps at the response curve which results in inconstant MCF values.

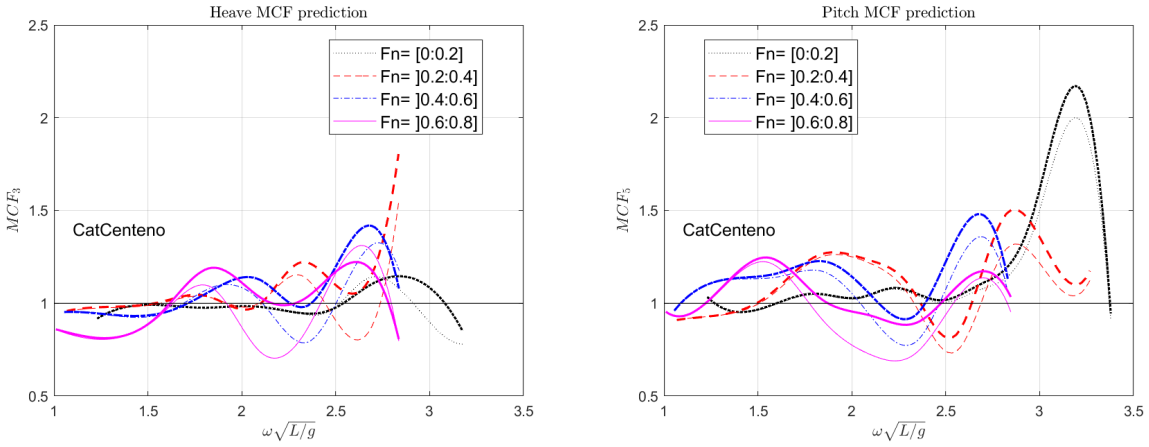

Figure 7.3: Averaged MCF of CatCenteno results for heave (left) and pitch (right).

Model correction factor values for the case of computations using CatCenteno are shown in Figure 7.3. The results when including a two-dimensional interaction scheme show different characteristics regarding the resonance peaks, and the general behaviour of the curve is more inconstant.

For heave motion, left side of Figure 7.3, at low Froude numbers interval the MCF is very close to one, showing some under-prediction at the higher frequencies. To note that once the Froude numbers tested are higher, the behaviour of such method is to over-predict the resonance peaks. Because of this, the attention is regarding the lower values of the curves as they fit better the locations of resonance frequencies too. These locations show once more the effect of forward speed and encounter resonance frequency, their MCF values show the over-predictions and with the increased speed they become lower and their location at lower frequencies. When including the viscous effects on CatCenteno computations,

the values of MCF become closer to one at the resonance frequencies. This effect is noticed only around these frequencies and more efficient for higher Froude numbers. In pitch MCF using CatCenteno, the curves show wider pattern of peaks and pits. The under-prediction at low frequencies is less significant than Fonseca method, traducing an improvement in results when accounting interaction. It is seen to that the inclusion of viscous effects improves results at higher Froude numbers by resulting in MFC values closer to one at midrange frequencies.

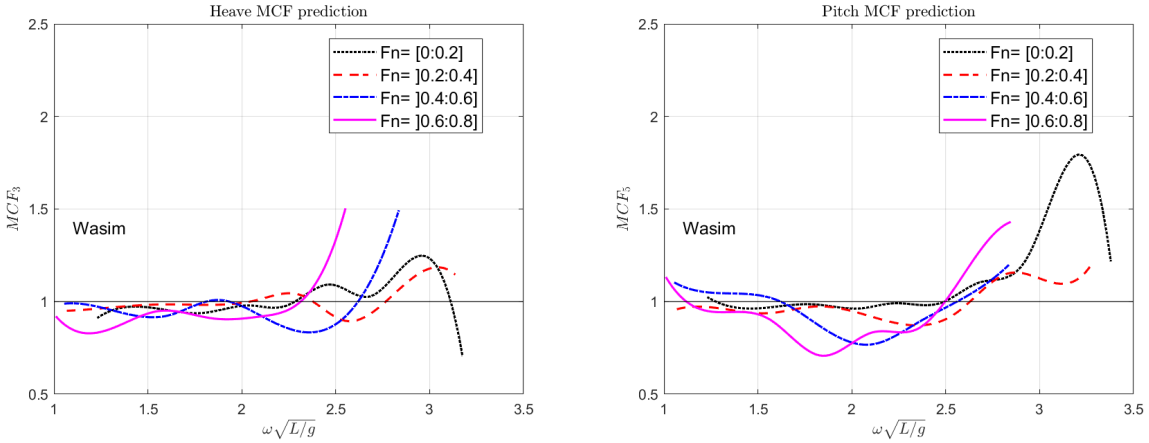

Figure 7.4: Averaged MCF of Wasim results for heave (left) and pitch (right).

The last set of figures, 7.4, refers to the computations of averaged MCF for Wasim results. The overall results are better having values closer to 1, at the relevant frequency domain. The figure shows a slightly over-prediction of heave motion at all Froude numbers. The high speed combined with high frequencies gives very high values of MCF and it is considered to be the same situation of close to zero response values. In this case the location of resonance frequencies is not well observed for heave results, but only for pitch where it is represented by lower values of the curves. This values show bigger over-predictions with the increase of speed and become wider, ranging a bigger interval of frequencies.

With this type of study it is possible to analyse the average behaviour of the transfer functions. Because the MCF is frequency dependent it is possible to observe the location of errors, which in these cases are mainly located around natural encounter frequencies. The sequence of results show that there are improvements on response values when accounting hydrodynamic interaction. In general the heave predictions come with MCF values closer to one and with results that indicate lack of precision at resonance frequencies. As for pitch motion, MCF figures show lack of precision of the methods, for the strip theories it comes under-predicted and for panel method used over-predicted. Inclusion of end-terms in Fonseca do not necessary bring better results, especially due to the lack of interaction of the method, while viscous effects in CatCenteno do bring some improvement in results but only for the very high Froude numbers. The location of resonance frequencies is not so easy to observe with CatCenteno, due to wider ranges in frequency. The figures have also shown the correlation coefficient result between the tested variables, RMSE and the ship's speed. This difference is observed by the amplitude and peaks locations of MCF curves, representing the resonance frequencies and differences in motion amplitudes.

Chapter 8

Conclusions

Computations of wave induced motions on catamarans were studied, comparing results with experimental data found in the bibliography. It is understood that catamarans can have relatively complex considerations to take into account. One of most important is the hydrodynamic interaction between demi-hulls. To better understand the effect of hydrodynamic interaction several objectives were defined, steps in which this work is based on. The use of several numerical methods to compute catamaran motions was done resulting in comparison between different levels on hydrodynamic interaction. Along the study of such methods experimental data was collected, with seven experimental hull models used for validations a good amount of results using the methods were obtained. The methods results are analysed and compared to the experimental data by the means of RAO figures and RMSE. With the pool of results a further study is done, using performance metrics philosophy two types of model errors are studied, a frequency independent and frequency dependent.

8.1 Achievements obtained

8.1.1 Software

A compilation on the existing methods to predict catamaran motions is accomplished, being established the need to include hydrodynamic interaction between demi-hulls. Also it is noted the need to have methods that allow fast computations, in order to include them in design stages. Namely, strip theory based methods or three-dimensional as Rankine panel method. These methods are based on potential flow computations, having lower times of computations than CFD methods which include viscous effects by means of boundary layer models. With the chosen methods three levels of interaction are used; a no-interaction using Fonseca software, two-dimensional interaction by the use of a strip theory based software CatCenteno and the fully three-dimensional considered by Wasim commercial software. Post processing of single-hull motions results from Fonseca is done to the twin-hull case, this because the need compare results for catamaran motions in different headings, $\beta \neq 180^\circ$. An important aspect of strip theory software found is the ability to create automation of computations, this was accomplished saving time and could be included in optimisation processes by seakeeping criteria. However it is also

possible to achieve the same with Wasim software, with a higher lever of automation and consuming more time on computations. This was not attempted due to the lack of time for this work.

8.1.2 Interaction

Relatively to no-interaction comes the formulation of exciting forces, as discussed in Chapter 4, when transforming form the single-hull case to twin-hull exciting forces have to consider the phase that each demi-hull is subjected too. Equations 4.7, 4.8 and 4.9 are the result of such consideration, it may happen that experimented frequencies are so that the outcome of exciting forces are close or equal to zero. This no-interaction scheme is considered to be relevant in high speed cases, as the last example from Figure 4.1. The original software does not include the effect of end-terms, however in the post-processing phase it was possible to include them creating extra results from computations.

More results are obtained with two-dimensional interaction scheme, CatCenteno software uses the same method to compute the hydrodynamic coefficients as Fonseca, but due to hull symmetry implementation result comes as a sum of the symmetric and anti-symmetric solutions from Frank's close fit. The first case seen in Figure 4.1 exemplifies this case. Results from application of this method compared to the ones found in the literature show reasonable agreement, such results are discussed and studied in Chapter 4.2. It is found that results from this implementation are relatively precise when the models have low speeds. Prediction of resonance frequency due to the water column motion between the demi-hulls is justified by hydrodynamic coefficients values. For higher Froude numbers, considerations on the interaction limit are introduced, based on two-dimensional formulation. With the result of Equation 4.16 the strange results found in Figure 4.7 are justified as limit of interaction between demi-hulls. This code has other feature that could be included in the computations, cross-flow empiric method. Because of this the results of this software include both options.

For fully three-dimensional, Wasim software, such computations were not performed. The possibility to develop results on the hydrodynamic coefficients and simplified hull forms was given relatively late and the focus remained on more realistic case studies. However this method of accounting interaction is far more sophisticated, a schematic is found in the mid case of Figure 4.1. Besides the three-dimensional radiation problem, other very important aspect that Wasim software includes is interaction between standing wave pattern created around the demi-hulls and ship's motion. Such ability is of extreme importance for high-speed vessels, and it is possible that if such results are included in strip theory computations the interval of applicability would be maximized.

8.1.3 Case studies

To test the numerical methods available for this work several models experimented in towing tanks where found, description of these case studies and their implementation with software can be found in Chapter 5. A total of 7 different geometries were tested within these some have different characteristics which resulted in a wide range of results. The general type of model is of smooth hull's surface and wet-transom, because of this the models motions are computed including end-terms. Delft 372 is the

opposite case being a model that do not present a wet-transom. Other interesting characteristic found is the hard chine hull of VOSPER catamaran, this characteristic justified the use of cross-flow method in Centeno et al. (2000). One of the models represented difficulty, El Pardo model has a wave piercing bow type which could not be modelled properly using CatCenteno and Fonseca software. Wasim software allows geometries of such type, however this model was simplified being modified excluding the wave piercing bow. For each model here used several experimented conditions were found, this is due to the various speeds and headings. Resulting from this conditions a total of 48 combinations are available. Considering that each one of these combinations results in 3 different methods and in heave, pitch and roll motions results a substantial amount of data is collected.

8.2 Results conclusion

The first part of results is referent to the direct comparison between experimental values and wave induced motions, from this part several conclusions can be taken. The codes that showed more stable results are Wasim and Fonseca. CatCenteno code has few validations works associated and the two-dimensional approach has a problem regarding exaggerated spacing of demi-hulls, similar results are found in van't Veer and Siregar (1995). Curves resulting from computations using CatCenteno are not smooth at peak transitions, in fact many RAO figures appear with numerical errors and may not translate specific results of the method.

- Heave motion results are better predicted than pitch motions for catamarans. Resonance frequencies are generally well predicted by the three methods however it appears to exist a limit when strip theory based codes fail to give the same type of curve at resonance peak, $Fn > 0.6$. The experimented peaks are wider than the predictions of strip theory codes, while Wasim show resulting curves in better agreement.

- Pitch motions in catamarans are not so well predicted for the general cases, Wasim has the best curve fit and interestingly Fonseca without interaction shows reasonable curves but the resonance frequencies are not well predicted being slightly shifted to the experimented ones. Presence of secondary humps in the responses also indicate the existence of non-linearities in this mode of motion.

- Roll motions are less in number of computations, however it was observed that inclusion of any type of interaction is beneficial to RAO curves results. Wasim computations show better agreement regarding the shape of curves, and in some cases CatCenteno also show good fitting curves. Fonseca computations, without interaction and with post-processing to compute roll motion of twin-hulls, show well behaved curves but always with bigger values along the frequency domain.

It was found relation between good RMSE values and interaction schemes, which depended on forward speed and hull spacing. Wasim performs with precision for the widest range of these variables. Fonseca, being well implemented can perform good for wider hull spacings. The use of end-terms improves the results for higher Froude numbers, meaning less interaction between hulls.

- The above observations together with the average RMSE computed, dictate that the best method to apply in catamaran motions studies is Wasim. However, Fonseca including end-terms can perform good for longitudinal motions, with some discrepancies in the location of resonance frequencies.

Regarding the first part of model errors study, a frequency independent model error, it is observed that for heave motion the methods that needs less linear correction are Fonseca when including end-terms, and CatCenteno when including viscous effects. For pitch and roll motions this type of model demonstrates that CatCenteno with viscous effects does not need readjustment, having $\overline{\hat{a_5}}$ and $\overline{\hat{a_4}}$ equal to 1 in average. Other important observation is the failure to find a linear correlation of FIME results and the variables defined in the chapter. However when changing the control variable to RMSE an acceptable degree of correlation with Froude number is found. However for roll motion this was not found. Although there is some significance regarding heading and waterline coefficients on computations using Fonseca. For CatCenteno when including end-terms, either wave angle and Froude number demonstrated some linear relation to RMSE roll values. This results justified that a continuation of roll motions errors study would not generate conclusive results.

- Application of a constant model error, which is not frequency dependent is not sufficient for the case of catamaran motion computations.

Due to correlation coefficient results, intervals of Froude numbers were created and an averaged model correction factor was applied. The results are expressed in Figures 7.2, 7.3 and 7.4 from those it is concluded that Wasim gives better results, closer to 1, for a wider range in frequency domain. For all the methods there are significant differences for the higher frequency domains, it is concluded that since response amplitudes are very small or equal to zero, such frequencies are not representative in the study.

- The relevance of Froude number is found, since frequencies at which errors are more significant are close to natural encounter frequencies.

- Wasim gives better results, closer to 1, for a wider range in frequency domain, reflecting the general precision of the method.

For no-interaction method, using Fonseca, it is possible to observe that inclusion of end-term may not traduce benefits to all the Froude numbers intervals and for pitch motion results bigger corrections are needed when including such effect. The application of an averaged MCF on CatCenteno results show very inconstant curves along the frequency domain, crossing several time the reference value 1. However when including viscous effects, results appear to be improved for both heave and pitch, with special effect for higher Froude numbers intervals.

- The results using no-interaction methods for catamaran motions can perform good when comparing a generic metric like RMSE. However the lack of some degree of interaction gives errors at resonance frequencies.

- CatCenteno only gives good results when including with cross-flow. Such empiric method could be applied to higher level of interactions and therefore improving their results. This is possible in Wasim by increasing the critical damping.

8.3 Future Work

As a continuation on this work there are some interesting studies that could be useful for the future, namely:

1. A more comprehensive study on the hydrodynamic coefficients, the comparison of coefficients was not done for the three-dimensional case. Having a more detailed analysis of the mathematical formulations and therefore justifying the differences on motion results. Such study could be applied on a existent catamaran hull form.

2. Since the type of vessels here studied operate at relatively high speeds, and it is known that there are strip theory based methods that allow to obtain motion transfer functions with a wider range of speeds. Application of fast strip theory methods in a comparison study could bring better results when keeping the hypothesis of no-interaction. For the two-dimensional strip theory code used, it was found that improvements can be done. The geometric definition of the hull is very simplified and further debugging of the code is recommended.

3. The experiments data collected is largely referent to head and bow waves, in a realistic situation a vessel will operate with other conditions, it is suggested to perform comparisons studies for wider range of headings and modes of motion. Other limitation was the type of catamarans bows which were modelled in a very simplistic way. A comparative study of bow types when including three-dimensional interaction is a possible work to be done. Results of wave resistance and cross-deck loads could be possibly included on these type of studies.

4. Due to the computational evolution and therefore ability to perform fully three-dimensional computations with panel methods it may be possible to create an optimization regarding seakeeping criteria using such tools.

Bibliography

Seakeeping experiments guidelines 7.5-02.07. 02.1. ITTC Recommended Procedures, 2017.

A. H. S. Ang, W. H. Tang, et al. *Probability concepts in engineering: emphasis on applications in civil & environmental engineering*, volume 1. Wiley New York, 2007.

F. P. Arribas and J. A. C. Fernández. Strip theories applied to the vertical motions of high speed crafts. *Ocean Engineering*, 33(8-9):1214–1229, 2006.

E. Begovic, G. Boccadamo, and I. Zotti. On the viscous forces on the motions of high speed hulls. In *Proceedings of the HIPER 02 Conference, Bergen, Norway*, pages 47–59, 2002.

V. Bertram. *Practical ship hydrodynamics*. Elsevier, 2012.

B. Bouscasse, R. Broglia, and F. Stern. Experimental investigation of a fast catamaran in head waves. *Ocean Engineering*, 72:318–330, 2013.

G. Bulian, A. Francescutto, and I. Zotti. Stability and roll motion of fast multihull vessels in beam waves. *Ships and Offshore Structures*, 3(3):215–228, 2008.

T. Bunnik, D. Van, G. Kapsenberg, Y. Shin, R. Huijsmans, G. B. Deng, G. Delhommeau, M. Kashiwagi, and B. Beck. A comparative study on state-of-the-art prediction tools for seakeeping. In *28th ONR Symposium on Naval hydrodynamics*, 2010.

T. Castiglione, F. Stern, S. Bova, and M. Kandasamy. Numerical investigation of the seakeeping behavior of a catamaran advancing in regular head waves. *Ocean Engineering*, 38(16):1806–1822, 2011.

R. Centeno, N. Fonseca, and C. Guedes Soares. Prediction of motions of catamarans accounting for viscous effects. *International shipbuilding progress*, 47(451):303–323, 2000.

R. Centeno, K. S. Varyani, and C. Guedes Soares. Experimental study on the influence of hull spacing on hard-chine catamaran motions. *Journal of ship research*, 45(3):216–227, 2001.

H. S. Chan. Prediction of motion and wave loads of twin-hull ships. *Marine structures*, 6(1):75–102, 1993.

S. S. Dhavalikar. Comparative study of seakeeping analysis results from various methods. In *ASME 2011 30th International Conference on Ocean, Offshore and Arctic Engineering*, pages 217–223. American Society of Mechanical Engineers, 2011.

N. Elsimillawy and N. S. Miller. Time simulation of ship motions: a guide to the factors degrading dynamic stability. *Society of Naval Architects and Marine Engineers-Transactions*, 94(Preprint No. 8), 1986.

O. Faltinsen and R. Zhao. Numerical predictions of ship motions at high forward speed. *Phil. Trans. R. Soc. Lond. A*, 334(1634):241–252, 1991.

O. Faltinsen, J. R. Hoff, J. Kvalsvold, and R. Zhao. Global loads on high-speed catamarans. *5th Int. Symp. on Practical Design of Ships and Mobile Units*, 1992.

O. M. Faltinsen. *Hydrodynamics of high-speed marine vehicles*, volume 474. Cambridge university press Cambridge, 2005.

C. C. Fang and H. S. Chan. Investigation of seakeeping characteristics of high-speed catamarans in waves. *Journal of Marine Science and Technology*, 12(1):7–15, 2004.

C.-C. Fang, H. Chan, and A. Incecik. Investigation of motions of catamarans in regular waves-i. *Ocean engineering*, 23(1):89–105, 1996.

D. Fathi and J. R. Hoff. Shipx vessel responses (veres). *Theory Manual, Marintek AS, Feb*, 13, 2004.

N. Fonseca. Apontamentos de dinâmica e hidrodinâmica do navio, 2009.

N. Fonseca and C. Guedes Soares. Time-domain analysis of large-amplitude vertical ship motions and wave loads. *Journal of Ship Research*, 42(2):139–152, 1998.

N. Fonseca and C. Guedes Soares. Viscous effects in the vertical motions of ships in waves. *The sea and the challenges for the future (in Portuguese)*, pages 59–84, 2000.

W. Frank. Oscillation of cylinders in or bellow the free surface of deep fluids. Technical Report 2375, Naval Ship Research and Development Center, Washington D. C., 1967.

J. Gerritsma and W. Beukelman. Analysis of the modified strip theory for the calculation of ship motions and wave bending moments. *International Shipbuilding Progress*, 14(156):319–337, 1967.

C. Guedes Soares, N. Fonseca, P. Santos, and A. Maron. Model tests of the motions of a catamaran hull in waves. In *Proceedings of the International Conference on Hydrodynamics of High-Speed Craft, Royal Institution of Naval Architects, London*, 1999.

O. A. Hermundstad. *Theoretical and experimental hydroelastic analysis of high speed vessels*. PhD thesis, The Norwegian Institute of Technology, 1995.

O. A. Hermundstad, J. V. Aarsnes, and T. Moan. Linear hydroelastic analysis of high-speed catamarans and monohulls. *Journal of Ship Research*, 43(1):48–63, 1999.

D. A. Hudson, W. G. Price, and P. Temerel. Seakeeping performance of high speed displacement craft. *FAST'95: 3rd Int. Conf. on Fast Sea Transportation*, 1995.

A. Incecik, B. F. Morrison, and A. J. Rodgers. Experimental investigation of resistance and seakeeping characteristics of a catamaran design. *Proc. 1st Int. Conf. on Fast Sea Transportation, Norway*, pages 239–258, 1991.

H. D. Jones. Catamaran Motion Predictions in Regular Waves. Report 3700, Naval Ship Research and Development Center, 1972.

J. M. J. Journee and L. J. M. Adegeest. Theoretical manual of strip theory program "SEAWAY for Windows". *TU Delft Report*, 1370, 2003.

B. V. Korvin-Kroukovsky. Investigation of Ship Motions in Regular Waves. *SNAME Transactions*, 63: 386–435, 1955.

B. V. Korvin-Kroukovsky and W. R. Jacobs. Pitching and Heaving Motions of a Ship in Regular Waves. *SNAME Transactions*, 65:590–631, 1957.

D. Kring, Y. Huang, P. Sclacounos, T. Vada, and A. Braathen. Nonlinear ship motions and wave-induced loads by a rankine method. *Twenty-First Symposium on Naval Hydrodynamics*, 1997.

D. C. Kring. *Time domain ship motions by a three-dimensional Rankine panel method*. PhD thesis, Massachusetts Institute of Technology, 1994.

C. M. Lee and R. M. Curphey. Prediction of motion, stability and wave load of small-waterplane-area-twin-hull ships. *Transactions Society Naval Architects Marine Engineers*, 85:94–130, 1977.

C. M. Lee, H. Jones, and J. W. Bedel. Added mass and damping coefficients of heaving twin cylinders in a free surface. Report 3695, Naval Ship Research and Development Center, 1971.

C. M. Lee, H. D. Jones, and R. M. Curphey. Prediction of motion and hydrodynamic loads of catamarans. *Marine Technology*, 10:392–405, 1973.

F. M. Lewis. The inertia of the water surrounding a vibrating ship. *SNAME Transactions*, 37:1–20, 1929.

B. Molin. On the piston mode in moonpools. In *In Proc. 14th Int. Workshop on Water Waves and Floating Bodies*, 1999.

A. Nestegard, V. Hansen, O. Rognebakke, and B. Cerup-Simonsen. Achievements in Applications of Marine Hydrodynamics. In *ASME 2008 27th International Conference on Offshore Mechanics and Arctic Engineering*, pages 319–326. American Society of Mechanical Engineers, 2008.

T. F. Ogilvie and E. O. Tuck. A rational strip theory of ship motions: part I. Technical report, University of Michigan, 1969.

M. Ohkusu. On the motion of multihull ships in waves (I). *Report of Research Institute of Applied Mechanics, Kyushu University*, 18(60), 1970.

M. Ohkusu and M. Takaki. On the motion of multihull ships in waves (II). *Report of Research Institute of Applied Mechanics, Kyushu University*, 19(62), 1971.

H. Peng. *Numerical computation of multi-hull ship resistance and motion*. PhD thesis, Dalhousie University, 2001.

N. Salvesen, E. O. Tuck, and O. Faltinsen. Ship motions and sea loads. *Transactions Society Naval Architects Marine Engineers*, 78:250–287, 1970.

G. Schmidt. Linearized stern flow of a two-dimensional shallow-draft ship. *Journal of Ship Research*, 25 (4):236–242, 1981.

P. Temarel, W. Bai, A. Bruns, Q. Derbanne, D. Dessi, S. Dhavalikar, N. Fonseca, T. Fukasawa, X. Gu, A. Nestegård, et al. Prediction of wave-induced loads on ships: Progress and challenges. *Ocean Engineering*, 119:274–308, 2016.

B. Thwaites. *Incompressible aerodynamics*. Oxford University Press, 1960.

Y. Tian, G. S. Nearing, C. D. Peters-Lidard, K. W. Harrison, and L. Tang. Performance metrics, error modeling, and uncertainty quantification. *Monthly Weather Review*, 144(2):607–613, 2016.

R. Timman and J. N. Newman. The coupled damping coefficients of a symmetric ship. *Journal of ship Research*, 5(4):13, 1962.

F. Ursell. On the heaving motion of a circular cylinder on the surface of a fluid. *Quarterly Journal of Mechanics and Applied Mathematics*, 2(2):218–231, 1949.

A. P. van't Veer. Analysis of motions and loads on a catamaran vessel in waves. *FAST'97: 4th Int. Conf. on Fast Sea Transportation*, 1997.

A. P. Van't Veer. *Behaviour of catamarans in waves.* PhD thesis, TU Delft, Delft University of Technology, 1998a.

A. P. van't Veer and F. R. Siregar. The interaction effects on a catamaran traveling with forward speed in waves. *FAST'95: 3rd Int. Conf. on Fast Sea Transportation*, 1995.

R. Van't Veer. Experimental results of motions, hydrodynamic coefficients and wave loads on the 372 catamaran model. *TU Delft report*, (1129), 1998b.

R. Van't Veer. Experimental results of motions and structural loads on the 372 catamaran model in head and oblique waves. *TU Delft report*, (1130), 1998c.

K. S. Varyani, R. M. Gatiganti, and M. Gerigk. Motions and slamming impact on catamaran. *Ocean engineering*, 27(7):729–747, 2000.

D. N. Veritas. Sesam user manual wasim: wave loads on vessels with forward speed, 2011.

S. Wang and R. Wahab. Heaving oscillations of twin cylinders in a free surface. *Journal of Ship Research*, (1), 1971.

I. Watanabe and C. Guedes Soares. Comparative study on the time-domain analysis of non-linear ship motions and loads. *Marine structures*, 12(3):153–170, 1999.

J. F. Wellicome, P. Temarel, A. F. Molland, and P. R. Couser. Experimental measurements of the sea-keeping characteristics of fast displacement catamarans in long-crested head-seas. Technical Report Ship Science Report 89, University of Southampton, 1995.

J. Xia and Z. Wang. Time-domain hydroelasticity theory of ships responding to waves. *Journal of Ship Research*, 41(4):286–300, 1997.

Appendix A

RAO figures

In this appendix the reader finds the graphical results for Response Amplitude Operators.

Caption of figures includes:

1. Model name
2. Froude number, Fn
3. Heading angle, β
4. Hull spacing, S/L
5. Interaction at heave natural frequency, $Int = 1 - \tau_{n3} S/L$

A.1 NPL 4b round bilge series

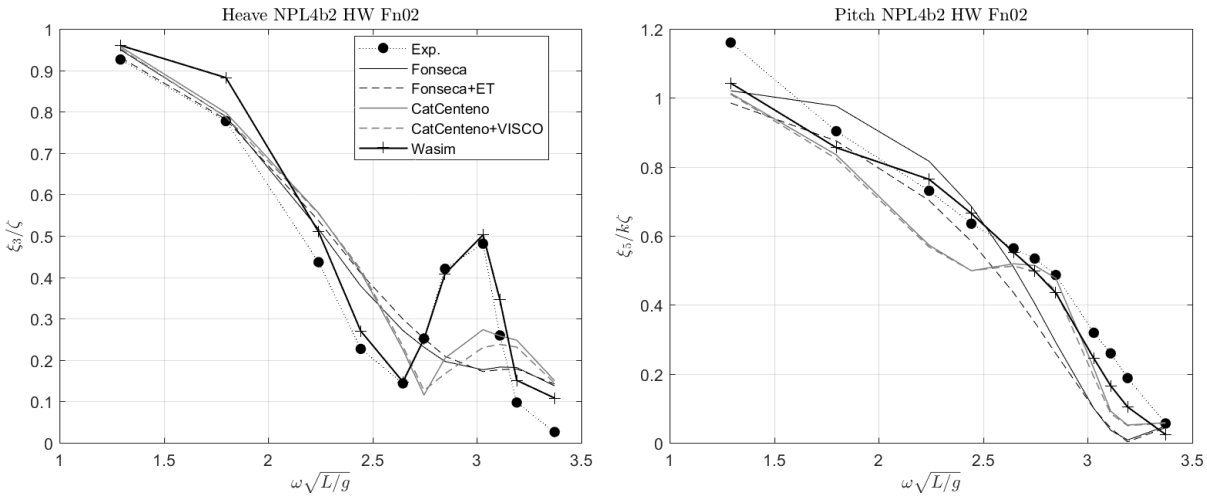

Figure A.1: Motion RAO, NPL 4b, $Fn = 0.2$, $\beta = 180°$, $S/L = 0.2$, $Int = 0.83$.

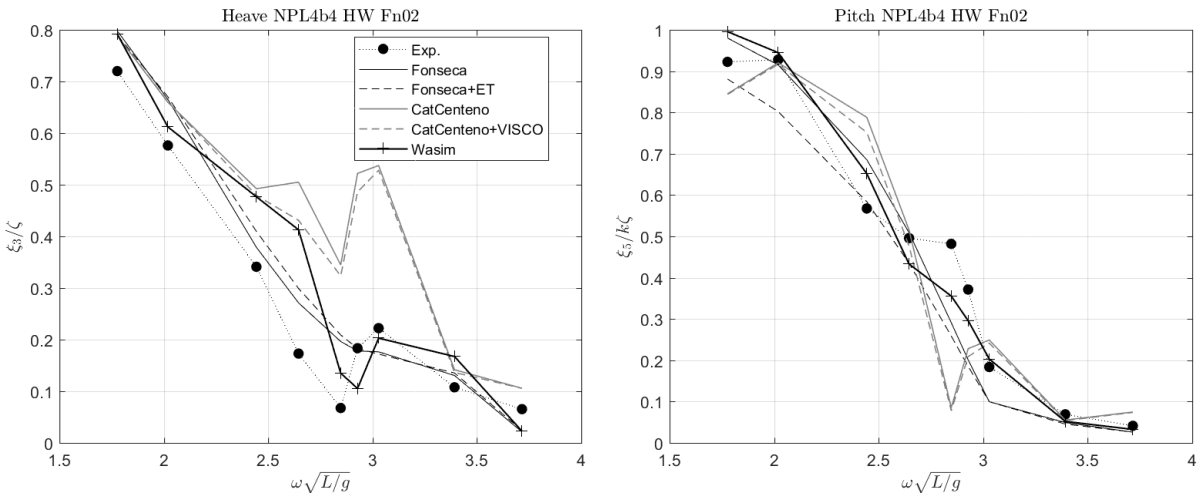

Figure A.2: Motion RAO, NPL 4b, $Fn = 0.2$, $\beta = 180°$, $S/L = 0.4$, $Int = 0.67$.

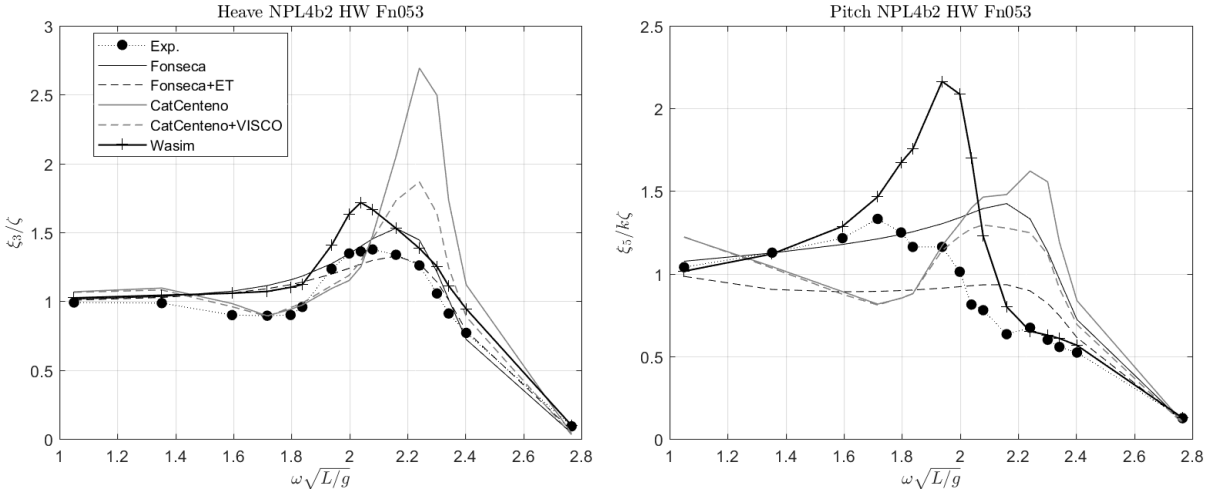

Figure A.3: Motion RAO, NPL 4b, $Fn = 0.53$, $\beta = 180°$, $S/L = 0.2$, $Int = 0.56$.

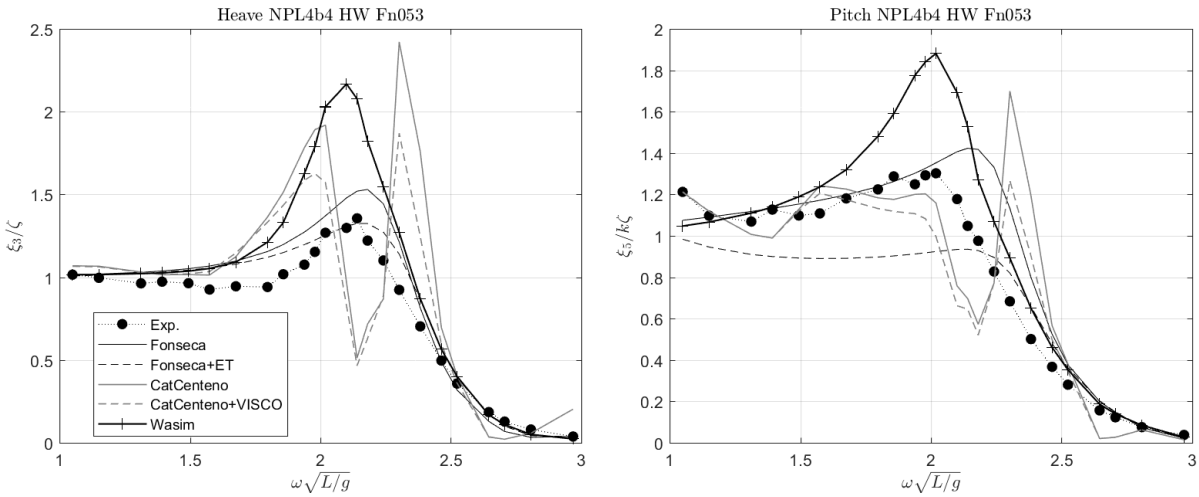

Figure A.4: Motion RAO, NPL 4b, $Fn = 0.53$, $\beta = 180°$, $S/L = 0.4$, $Int = 0.12$.

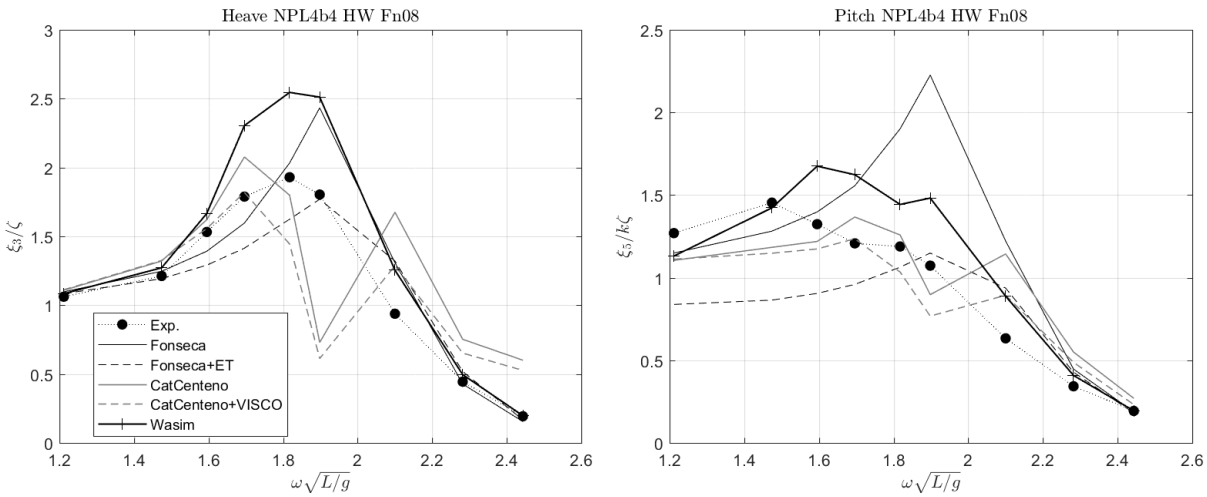

Figure A.5: Motion RAO, NPL 4b, $Fn = 0.8$, $\beta = 180°$, $S/L = 0.4$, $NoInt$.

A.2 NPL 5b round bilge series

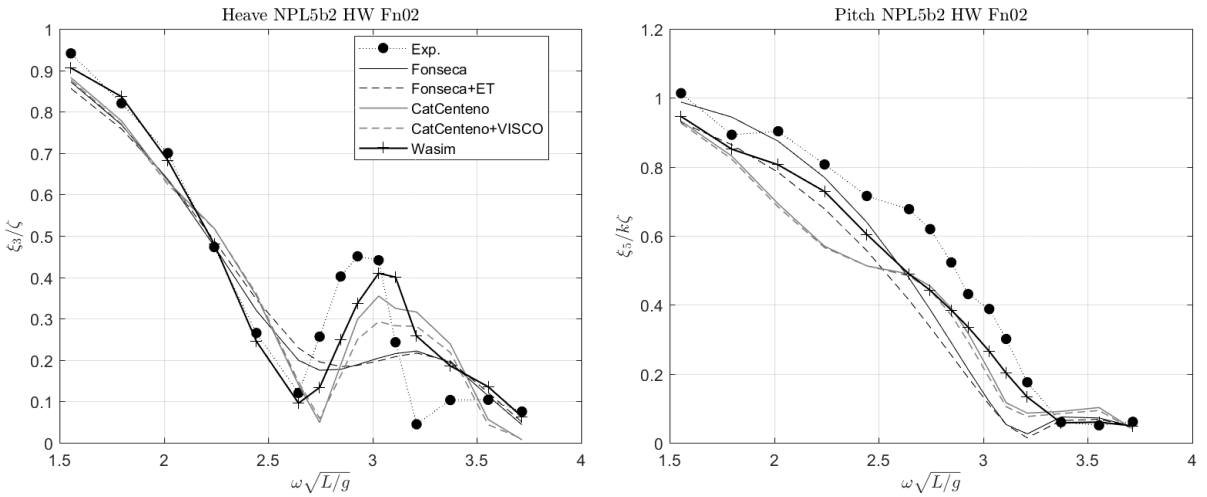

Figure A.6: Motion RAO, NPL 5b, $Fn = 0.2$, $\beta = 180°$, $S/L = 0.2$, $Int = 0.81$.

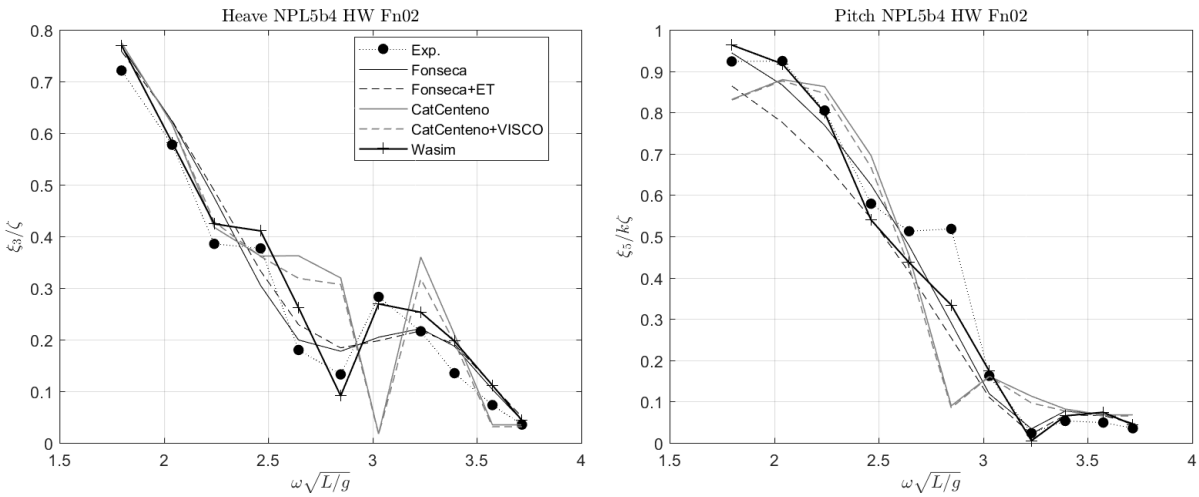

Figure A.7: Motion RAO, NPL 5b, $Fn = 0.2$, $\beta = 180°$, $S/L = 0.4$, $Int = 0.63$.

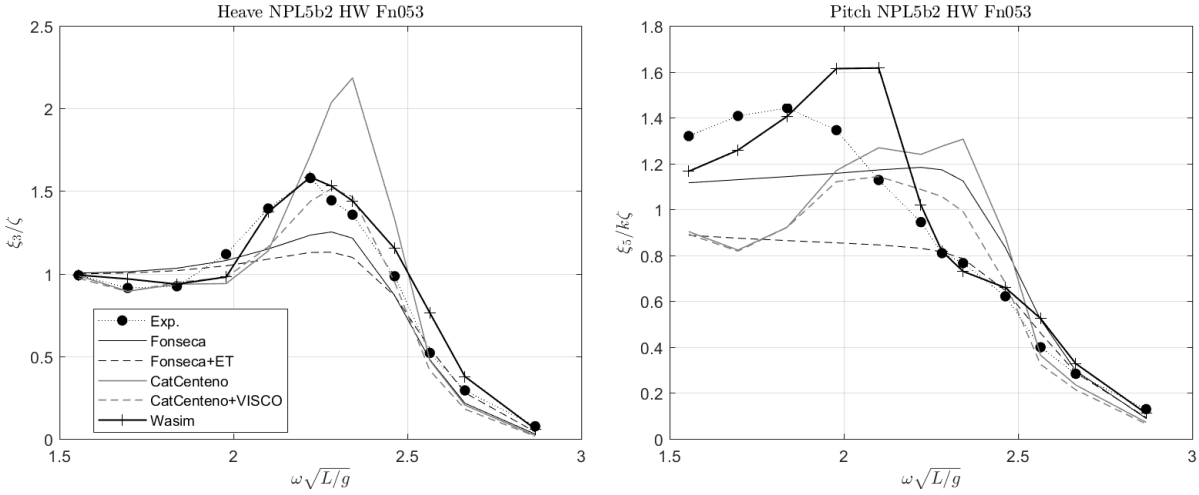

Figure A.8: Motion RAO, NPL 5b, $Fn = 0.53$, $\beta = 180°$, $S/L = 0.2$, $Int = 0.51$.

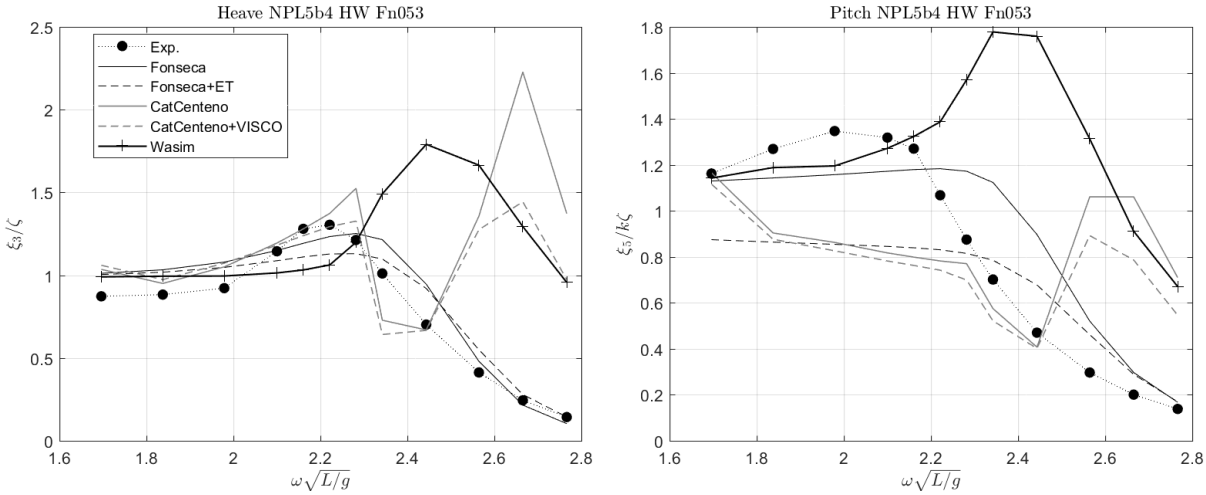

Figure A.9: Motion RAO, NPL 5b, $Fn = 0.53$, $\beta = 180°$, $S/L = 0.4$, $Int = 0.02$.

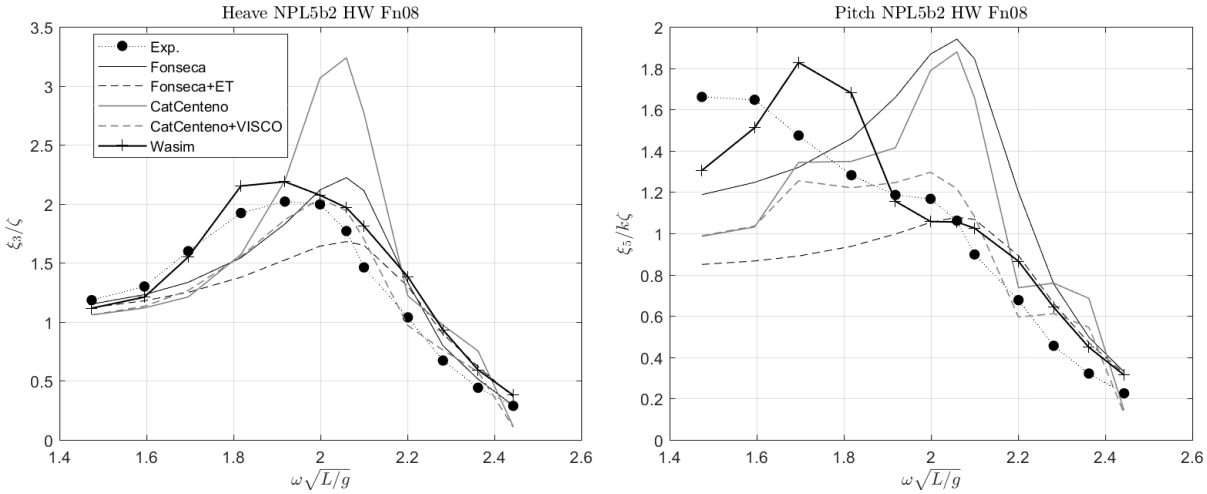

Figure A.10: Motion RAO, NPL 5b, $Fn = 0.8$, $\beta = 180°$, $S/L = 0.2$, $Int = 0.26$.

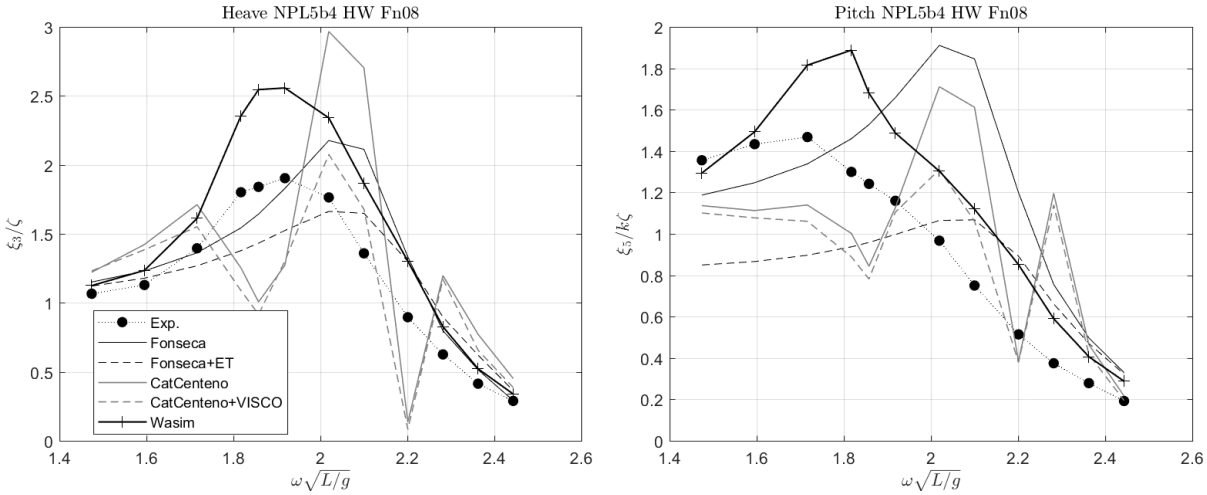

Figure A.11: Motion RAO, NPL 5b, $Fn = 0.8$, $\beta = 180°$, $S/L = 0.4$, $NoInt$.

A.3 NPL 6b round bilge series

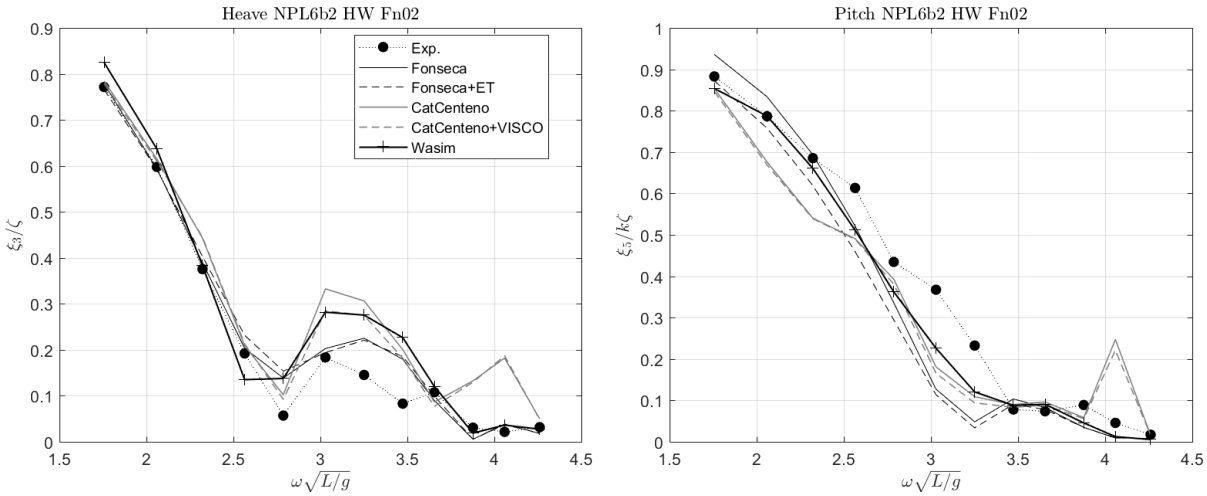

Figure A.12: Motion RAO, NPL 6b, $Fn = 0.2$, $\beta = 180°$, $S/L = 0.2$, $Int = 0.80$.

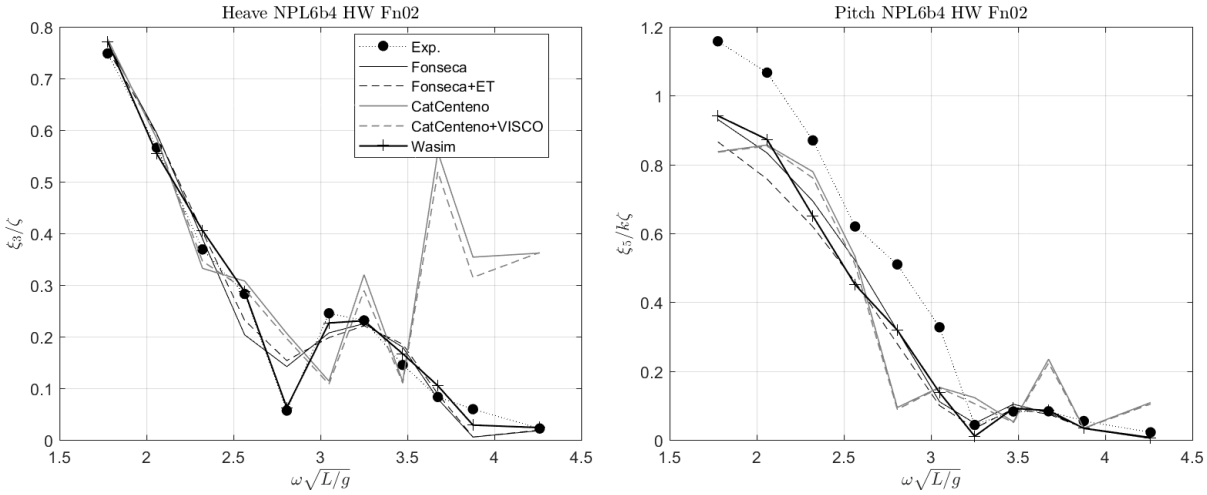

Figure A.13: Motion RAO, NPL 6b, $Fn = 0.2$, $\beta = 180°$, $S/L = 0.4$, $Int = 0.60$.

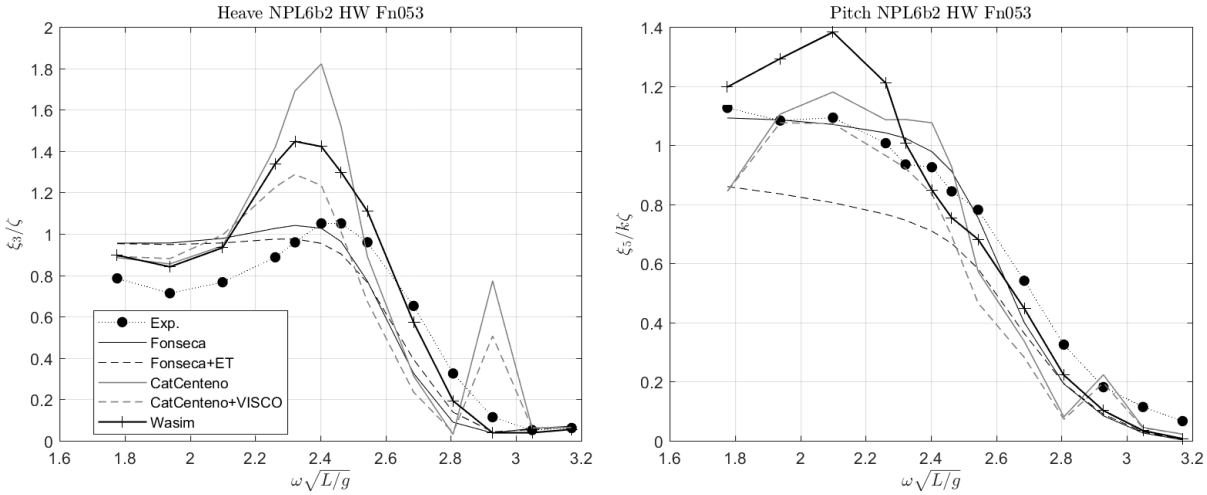

Figure A.14: Motion RAO, NPL 6b, $Fn = 0.53$, $\beta = 180°$, $S/L = 0.2$, $Int = 0.47$.

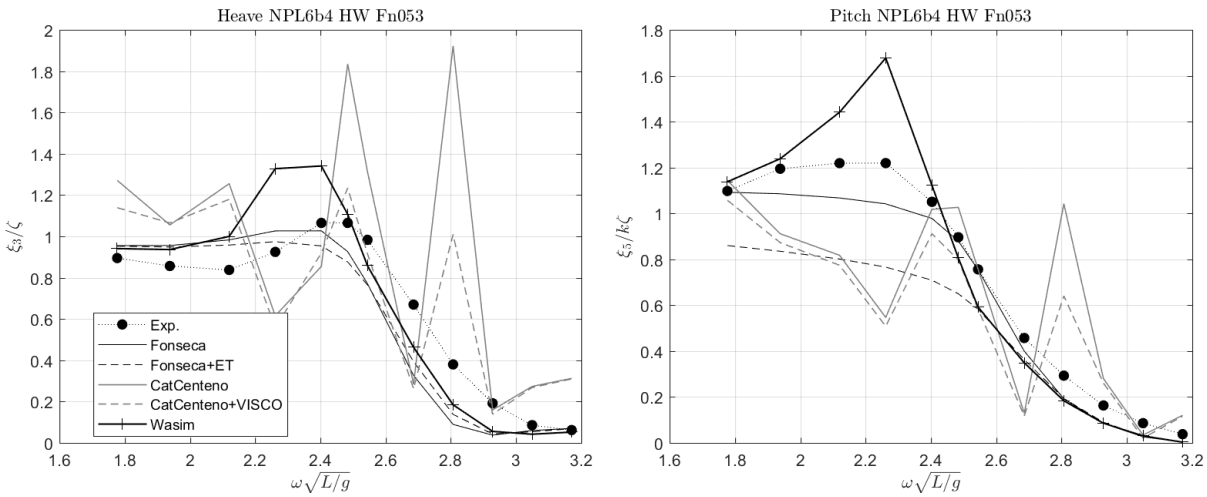

Figure A.15: Motion RAO, NPL 6b, $Fn = 0.53$, $\beta = 180°$, $S/L = 0.4$, $NoInt$.

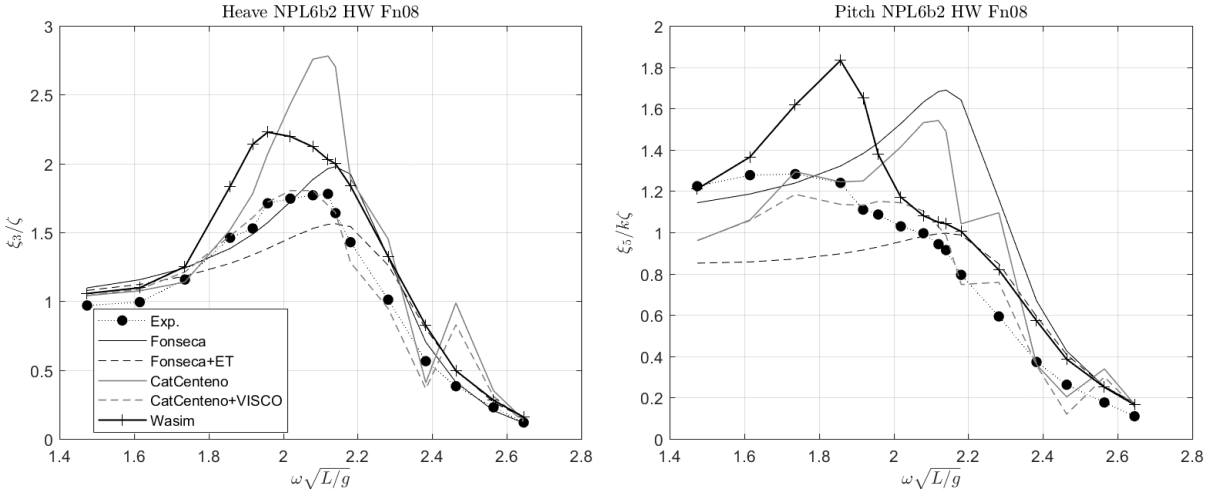

Figure A.16: Motion RAO, NPL 6b, $Fn = 0.8$, $\beta = 180°$, $S/L = 0.2$, $Int = 0.20$.

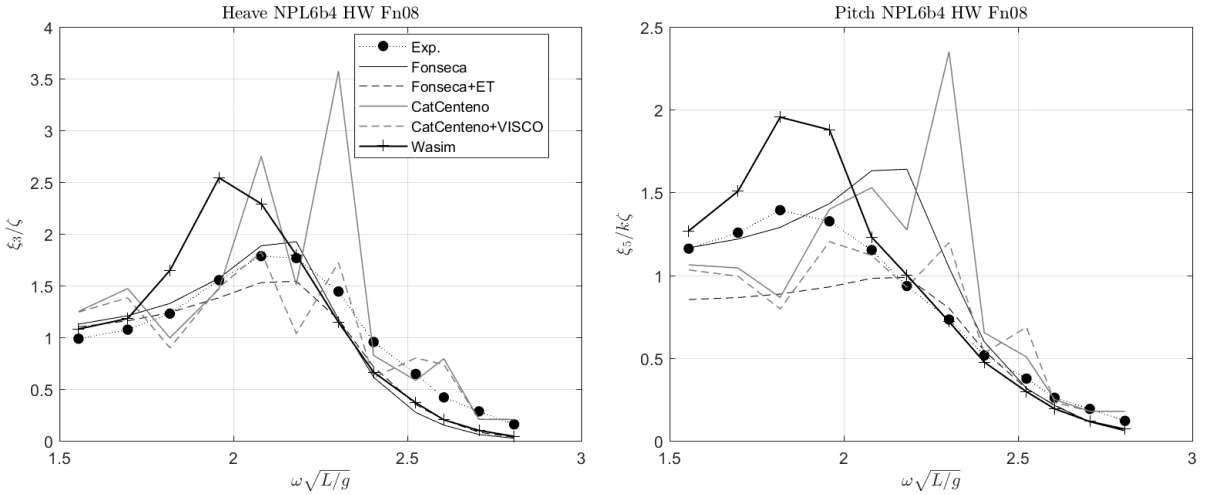

Figure A.17: Motion RAO, NPL 6b, $Fn = 0.8$, $\beta = 180°$, $S/L = 0.4$, $NoInt$.

A.4 MARINTEK

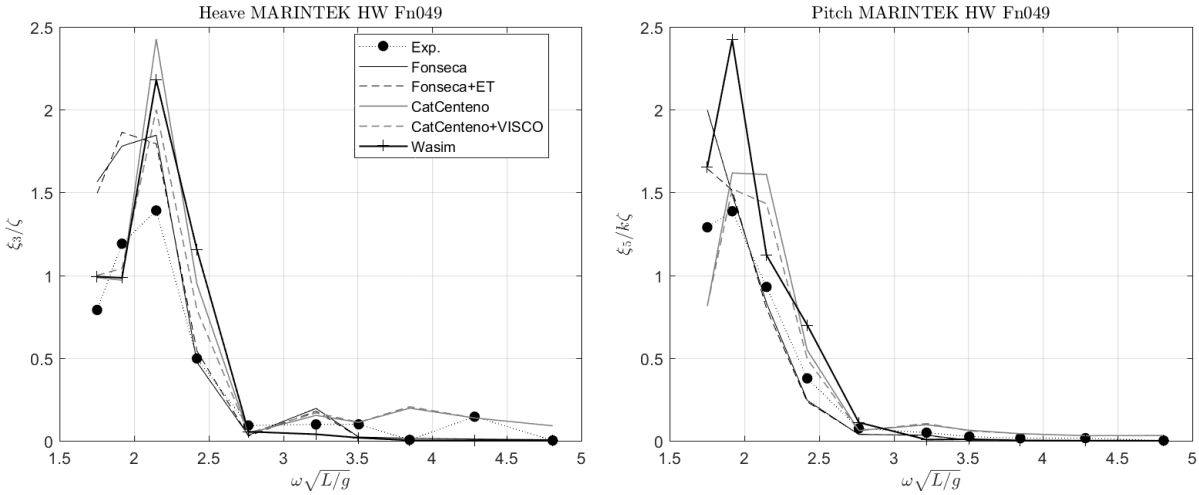

Figure A.18: Motion RAO, MARINTEK, $Fn = 0.49$, $\beta = 180°$, $S/L = 0.199$, $Int = 0.62$.

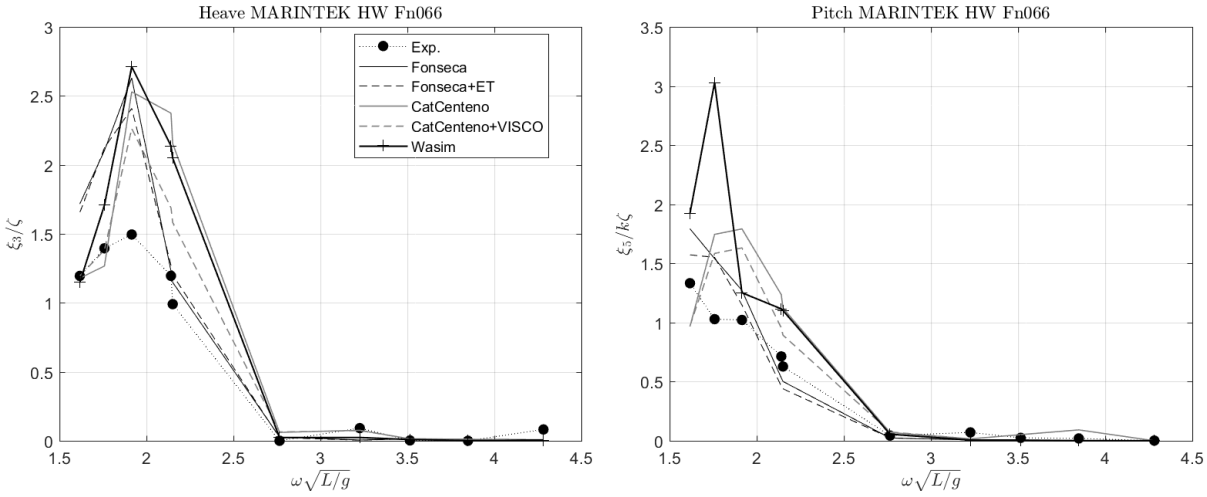

Figure A.19: Motion RAO, MARINTEK, $Fn = 0.66$, $\beta = 180°$, $S/L = 0.199$, $Int = 0.49$.

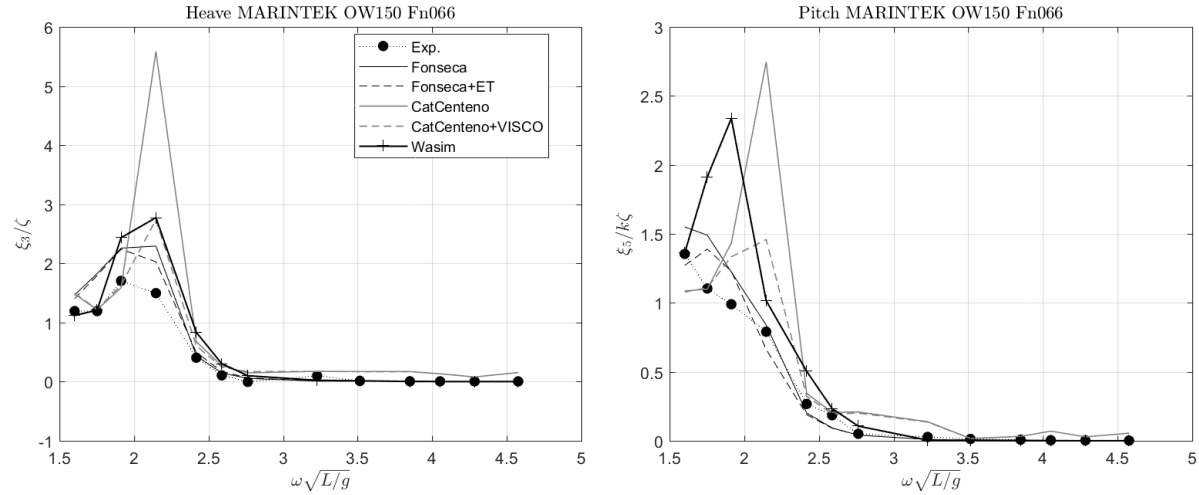

Figure A.20: Motion RAO, MARINTEK, $Fn = 0.66$, $\beta = 150°$, $S/L = 0.199$, $Int = 0.49$.

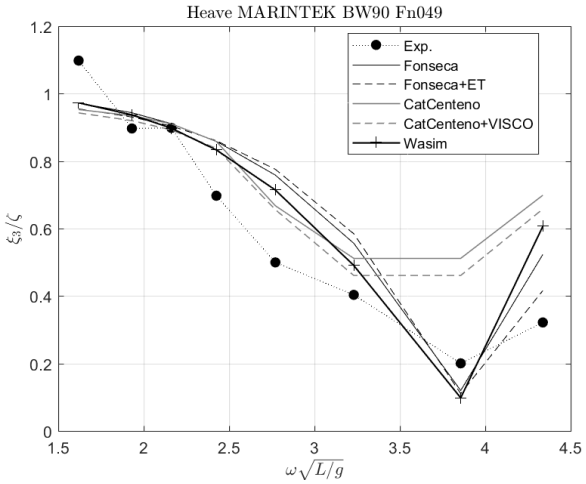

Figure A.21: Motion RAO, MARINTEK, $Fn = 0.49$, $\beta = 90°$, $S/L = 0.199$, $Int = 0.62$.

A.5 DELFT 372

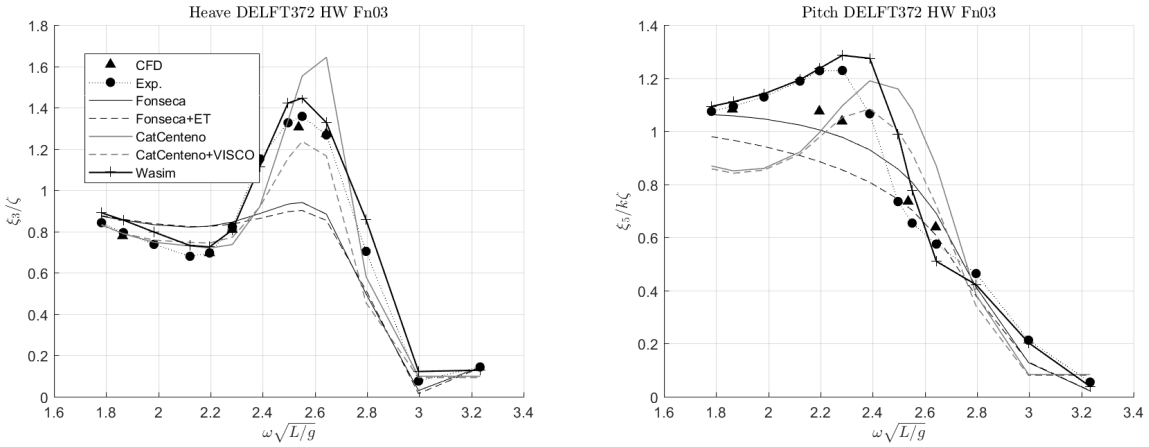

Figure A.22: Motion RAO, DELFT 372, $Fn = 0.3$, $\beta = 180°$, $S/L = 0.233$, $Int = 0.70$.

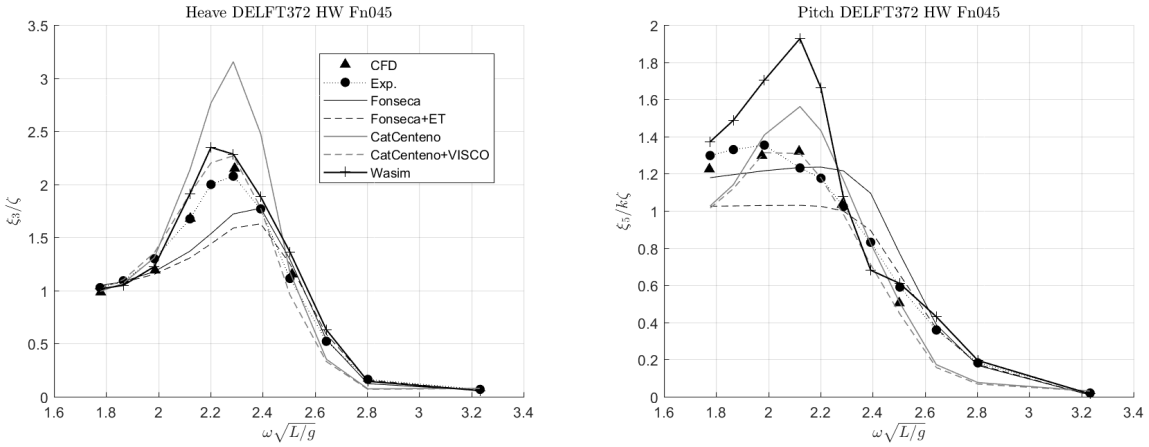

Figure A.23: Motion RAO, DELFT 372, $Fn = 0.45$, $\beta = 180°$, $S/L = 0.233$, $Int = 0.54$.

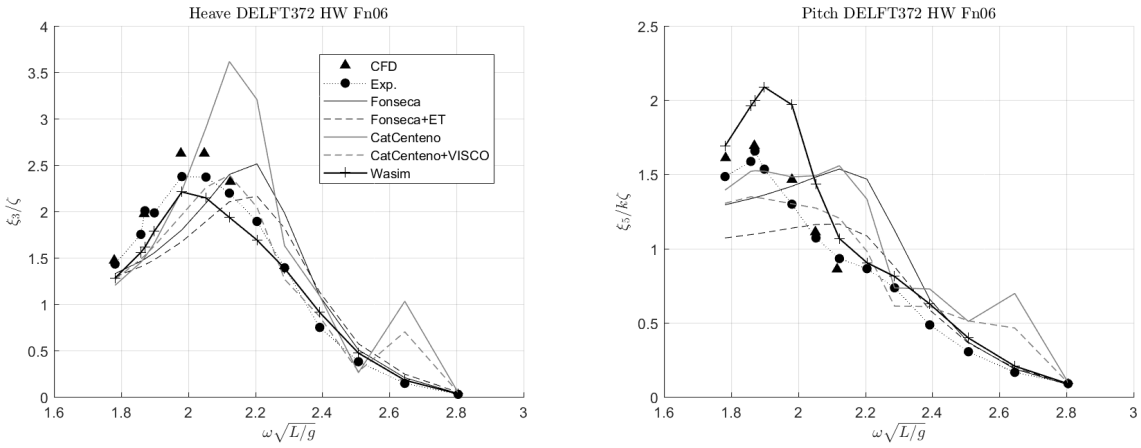

Figure A.24: Motion RAO, DELFT 372, $Fn = 0.6$, $\beta = 180°$, $S/L = 0.233$, $Int = 0.39$.

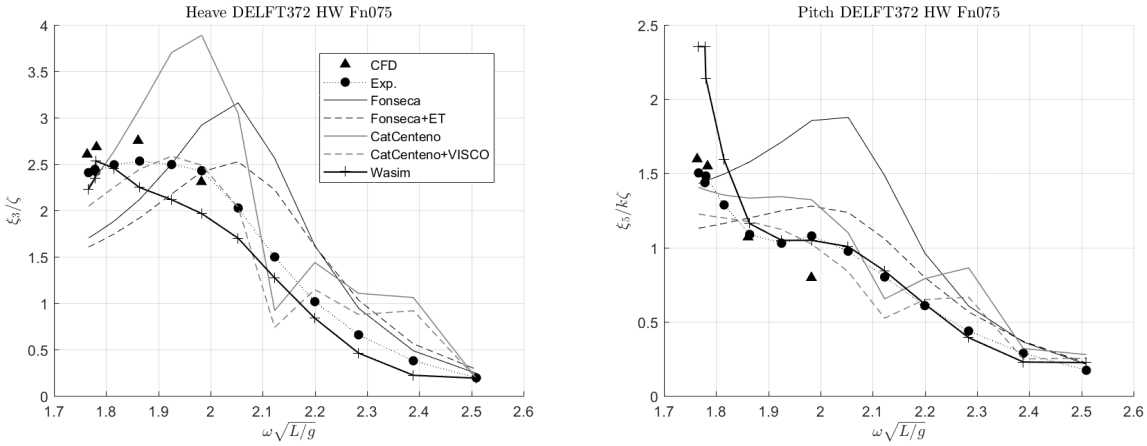

Figure A.25: Heave and Pitch, DELFT 372, $Fn = 0.75$, $\beta = 180°$, $S/L = 0.233$, $Int = 0.24$.

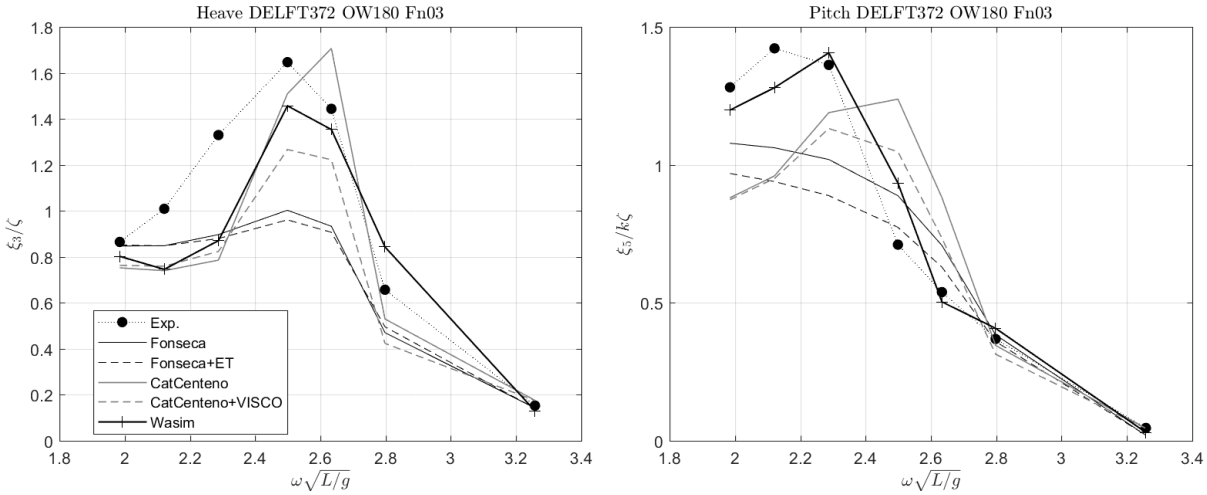

Figure A.26: Motion RAO, DELFT 372, $Fn = 0.3$, $\beta = 180°$, $S/L = 0.233$, $Int = 0.70$.

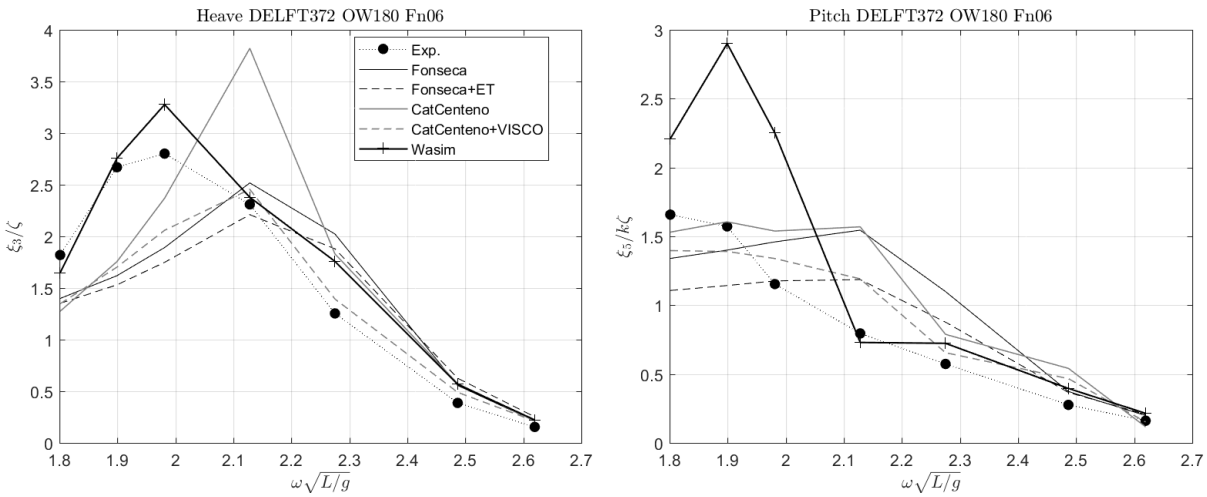

Figure A.27: Motion RAO, DELFT 372, $Fn = 0.6$, $\beta = 180°$, $S/L = 0.233$, $Int = 0.39$.

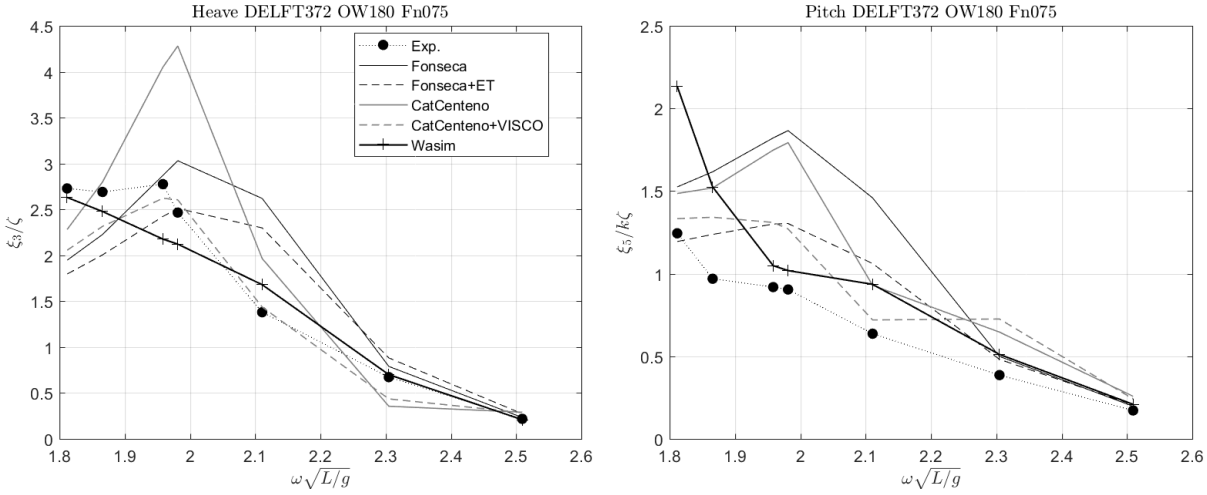

Figure A.28: Motion RAO, DELFT 372, $Fn = 0.75$, $\beta = 180°$, $S/L = 0.233$, $Int = 0.24$.

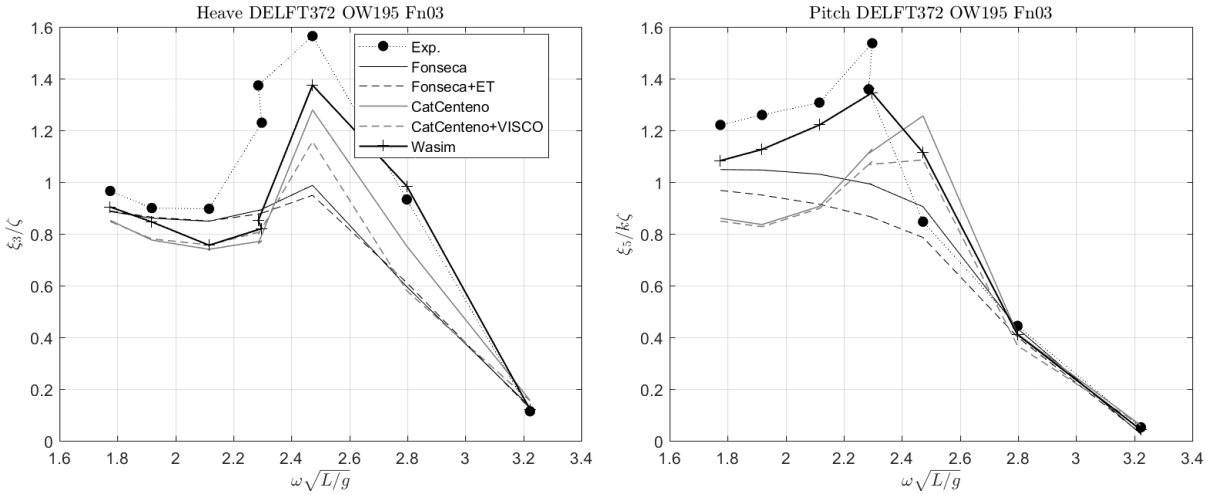

Figure A.29: Motion RAO, DELFT 372, $Fn = 0.3$, $\beta = 195°$, $S/L = 0.233$, $Int = 0.70$.

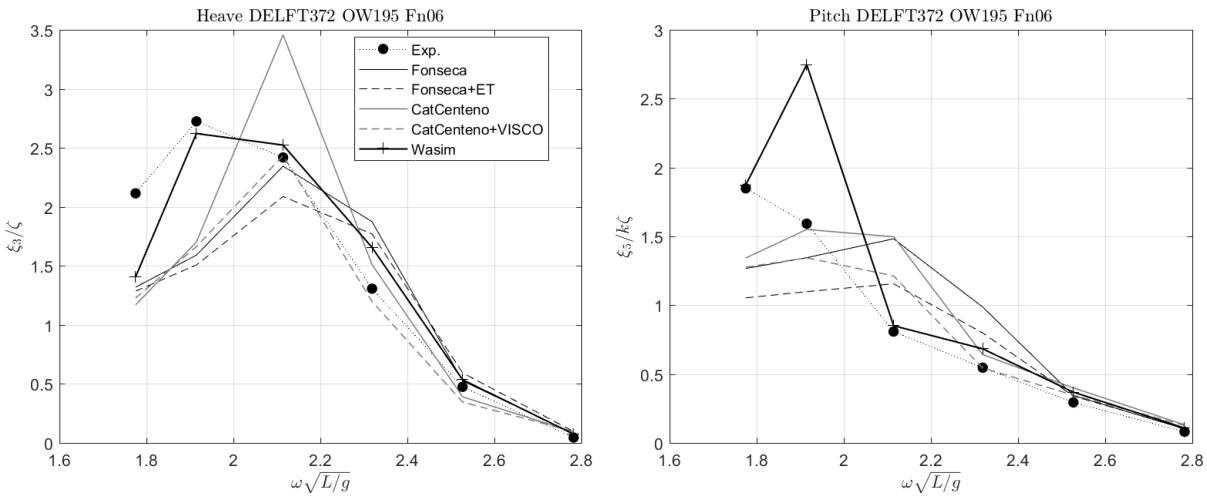

Figure A.30: Motion RAO, DELFT 372, $Fn = 0.6$, $\beta = 195°$, $S/L = 0.233$, $Int = 0.39$.

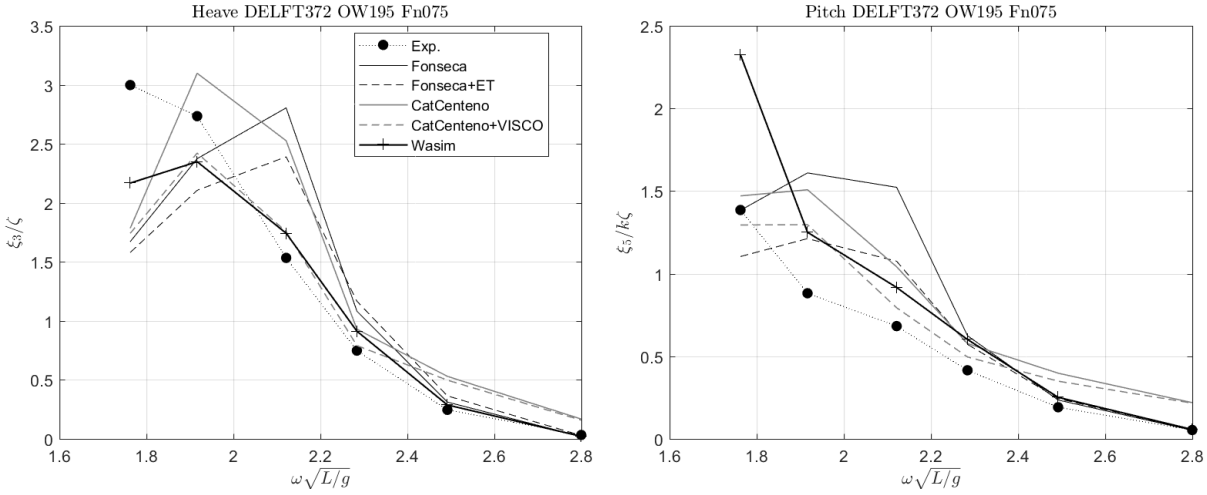

Figure A.31: Motion RAO, DELFT 372, $Fn = 0.75$, $\beta = 195°$, $S/L = 0.233$, $Int = 0.24$.

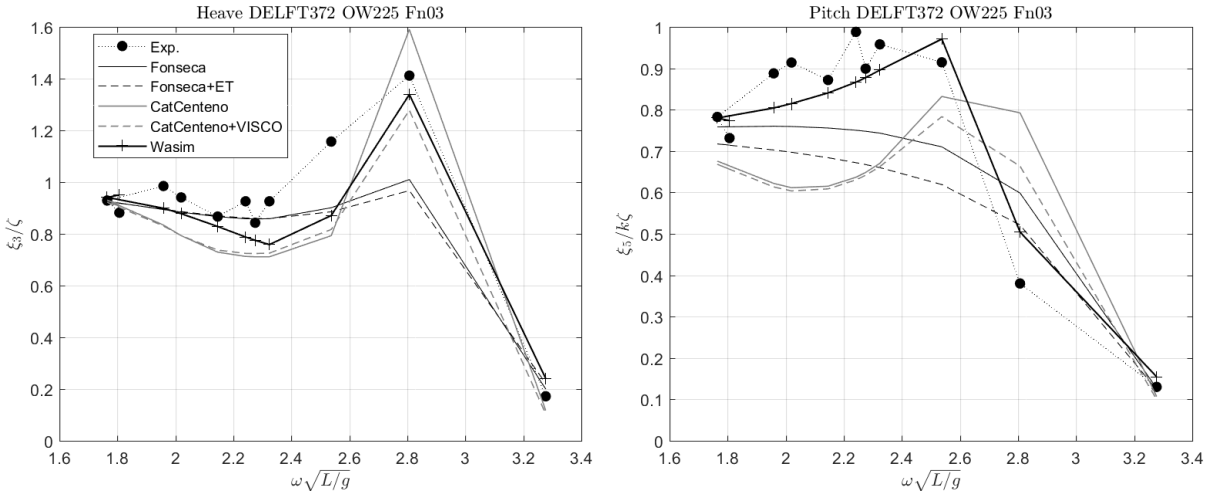

Figure A.32: Motion RAO, DELFT 372, $Fn = 0.3$, $\beta = 225°$, $S/L = 0.233$, $Int = 0.70$.

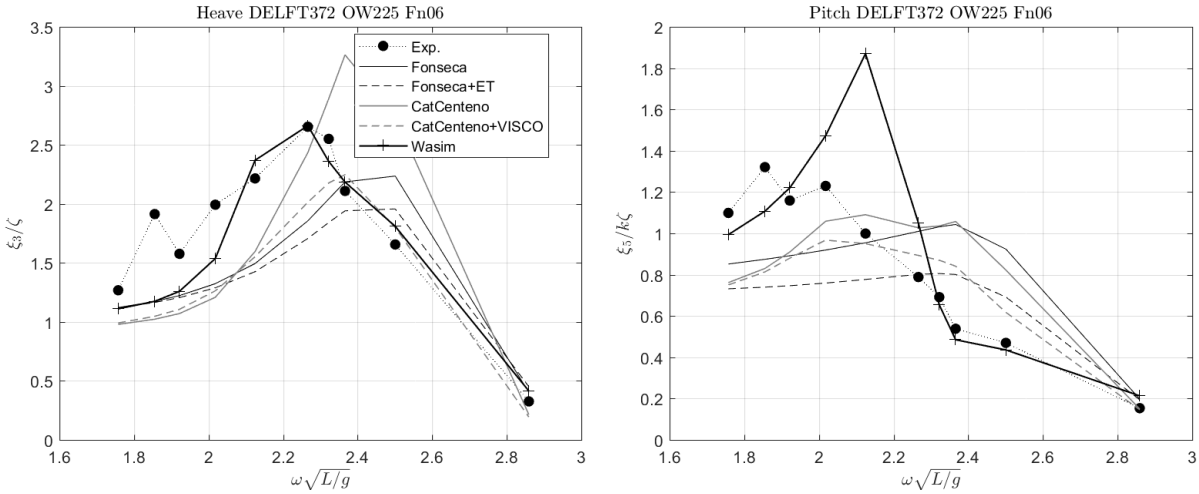

Figure A.33: Motion RAO, DELFT 372, $Fn = 0.6$, $\beta = 225°$, $S/L = 0.233$, $Int = 0.39$.

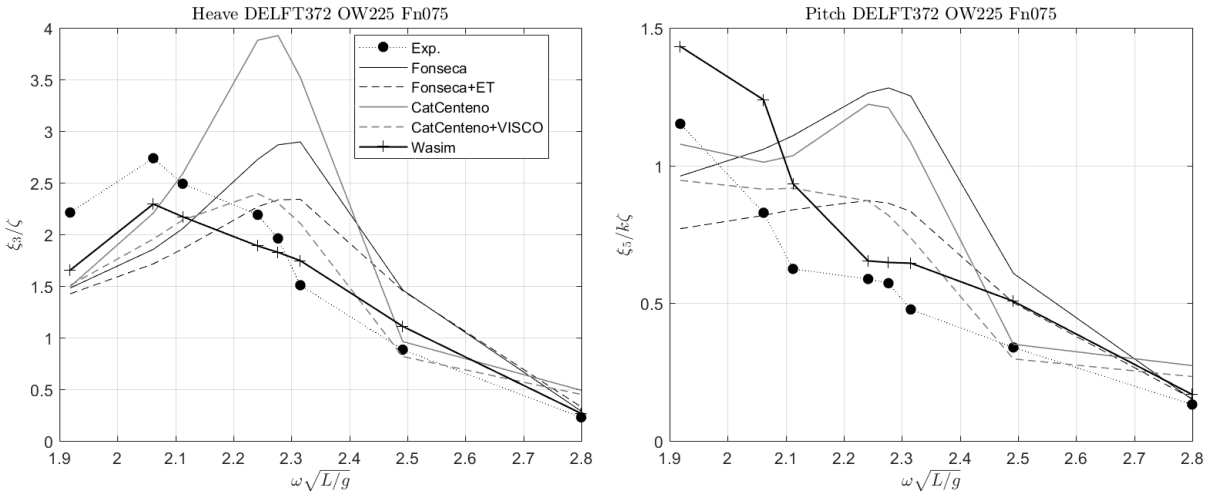

Figure A.34: Motion RAO, DELFT 372, $Fn = 0.75$, $\beta = 225°$, $S/L = 0.233$, $Int = 0.24$.

A.6 El Pardo

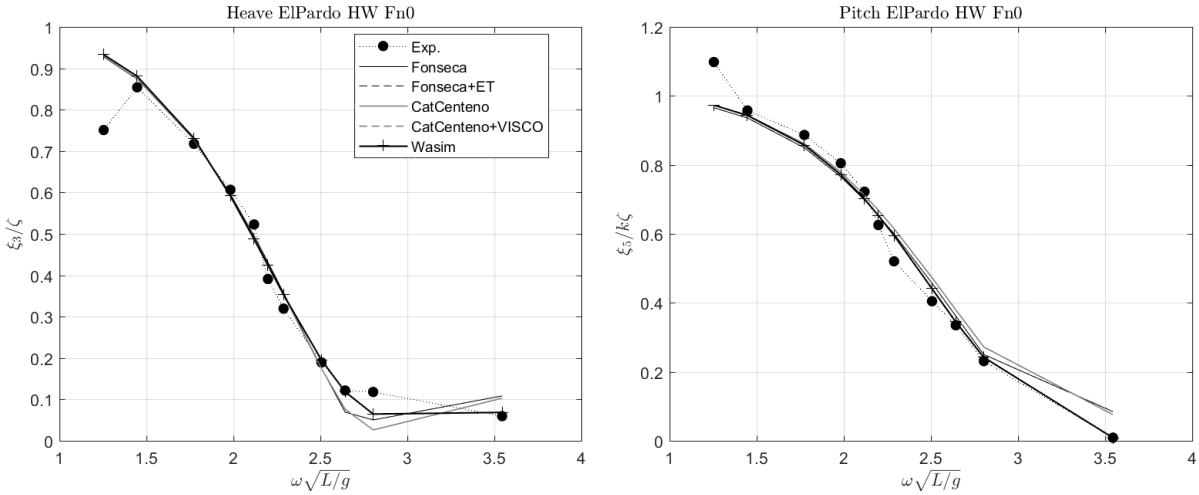

Figure A.35: Motion RAO, El Pardo, $Fn = 0.0$, $\beta = 180°$, $S/L = 0.2$, $Int = 1$.

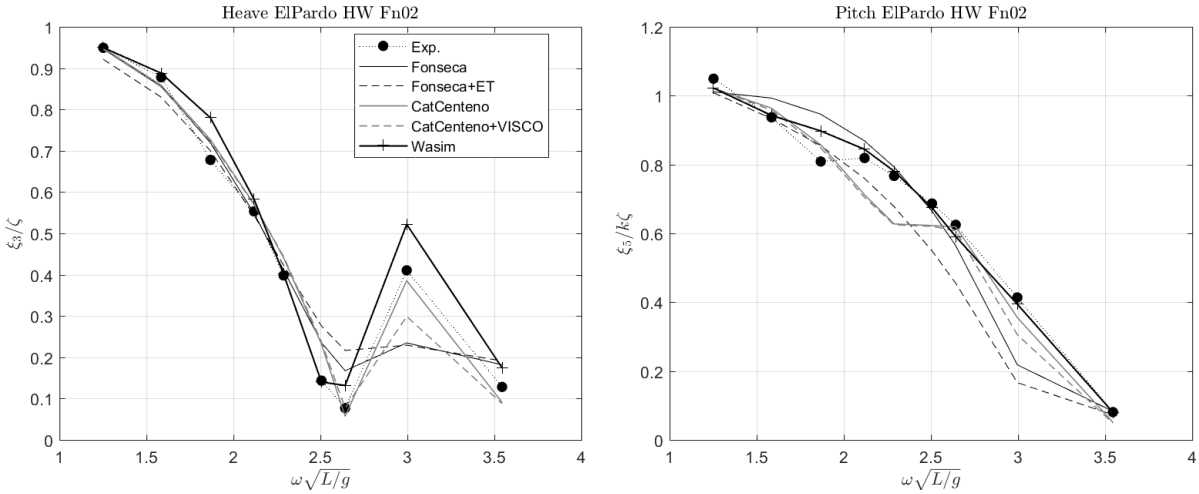

Figure A.36: Motion RAO, El Pardo, $Fn = 0.2$, $\beta = 180°$, $S/L = 0.2$, $Int = 0.81$.

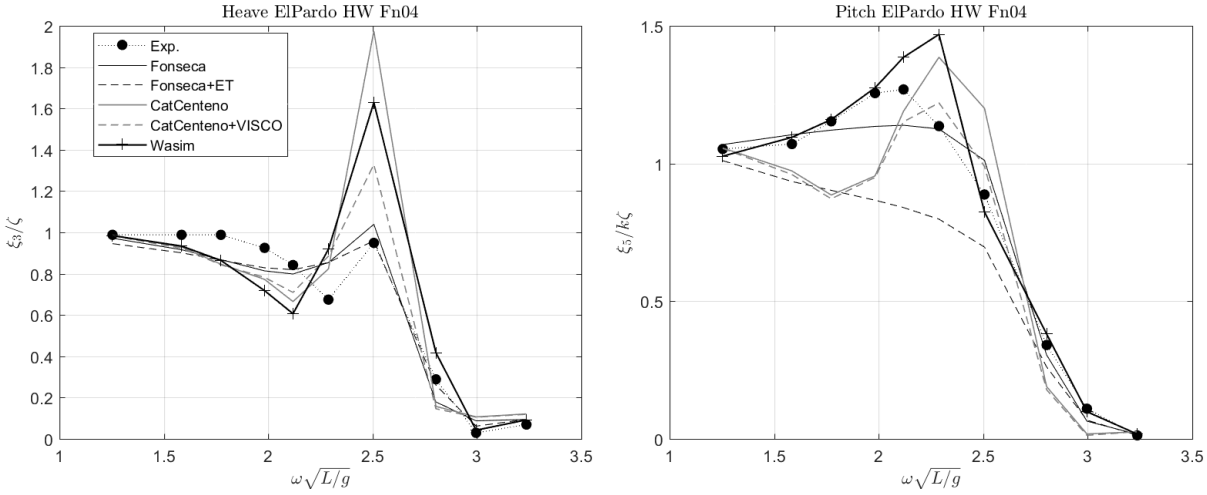

Figure A.37: Motion RAO, El Pardo, $Fn = 0.4$, $\beta = 180°$, $S/L = 0.2$, $Int = 0.63$.

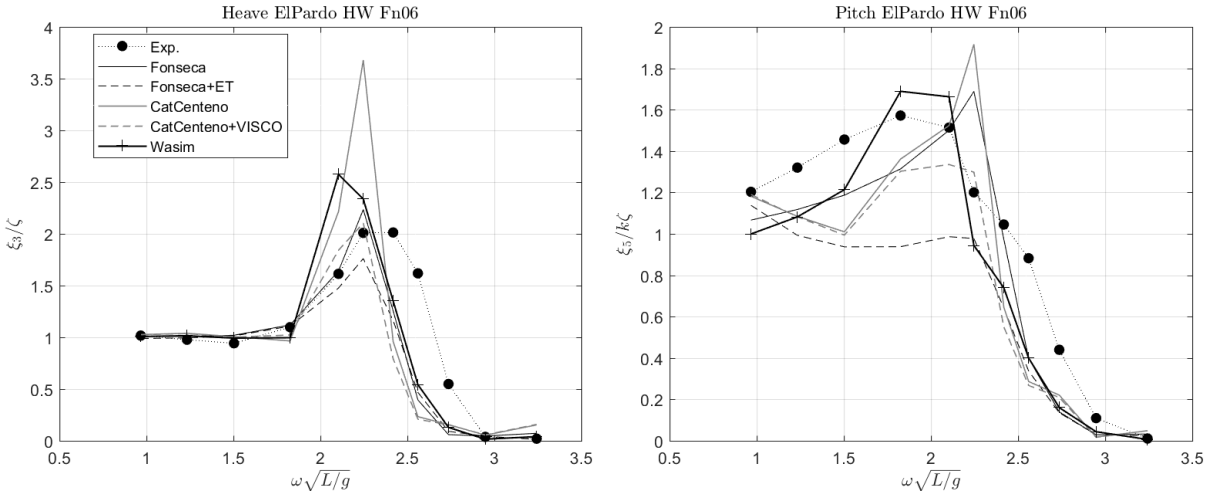

Figure A.38: Motion RAO, El Pardo, $Fn = 0.6$, $\beta = 180°$, $S/L = 0.2$, $Int = 0.44$.

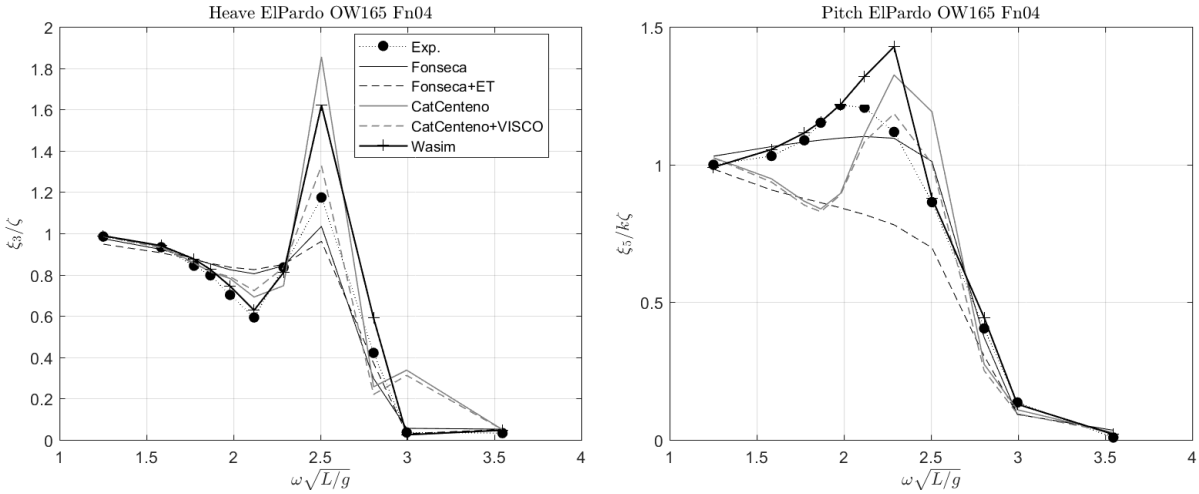

Figure A.39: Motion RAO, El Pardo, $Fn = 0.4$, $\beta = 165°$, $S/L = 0.2$, $Int = 0.63$.

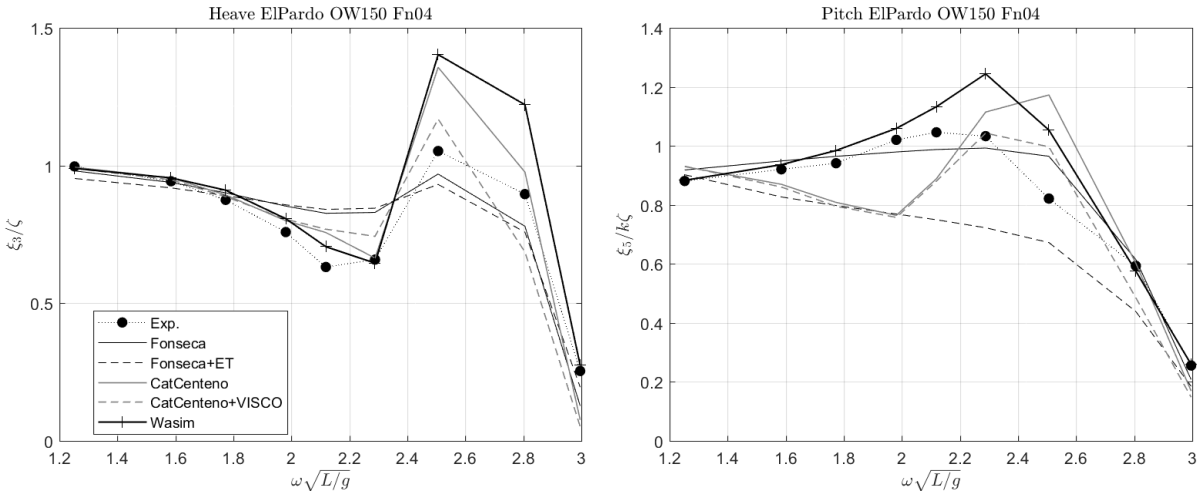

Figure A.40: Motion RAO, El Pardo, $Fn = 0.4$, $\beta = 150°$, $S/L = 0.2$, $Int = 0.63$.

A.7 VOSPER

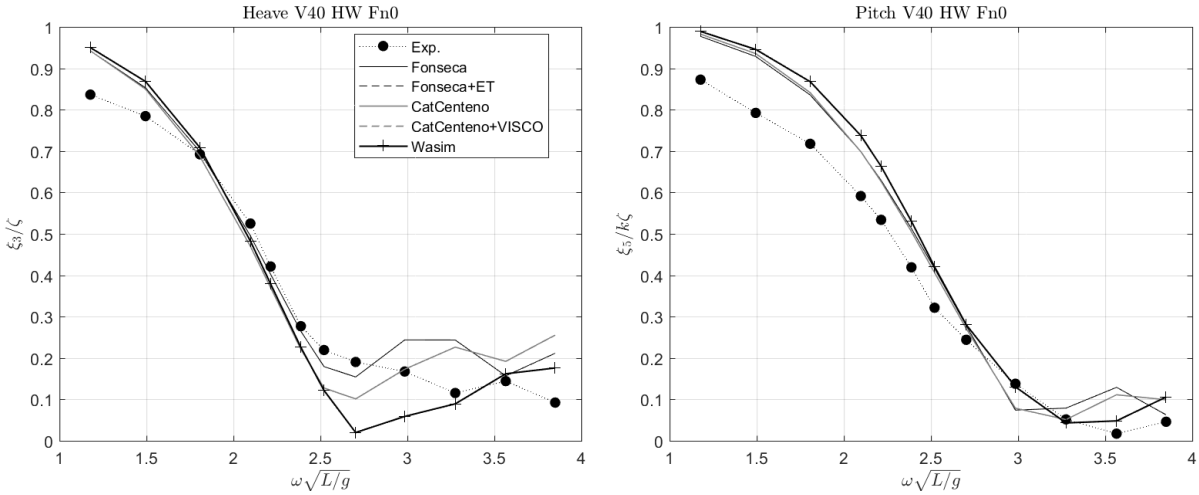

Figure A.41: Motion RAO, VOSPER V40, $Fn = 0.0$, $\beta = 180°$, $S/L = 0.195$, $Int = 1$.

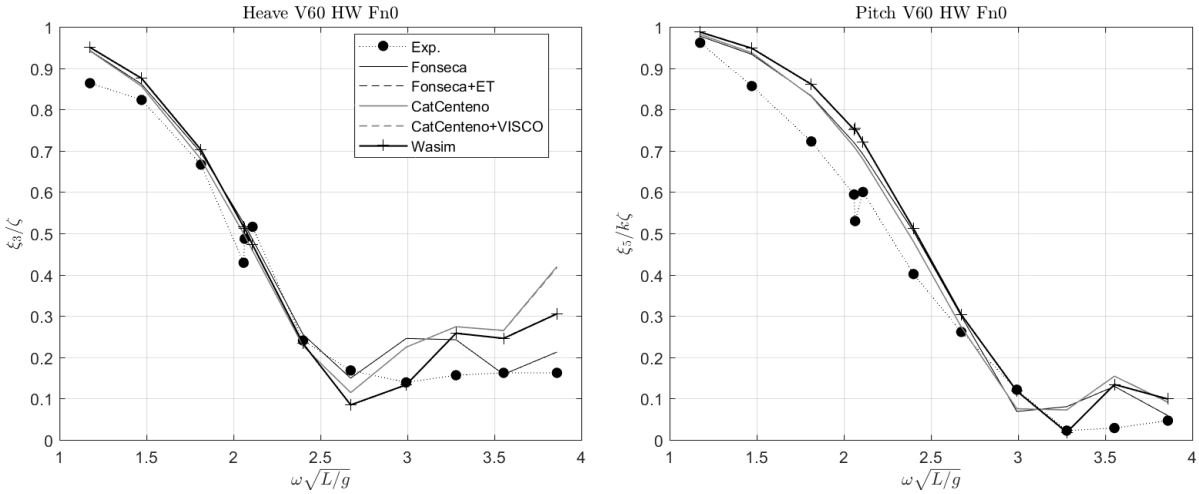

Figure A.42: Motion RAO, VOSPER V60, $Fn = 0.0$, $\beta = 180°$, $S/L = 0.293$, $Int = 1$.

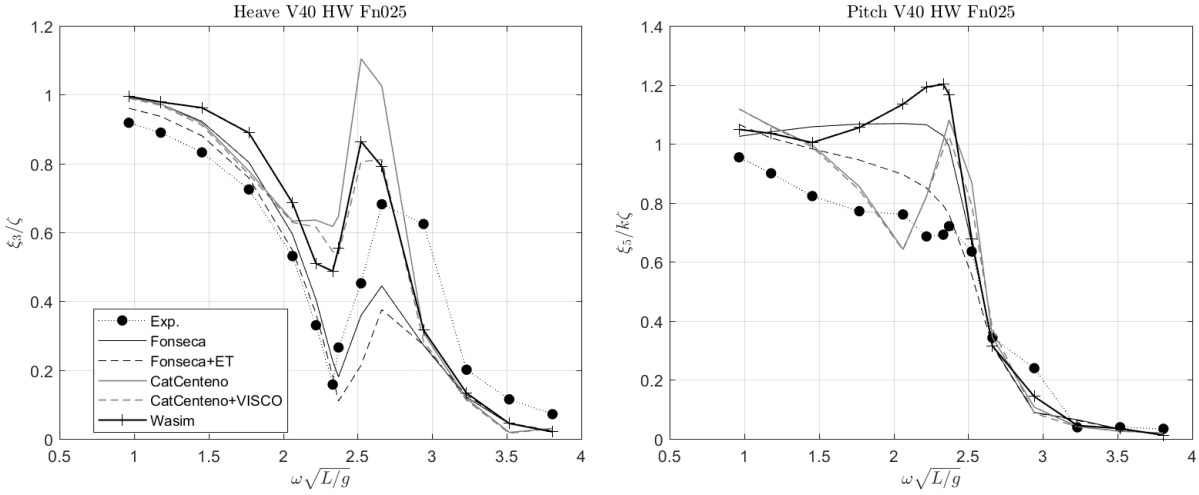

Figure A.43: Motion RAO, VOSPER V40, $Fn = 0.25$, $\beta = 180°$, $S/L = 0.195$, $Int = 0.81$.

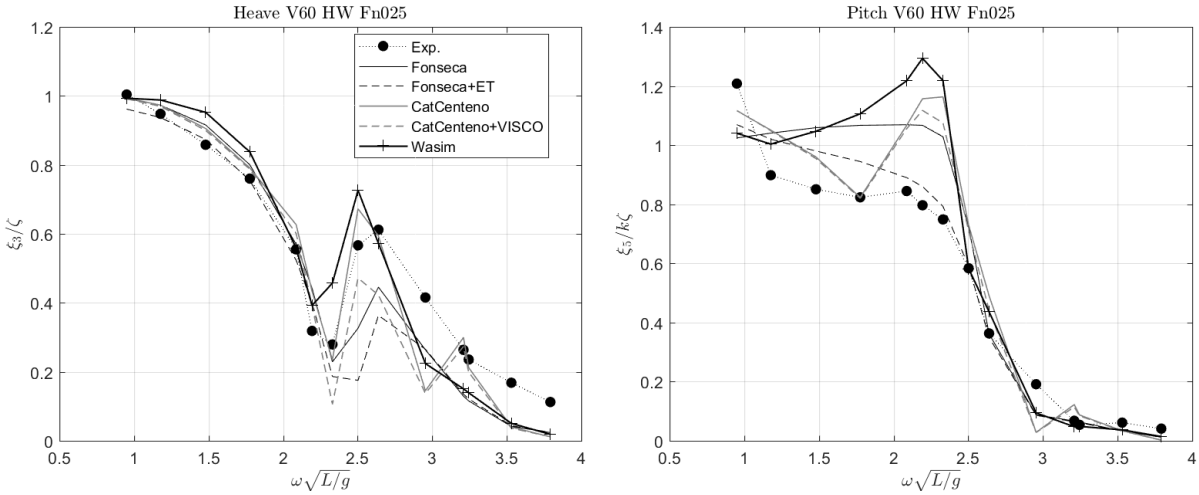

Figure A.44: Motion RAO, VOSPER V60, $Fn = 0.25$, $\beta = 180°$, $S/L = 0.293$, $Int = 0.72$.

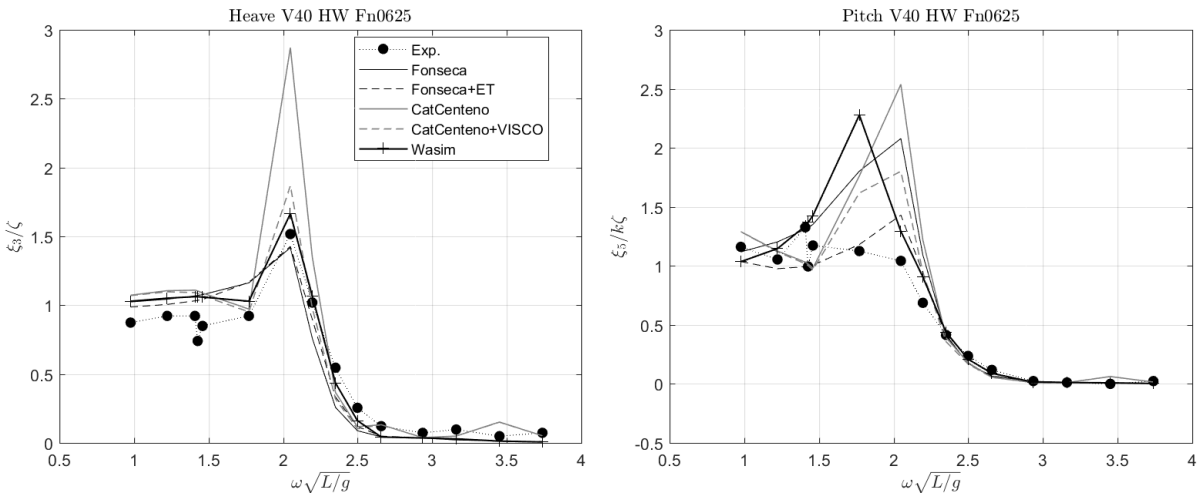

Figure A.45: Motion RAO, VOSPER V40, $Fn = 0.625$, $\beta = 180°$, $S/L = 0.195$, $Int = 0.53$.

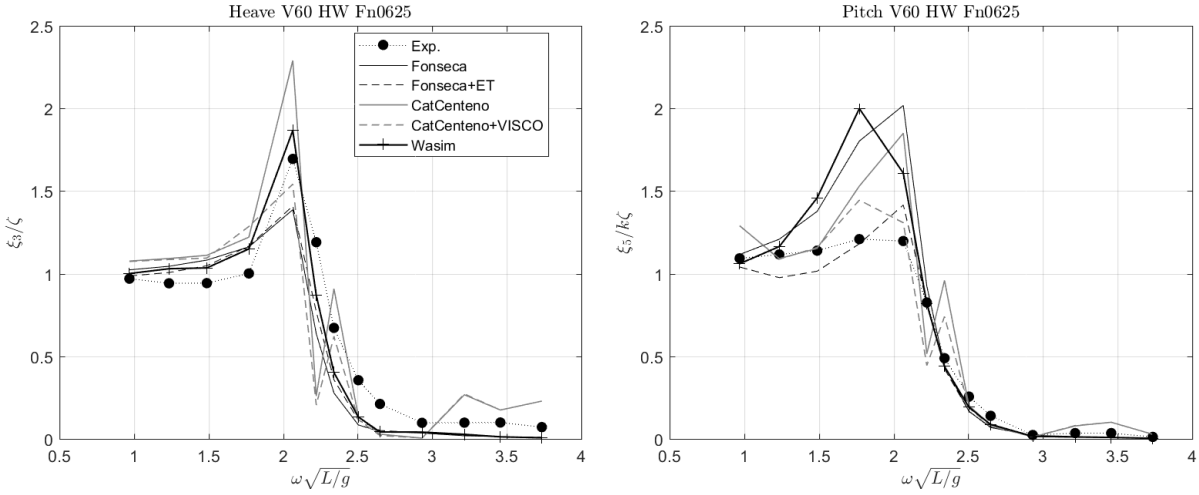

Figure A.46: Motion RAO, VOSPER V60, $Fn = 0.625$, $\beta = 180°$, $S/L = 0.293$, $Int = 0.29$.

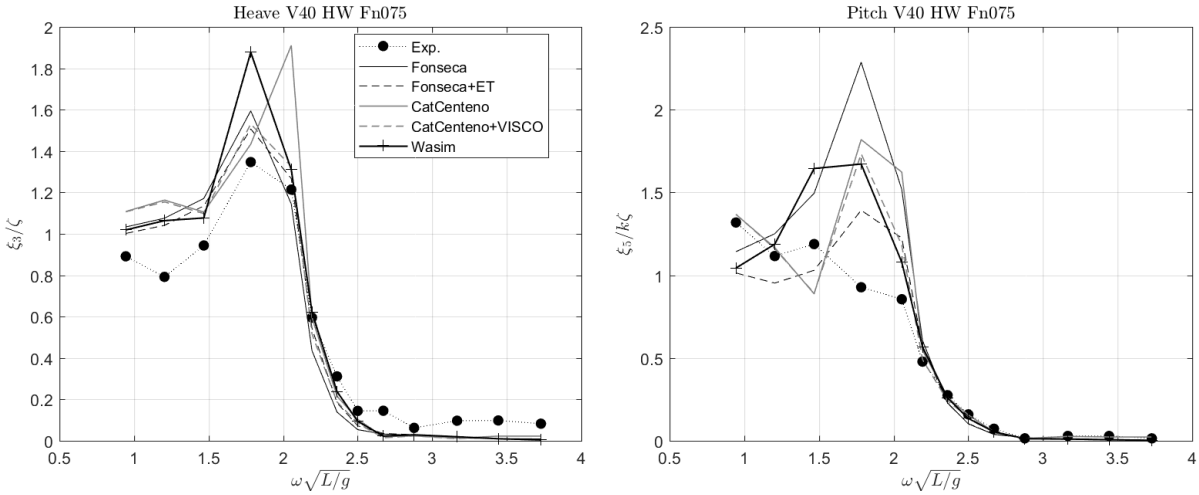

Figure A.47: Motion RAO, VOSPER V40, $Fn = 0.75$, $\beta = 180°$, $S/L = 0.195$, $Int = 0.43$.

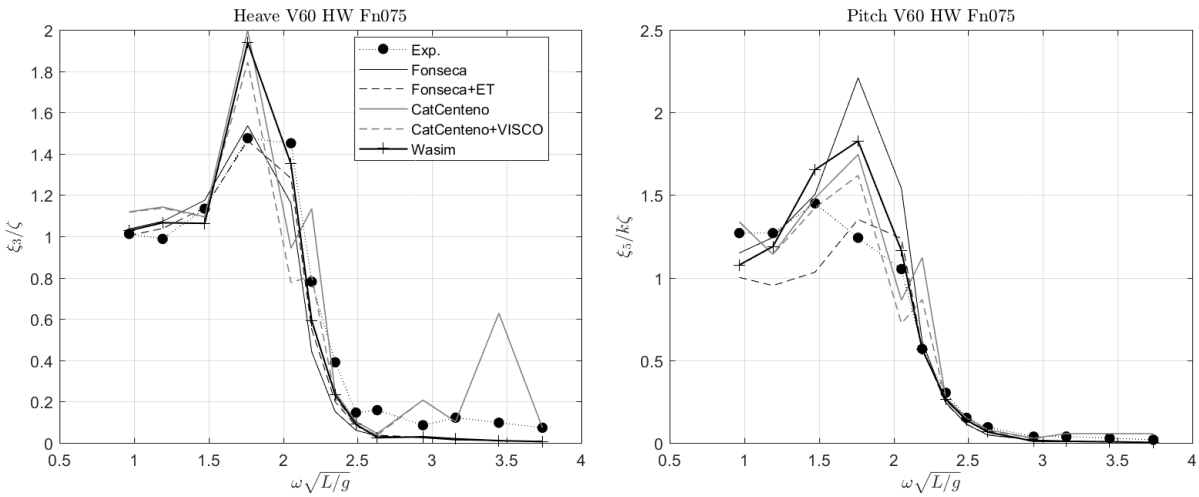

Figure A.48: Motion RAO, VOSPER V60, $Fn = 0.75$, $\beta = 180°$, $S/L = 0.293$, $Int = 0.15$.

A.8 Roll motion RAO

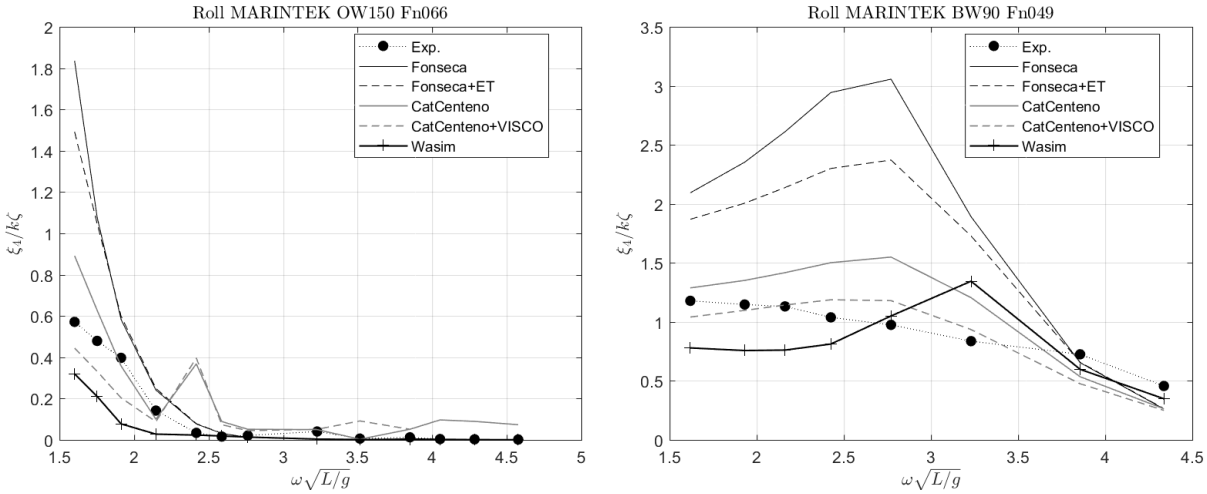

Figure A.49: Motion RAO (Roll), MARINTEK, $Fn = 0.66$, $\beta = 150°$ (left) and $Fn = 0.49$, $\beta = 90°$ (right).

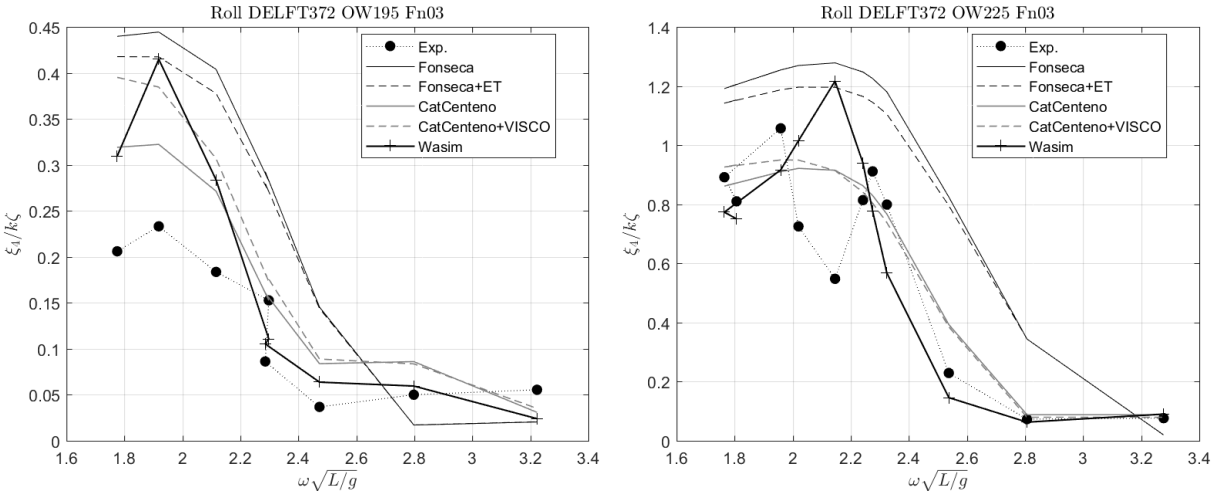

Figure A.50: Motion RAO (Roll) DELFT 372, $Fn = 0.3$, $\beta = 195, 225°$, $S/L = 0.233$, $Int = 0.70$.

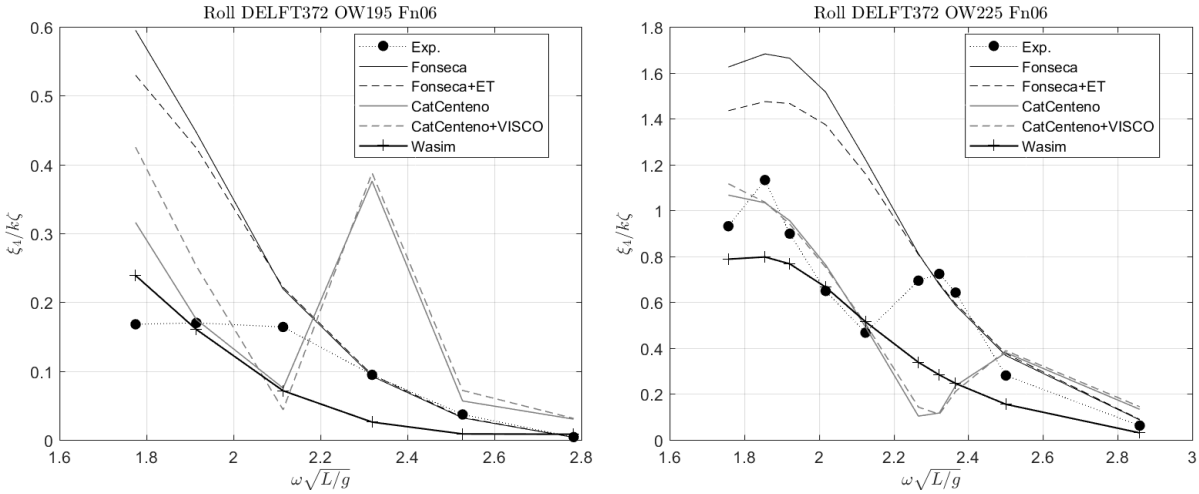

Figure A.51: Motion RAO (Roll) DELFT 372, $Fn = 0.6$, $\beta = 195, 225°$, $S/L = 0.233$, $Int = 0.39$.

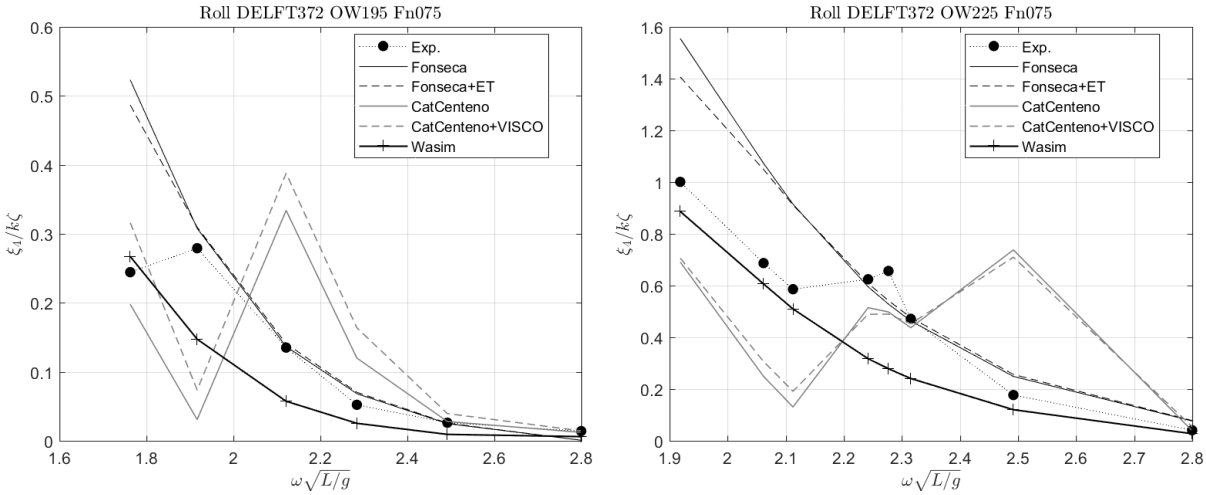

Figure A.52: Motion RAO (Roll) DELFT 372, $Fn = 0.75$, $\beta = 195, 225°$, $S/L = 0.233$, $Int = 0.24$.

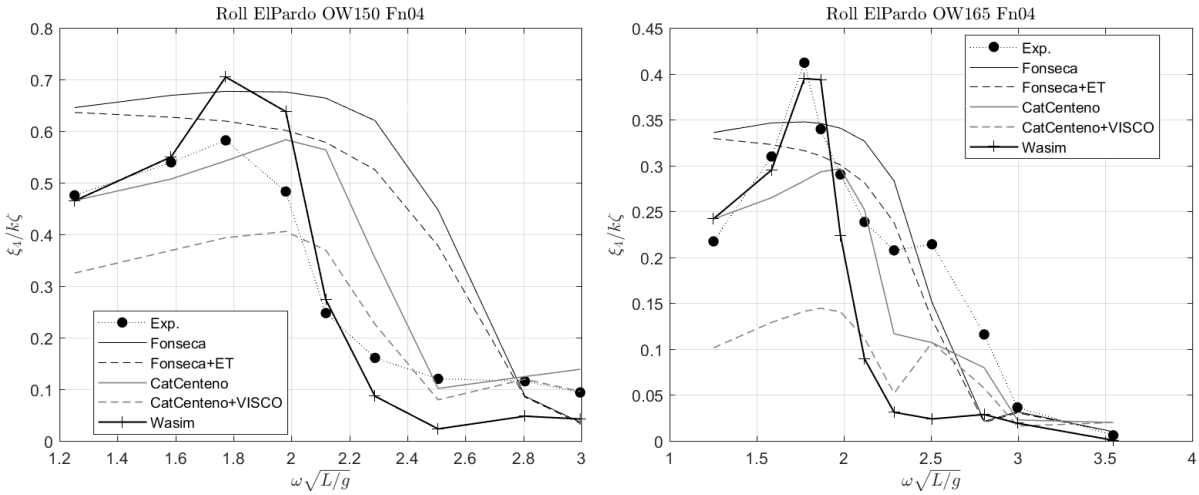

Figure A.53: Motion RAO (Roll), El Pardo, $Fn = 0.4$, $\beta = 150°$ (left) $\beta = 165°$ (right), $S/L = 0.2$, $Int = 0.63$.

Appendix B

Root mean square error tables

$$e_j = \sqrt{\frac{1}{N}\sum_{i=1}^{N}(X_i - H_i)^2} \tag{B.1}$$

Being X_i the experimental data, considered to be the correct one. The computations results are expressed as H_i, which differ of method. Belongs to the performance metrics widely used by authors to quantify the error with more significance to the bigger differences since it is the squared.

B.1 Heave and Pitch motions RMSE

Table B.1: Root mean square error for heave and pitch motions, NPL 4b round bilge.

			Catamaran model: NPL 4b $S/L = 0.20$									
			Fonseca		Fonseca+ET		CatCen		CatCen+visco		Wasim	
Fn	β	Int	e_3	e_5	e_3	e_5	e_3	e_5	e_3	e_5	e_3	e_5
0.20	180	0.83	0.14	0.14	0.15	0.16	0.14	0.11	0.15	0.12	0.06	0.06
0.53	180	0.56	0.14	0.39	0.11	0.23	0.59	0.53	0.26	0.38	0.20	0.48

			Catamaran model: NPL 4b $S/L = 0.40$									
			Fonseca		Fonseca+ET		CatCen		CatCen+visco		Wasim	
Fn	β	Int	e_3	e_5	e_3	e_5	e_3	e_5	e_3	e_5	e_3	e_5
0.20	180	0.67	0.07	0.10	0.08	0.11	0.22	0.16	0.20	0.16	0.10	0.07
0.53	180	0.12	0.16	0.20	0.10	0.22	0.52	0.30	0.39	0.24	0.38	0.28
0.80	180	$NoInt$	0.26	0.51	0.22	0.32	0.48	0.23	0.47	0.20	0.38	0.26

Table B.2: Root mean square error for heave and pitch motions, NPL 5b round bilge.

			Catamaran model: NPL 5b $S/L = 0.20$									
			Fonseca		Fonseca+ET		CatCen		CatCen+visco		Wasim	
Fn	β	Int	e_3	e_5	e_3	e_5	e_3	e_5	e_3	e_5	e_3	e_5
0.20	180	0.81	0.13	0.16	0.13	0.18	0.13	0.15	0.13	0.16	0.09	0.10
0.53	180	0.51	0.15	0.23	0.20	0.31	0.33	0.35	0.11	0.29	0.10	0.18
0.80	180	0.26	0.29	0.52	0.29	0.40	0.68	0.48	0.20	0.30	0.20	0.21

			Catamaran model: NPL 5b $S/L = 0.40$									
			Fonseca		Fonseca+ET		CatCen		CatCen+visco		Wasim	
Fn	β	Int	e_3	e_5	e_3	e_5	e_3	e_5	e_3	e_5	e_3	e_5
0.20	180	0.63	0.05	0.08	0.05	0.11	0.13	0.14	0.11	0.14	0.04	0.06
0.53	180	0.02	0.13	0.22	0.13	0.30	0.74	0.47	0.51	0.41	0.64	0.66
0.80	180	$NoInt$	0.30	0.52	0.27	0.36	0.70	0.46	0.51	0.36	0.42	0.32

Table B.3: Root mean square error for heave and pitch motions, NPL 6b round bilge.

			Catamaran model: NPL 6b $S/L = 0.20$									
			Fonseca		Fonseca+ET		CatCen		CatCen+visco		Wasim	
Fn	β	Int	e_3	e_5	e_3	e_5	e_3	e_5	e_3	e_5	e_3	e_5
0.20	180	0.80	0.05	0.10	0.05	0.11	0.09	0.11	0.08	0.11	0.07	0.07
0.53	180	0.47	0.17	0.08	0.15	0.20	0.42	0.15	0.25	0.16	0.24	0.14
0.80	180	0.20	0.19	0.45	0.19	0.23	0.54	0.32	0.14	0.12	0.32	0.26

			Catamaran model: NPL 6b $S/L = 40$									
			Fonseca		Fonseca+ET		CatCen		CatCen+visco		Wasim	
Fn	β	Int	e_3	e_5	e_3	e_5	e_3	e_5	e_3	e_5	e_3	e_5
0.20	180	0.60	0.04	0.15	0.04	0.18	0.21	0.19	0.19	0.19	0.02	0.15
0.53	180	$NoInt$	0.17	0.09	0.15	0.26	0.56	0.34	0.30	0.31	0.18	0.17
0.80	180	$NoInt$	0.21	0.27	0.20	0.24	0.71	0.52	0.31	0.25	0.38	0.25

Table B.4: Root mean square error for heave and pitch motions, MARINTEK.

			Catamaran model: MARINTEK $S/L = 0.20$									
			Fonseca		Fonseca+ET		CatCen		CatCen+visco		Wasim	
Fn	β	Int	e_3	e_5	e_3	e_5	e_3	e_5	e_3	e_5	e_3	e_5
0.49	180	0.62	0.35	0.23	0.34	0.13	0.38	0.28	0.24	0.23	0.34	0.37
0.66	180	0.49	0.46	0.24	0.41	0.21	0.62	0.42	0.35	0.31	0.60	0.69
0.66	150	0.49	0.33	0.14	0.28	0.12	1.14	0.56	0.38	0.23	0.43	0.45
0.49	90	0.62	0.15	...	0.15	...	0.20	...	0.18	...	0.15	...

Table B.5: Root mean square error for heave and pitch motions, Delft 372.

			Catamaran model: Delft 372 $S/L = 0.23$									
			Fonseca		Fonseca+ET		CatCen		CatCen+visco		Wasim	
Fn	β	Int	e_3	e_5	e_3	e_5	e_3	e_5	e_3	e_5	e_3	e_5
0.30	180	0.70	0.22	0.13	0.24	0.19	0.14	0.25	0.12	0.21	0.07	0.10
0.60	180	0.39	0.38	0.32	0.38	0.29	0.65	0.31	0.28	0.20	0.19	0.31
0.45	180	0.54	0.21	0.13	0.26	0.18	0.48	0.18	0.14	0.14	0.17	0.29
0.75	180	0.24	0.63	0.46	0.57	0.23	0.69	0.20	0.32	0.17	0.24	0.40
0.30	180	0.70	0.36	0.22	0.38	0.28	0.26	0.34	0.29	0.29	0.23	0.11
0.60	180	0.39	0.63	0.39	0.66	0.33	0.75	0.36	0.50	0.22	0.28	0.69
0.75	180	0.24	0.62	0.65	0.58	0.29	0.89	0.53	0.32	0.28	0.30	0.42
0.30	195	0.70	0.32	0.27	0.33	0.36	0.31	0.33	0.33	0.33	0.25	0.14
0.60	195	0.39	0.61	0.42	0.65	0.42	0.72	0.35	0.57	0.31	0.33	0.48
0.75	195	0.24	0.78	0.46	0.75	0.25	0.67	0.32	0.55	0.20	0.39	0.43
0.30	225	0.70	0.15	0.16	0.16	0.21	0.18	0.25	0.16	0.24	0.12	0.07
0.60	225	0.39	0.54	0.33	0.58	0.32	0.69	0.32	0.51	0.26	0.31	0.31
0.75	225	0.24	0.78	0.49	0.64	0.25	1.21	0.42	0.48	0.21	0.32	0.23

Table B.6: Root mean square error for heave and pitch motions, El Pardo.

			Catamaran model: El Pardo $S/L = 0.20$									
			Fonseca		Fonseca+ET		CatCen		CatCen+visco		Wasim	
Fn	β	Int	e_3	e_5	e_3	e_5	e_3	e_5	e_3	e_5	e_3	e_5
0.00	180	1.00	0.06	0.06	0.06	0.06	0.07	0.06	0.07	0.06	0.06	0.05
0.20	180	0.81	0.08	0.09	0.09	0.12	0.04	0.07	0.06	0.08	0.06	0.04
0.40	180	0.63	0.10	0.07	0.08	0.24	0.34	0.19	0.17	0.16	0.26	0.11
0.40	165	0.63	0.10	0.07	0.11	0.23	0.23	0.20	0.12	0.18	0.15	0.10
0.40	150	0.63	0.11	0.06	0.12	0.19	0.13	0.17	0.12	0.14	0.16	0.11
0.60	180	0.44	0.46	0.27	0.46	0.39	0.76	0.35	0.58	0.31	0.51	0.25

Table B.7: Root mean square error for heave and pitch motions, Vosper.

			Catamaran model: Vosper V40 $S/L = 0.20$									
			Fonseca		Fonseca+ET		CatCen		CatCen+visco		Wasim	
Fn	β	Int	e_3	e_5	e_3	e_5	e_3	e_5	e_3	e_5	e_3	e_5
0.00	180	1.00	0.07	0.09	0.07	0.09	0.08	0.09	0.08	0.09	0.08	0.10
0.25	180	0.81	0.13	0.21	0.15	0.11	0.29	0.17	0.21	0.16	0.21	0.27
0.63	180	0.53	0.18	0.35	0.15	0.16	0.39	0.45	0.18	0.27	0.14	0.33
0.75	180	0.43	0.16	0.43	0.12	0.20	0.24	0.34	0.15	0.26	0.18	0.26

			Catamaran model: Vosper V60 $S/L = 0.29$									
			Fonseca		Fonseca+ET		CatCen		CatCen+visco		Wasim	
Fn	β	Int	e_3	e_5	e_3	e_5	e_3	e_5	e_3	e_5	e_3	e_5
0.00	180	1.00	0.06	0.09	0.06	0.09	0.10	0.09	0.10	0.09	0.07	0.11
0.25	180	0.72	0.12	0.17	0.15	0.08	0.10	0.18	0.12	0.16	0.11	0.24
0.63	180	0.29	0.24	0.29	0.20	0.09	0.34	0.26	0.32	0.16	0.16	0.26
0.75	180	0.15	0.16	0.30	0.11	0.18	0.28	0.22	0.27	0.17	0.16	0.19

B.2 Roll mode of motion RMSE

Table B.8: Root mean square error for roll motion.

		Catamaran model: Delft 372				
		Fonseca	Fonseca+ET	CatCen	CatCen+visco	Wasim
Fn	β	e_4	e_4	e_4	e_4	e_4
0.30	195	0.17	0.15	0.07	0.10	0.08
0.60	195	0.21	0.18	0.14	0.17	0.06
0.75	195	0.11	0.10	0.13	0.14	0.06
0.30	225	0.42	0.37	0.15	0.15	0.25
0.60	225	0.52	0.42	0.31	0.31	0.25
0.75	225	0.27	0.23	0.33	0.30	0.20

		Catamaran model: MARINTEK				
		Fonseca	Fonseca+ET	CatCen	CatCen+visco	Wasim
Fn	β	e_4	e_4	e_4	e_4	e_4
0.66	150	0.39	0.31	0.14	0.14	0.14
0.49	90	1.30	0.91	0.33	0.16	0.31

		Catamaran model: El Pardo				
		Fonseca	Fonseca+ET	CatCen	CatCen+visco	Wasim
Fn	β	e_4	e_4	e_4	e_4	e_4
0.40	165	0.07	0.06	0.06	0.15	0.10
0.40	150	0.26	0.20	0.13	0.11	0.08

Appendix C

Frequency independent model error tables

Following the formulation from 7.1 the resulting values for random variable a are obtained in each tested model and conditions.

C.1 Heave and pitch motions FIME

Table C.1: Frequency independent model error for heave and pitch motions, NPL 4b round bilge.

		Catamaran model: NPL 4b $S/L = 2$									
		Fonseca		Fonseca+ET		CatCen		CatCen+visco		Wasim	
Fn	β	$\hat{a_3}$	$\hat{a_5}$	$\hat{a_3}$	$\hat{a_5}$	$\hat{a_3}$	$\hat{a_5}$	$\hat{a_3}$	$\hat{a_5}$	$\hat{a_3}$	$\hat{a_5}$
0.20	180	0.96	1.04	0.95	1.15	0.94	1.14	0.94	1.16	0.92	1.06
0.53	180	0.91	0.76	0.96	1.06	0.69	0.71	0.86	0.83	0.85	0.69

		Catamaran model: NPL 4b $S/L = 4$									
		Fonseca		Fonseca+ET		CatCen		CatCen+visco		Wasim	
Fn	β	$\hat{a_3}$	$\hat{a_5}$	$\hat{a_3}$	$\hat{a_5}$	$\hat{a_3}$	$\hat{a_5}$	$\hat{a_3}$	$\hat{a_5}$	$\hat{a_3}$	$\hat{a_5}$
0.20	180	0.87	0.99	0.86	1.12	0.65	0.98	0.68	1.00	0.83	0.98
0.53	180	0.87	0.88	0.92	1.20	0.70	0.94	0.82	1.04	0.72	0.80
0.80	180	0.91	0.72	1.06	1.18	0.91	0.98	1.03	1.09	0.79	0.84

Table C.2: Frequency independent model error for heave and pitch motions, NPL 5b round bilge.

Catamaran model: NPL 5b $S/L = 2$

		Fonseca		Fonseca+ET		CatCen		CatCen+visco		Wasim	
Fn	β	$\hat{a_3}$	$\hat{a_5}$	$\hat{a_3}$	$\hat{a_5}$	$\hat{a_3}$	$\hat{a_5}$	$\hat{a_3}$	$\hat{a_5}$	$\hat{a_3}$	$\hat{a_5}$
0.20	180	1.09	1.10	1.08	1.22	1.02	1.24	1.05	1.26	1.00	1.15
0.53	180	1.10	0.97	1.14	1.32	0.83	0.95	1.04	1.11	0.96	0.93
0.80	180	0.93	0.76	1.10	1.21	0.73	0.82	1.03	1.07	0.91	0.94

Catamaran model: NPL 5b $S/L = 4$

		Fonseca		Fonseca+ET		CatCen		CatCen+visco		Wasim	
Fn	β	$\hat{a_3}$	$\hat{a_5}$	$\hat{a_3}$	$\hat{a_5}$	$\hat{a_3}$	$\hat{a_5}$	$\hat{a_3}$	$\hat{a_5}$	$\hat{a_3}$	$\hat{a_5}$
0.20	180	0.94	1.04	0.93	1.16	0.85	1.01	0.87	1.03	0.93	1.03
0.53	180	0.93	0.93	0.98	1.27	0.59	0.98	0.74	1.13	0.65	0.63
0.80	180	0.90	0.72	1.03	1.12	0.76	0.86	0.98	1.02	0.77	0.78

Table C.3: Frequency independent model error for heave and pitch motions, NPL 6b round bilge.

Catamaran model: NPL 6b $S/L = 2$

		Fonseca		Fonseca+ET		CatCen		CatCen+visco		Wasim	
Fn	β	$\hat{a_3}$	$\hat{a_5}$	$\hat{a_3}$	$\hat{a_5}$	$\hat{a_3}$	$\hat{a_5}$	$\hat{a_3}$	$\hat{a_5}$	$\hat{a_3}$	$\hat{a_5}$
0.20	180	0.95	1.01	0.95	1.11	0.86	1.13	0.88	1.14	0.88	1.07
0.53	180	0.94	0.99	0.98	1.32	0.67	0.98	0.85	1.12	0.77	0.92
0.80	180	0.91	0.71	1.05	1.09	0.72	0.80	0.98	1.01	0.80	0.80

Catamaran model: NPL 6b $S/L = 4$

		Fonseca		Fonseca+ET		CatCen		CatCen+visco		Wasim	
Fn	β	$\hat{a_3}$	$\hat{a_5}$	$\hat{a_3}$	$\hat{a_5}$	$\hat{a_3}$	$\hat{a_5}$	$\hat{a_3}$	$\hat{a_5}$	$\hat{a_3}$	$\hat{a_5}$
0.20	180	0.98	1.27	0.97	1.40	0.70	1.24	0.73	1.26	0.98	1.28
0.53	180	1.01	1.09	1.05	1.43	0.61	1.00	0.84	1.22	0.89	0.90
0.80	180	0.98	0.83	1.11	1.24	0.66	0.72	0.98	1.03	0.82	0.81

Table C.4: Frequency independent model error for heave and pitch motions, MARINTEK.

		Catamaran model: MARINTEK									
		Fonseca		Fonseca+ET		CatCen		CatCen+visco		Wasim	
Fn	β	$\hat{a_3}$	$\hat{a_5}$	$\hat{a_3}$	$\hat{a_5}$	$\hat{a_3}$	$\hat{a_5}$	$\hat{a_3}$	$\hat{a_5}$	$\hat{a_3}$	$\hat{a_5}$
0.49	180	0.67	0.79	0.67	0.89	0.66	0.81	0.77	0.89	0.69	0.66
0.66	180	0.67	0.77	0.70	0.83	0.61	0.65	0.75	0.74	0.61	0.50
0.66	150	0.71	0.83	0.75	0.91	0.38	0.53	0.72	0.81	0.67	0.59
0.49	90	0.90	...	0.91	...	0.87	...	0.90	...	0.91	...

Table C.5: Frequency independent model error for heave and pitch motions, Delft 372.

		Catamaran model: Delft 372									
		Fonseca		Fonseca+ET		CatCen		CatCen+visco		Wasim	
Fn	β	$\hat{a_3}$	$\hat{a_5}$	$\hat{a_3}$	$\hat{a_5}$	$\hat{a_3}$	$\hat{a_5}$	$\hat{a_3}$	$\hat{a_5}$	$\hat{a_3}$	$\hat{a_5}$
0.30	180	1.13	1.07	1.14	1.20	0.95	0.99	1.08	1.08	0.95	0.94
0.30	180	1.40	1.14	1.42	1.29	1.07	1.01	1.30	1.13	1.13	1.00
0.30	195	1.32	1.25	1.33	1.40	1.31	1.19	1.36	1.28	1.19	1.04
0.30	225	1.10	1.14	1.11	1.26	1.09	1.20	1.16	1.27	1.08	1.03
0.45	180	1.10	0.97	1.16	1.16	0.76	0.95	0.95	1.08	0.91	0.80
0.60	180	1.00	0.89	1.09	1.13	0.80	0.86	1.06	1.02	1.10	0.79
0.60	180	1.10	0.84	1.19	1.05	0.87	0.82	1.19	0.97	0.91	0.61
0.60	195	1.14	0.94	1.23	1.17	0.94	0.94	1.25	1.10	1.02	0.73
0.60	225	1.17	0.96	1.28	1.20	0.91	0.94	1.21	1.10	1.05	0.83
0.75	180	0.93	0.73	1.07	0.98	0.79	0.91	1.05	1.08	1.09	0.74
0.75	180	0.92	0.56	1.06	0.77	0.74	0.61	1.09	0.76	1.09	0.67
0.75	195	0.95	0.64	1.07	0.85	0.91	0.73	1.18	0.85	1.15	0.64
0.75	225	0.85	0.59	1.01	0.83	0.66	0.63	1.03	0.83	1.12	0.75

Table C.6: Frequency independent model error for heave and pitch motions, El Pardo.

		Catamaran model: El Pardo									
		Fonseca		Fonseca+ET		CatCen		CatCen+visco		Wasim	
Fn	β	$\hat{a_3}$	$\hat{a_5}$	$\hat{a_3}$	$\hat{a_5}$	$\hat{a_3}$	$\hat{a_5}$	$\hat{a_3}$	$\hat{a_5}$	$\hat{a_3}$	$\hat{a_5}$
0.00	180	0.94	1.02	0.94	1.02	0.94	1.01	0.94	1.01	0.94	1.02
0.20	180	0.99	0.98	1.00	1.07	0.98	1.04	0.99	1.05	0.94	0.99
0.40	180	1.01	1.02	1.03	1.28	0.79	1.00	0.95	1.08	0.87	0.94
0.40	165	0.98	1.02	0.98	1.27	0.83	1.03	0.94	1.10	0.88	0.94
0.40	150	0.97	0.99	0.98	1.22	0.91	0.99	0.97	1.06	0.87	0.91
0.60	180	1.06	1.05	1.19	1.42	0.74	1.01	1.05	1.18	0.91	1.09

Table C.7: Frequency independent model error for heave and pitch motions, Vosper.

		Catamaran model: Vosper V40									
		Fonseca		Fonseca+ET		CatCen		CatCen+visco		Wasim	
Fn	β	$\hat{a_3}$	$\hat{a_5}$	$\hat{a_3}$	$\hat{a_5}$	$\hat{a_3}$	$\hat{a_5}$	$\hat{a_3}$	$\hat{a_5}$	$\hat{a_3}$	$\hat{a_5}$
0.00	180	0.93	0.85	0.93	0.85	0.94	0.85	0.94	0.85	0.95	0.83
0.25	180	0.97	0.77	1.03	0.88	0.72	0.81	0.82	0.83	0.80	0.72
0.63	180	0.91	0.73	0.92	0.99	0.67	0.69	0.84	0.84	0.87	0.75
0.75	180	0.88	0.65	0.89	0.93	0.77	0.73	0.86	0.81	0.81	0.78

		Catamaran model: Vosper V60									
		Fonseca		Fonseca+ET		CatCen		CatCen+visco		Wasim	
Fn	β	$\hat{a_3}$	$\hat{a_5}$	$\hat{a_3}$	$\hat{a_5}$	$\hat{a_3}$	$\hat{a_5}$	$\hat{a_3}$	$\hat{a_5}$	$\hat{a_3}$	$\hat{a_5}$
0.00	180	0.92	0.88	0.92	0.88	0.91	0.88	0.91	0.88	0.92	0.85
0.25	180	1.02	0.84	1.07	0.95	0.96	0.83	1.02	0.85	0.94	0.78
0.63	180	1.06	0.75	1.07	1.01	0.81	0.80	0.95	0.92	0.97	0.78
0.75	180	1.04	0.78	1.05	1.10	0.85	0.87	0.92	0.94	0.93	0.88

C.2 Roll motion FIME

Table C.8: Frequency independent model error for roll motion.

		Catamaran model: Delft 372				
		Fonseca	Fonseca+ET	CatCen	CatCen+visco	Wasim
Fn	β	$\hat{a_4}$	$\hat{a_4}$	$\hat{a_4}$	$\hat{a_4}$	$\hat{a_4}$
0.30	195	0.46	0.49	0.69	0.58	0.65
0.60	195	0.36	0.40	0.47	0.40	0.92
0.75	195	0.60	0.64	0.65	0.56	1.19
0.30	225	0.64	0.68	0.93	0.92	0.89
0.60	225	0.59	0.65	1.00	0.99	1.29
0.75	225	0.72	0.75	1.07	1.10	1.27

		Catamaran model: MARINTEK				
		Fonseca	Fonseca+ET	CatCen	CatCen+visco	Wasim
Fn	β	$\hat{a_4}$	$\hat{a_4}$	$\hat{a_4}$	$\hat{a_4}$	$\hat{a_4}$
0.66	150	0.37	0.43	0.66	0.94	2.07
0.49	90	0.42	0.52	0.77	0.98	1.07

		Catamaran model: El Pardo				
		Fonseca	Fonseca+ET	CatCen	CatCen+visco	Wasim
Fn	β	$\hat{a_4}$	$\hat{a_4}$	$\hat{a_4}$	$\hat{a_4}$	$\hat{a_4}$
0.40	165	0.89	0.98	1.16	2.35	1.05
0.40	150	0.61	0.68	0.83	1.21	0.88